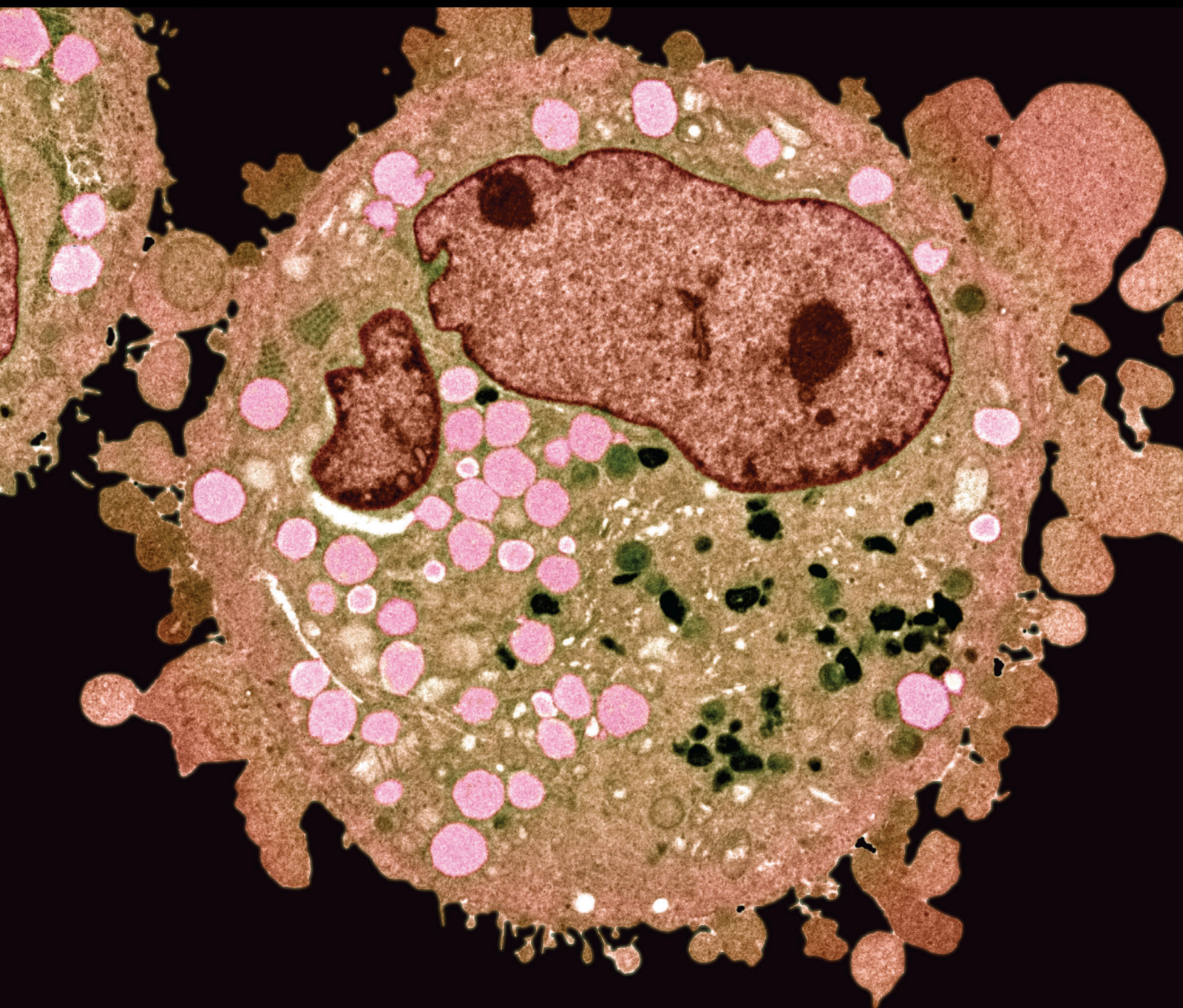


# Diagnosis, Therapy, and Prognosis for Hepatocellular Carcinoma

Lead Guest Editor: Zhigang Ren

Guest Editors: Xiaochao Ma, Zhenfeng Duan, and Xinhua Chen





---

# **Diagnosis, Therapy, and Prognosis for Hepatocellular Carcinoma**

Analytical Cellular Pathology

---

## **Diagnosis, Therapy, and Prognosis for Hepatocellular Carcinoma**

Lead Guest Editor: Zhigang Ren

Guest Editors: Xiaochao Ma, Zhenfeng Duan, and Xinhua  
Chen



---

Copyright © 2020 Hindawi Limited. All rights reserved.

This is a special issue published in "Analytical Cellular Pathology." All articles are open access articles distributed under the Creative Commons Attribution License, which permits unrestricted use, distribution, and reproduction in any medium, provided the original work is properly cited.

# Chief Editor

Dimitrios Karamichos, USA

---

## Editorial Board

Francisco Aguayo, Chile  
Consuelo Amantini, Italy  
Anna Batistatou, Greece  
Nady Braidy, Australia  
Silvia Cantara, Italy  
Monica Cantile, Italy  
Alain Chapel, France  
Domenico D'Arca, Italy  
Luigina Guasti, Italy  
Madhyastha Harishkumar, Japan  
Ekaterina Jordanova, The Netherlands  
Motohiro Kojima, Japan  
Maryou Lambros, United Kingdom  
Anant Madabhushi, USA  
Francesco A. Mauri, United Kingdom  
Alfredo Procino, Italy  
Liang Qiao, Australia  
Jonathan S. Reichner, USA  
Jorge Reis Filho, USA  
Carmela Ricciardelli, Australia  
José A. Sánchez-Alcázar, Spain  
Andrea Santarelli, Italy  
Nils Ole Schmidt, Germany  
Fernando Schmitt, Portugal  
Dorota L. Stankowska, USA  
Matthias B. Stope, Germany  
Sebastião Roberto Taboga, Brazil  
Giovanni Tuccari, Italy  
Sebastian Wachsmann-Hogiu, USA  
Man Yu, Canada

## Contents

### **Diagnosis, Therapy, and Prognosis for Hepatocellular Carcinoma**

Zhigang Ren , Xiaochao Ma, Zhenfeng Duan, and Xinhua Chen 

Editorial (2 pages), Article ID 8157406, Volume 2020 (2020)

### **Clinical Characteristics and Outcomes of Acute Lung Injury Caused by Transcatheter Arterial Chemoembolization for Hepatocellular Carcinoma: A Retrospective Cohort Study from a Single Institution in China**

Liang-jie Fang, Lu-yan Chen, Jun-hui Sun, and Jian-ying Zhou 

Research Article (7 pages), Article ID 4307651, Volume 2019 (2019)

### **miR-590-3p and Its Downstream Target Genes in HCC Cell Lines**

Mennatallah Elfar  and Asma Amleh 

Research Article (12 pages), Article ID 3234812, Volume 2019 (2019)

### **The Combination Strategy of Transarterial Chemoembolization and Radiofrequency Ablation or Microwave Ablation against Hepatocellular Carcinoma**

Zhentian Xu , Haiyang Xie , Lin Zhou , Xinhua Chen , and Shusen Zheng 

Review Article (7 pages), Article ID 8619096, Volume 2019 (2019)

### **Ginsenoside Rg3 Prolongs Survival of the Orthotopic Hepatocellular Carcinoma Model by Inducing Apoptosis and Inhibiting Angiogenesis**

Shen Hu , Yan Zhu, Xiangyang Xia , Xiaobo Xu , Fen Chen , Xudong Miao , and Xinmei Chen 

Research Article (7 pages), Article ID 3815786, Volume 2019 (2019)

### **Gene Ontology and Expression Studies of Strigolactone Analogues on a Hepatocellular Carcinoma Cell Line**

Mohammed Nihal Hasan, Syed Shoeb Razvi, Hani Choudhry , Mohammed A. Hassan, Said Salama Moselhy, Taha Abdullallah Kumosani, Mazin A. Zamzami , Khalid Omer Abualnaja, Majed A.

Halwani , Abdulrahman Labeed Al-Malki , Jiannis Ragoussis, Wei Wu, Christian Bronner, Tadao Asami , and Mahmoud Alhosin 

Research Article (10 pages), Article ID 1598182, Volume 2019 (2019)

### **Dynamics of the *O. felineus* Infestation Intensity and Egg Production in Carcinogenesis and Partial Hepatectomy in the Setting of Superinvasive Opisthorchiasis**

Vitaly G. Bychkov, Ludmila F. Kalyonova, Elena D. Khadieva, Semen D. Lazarev, Ilgiz R. Lukmanov, Vladimir A. Shidin, and Evgeny N. Morozov 

Research Article (5 pages), Article ID 8079368, Volume 2019 (2019)

### **Current Research Progress on Long Noncoding RNAs Associated with Hepatocellular Carcinoma**

Haihong Shi , Yuxin Xu, Xin Yi, Dandan Fang, and Xia Hou 

Review Article (8 pages), Article ID 1534607, Volume 2019 (2019)

**The Security Rating on Local Ablation and Interventional Therapy for Hepatocellular Carcinoma (HCC)  
and the Comparison among Multiple Anesthesia Methods**

Qianhui Jin , Xinhua Chen , and Shusen Zheng 

Review Article (7 pages), Article ID 2965173, Volume 2019 (2019)

## Editorial

# Diagnosis, Therapy, and Prognosis for Hepatocellular Carcinoma

Zhigang Ren <sup>1</sup>, Xiaochao Ma,<sup>2</sup> Zhenfeng Duan,<sup>3</sup> and Xinhua Chen <sup>4</sup>

<sup>1</sup>Department of Infectious Diseases, The First Affiliated Hospital of Zhengzhou University, Zhengzhou 450052, China

<sup>2</sup>University of Pittsburgh, Pennsylvania, USA

<sup>3</sup>David Geffen School of Medicine at University of Los Angeles, Los Angeles, CA, USA

<sup>4</sup>Department of Hepatobiliary and Pancreatic Surgery, The First Affiliated Hospital, School of Medicine, Zhejiang University, Hangzhou 310003, China

Correspondence should be addressed to Zhigang Ren; [fcrcenzg@zzu.edu.cn](mailto:fcrcenzg@zzu.edu.cn)

Received 18 January 2020; Accepted 20 January 2020; Published 3 February 2020

Copyright © 2020 Zhigang Ren et al. This is an open access article distributed under the Creative Commons Attribution License, which permits unrestricted use, distribution, and reproduction in any medium, provided the original work is properly cited.

Hepatocellular carcinoma (HCC) is one of the most common malignancies worldwide and the third leading cause of cancer-related death worldwide [1]. Currently, there are an estimated 29,200 new HCC cases in males and 11,510 cases in females in the United States in 2017, among which 29,000 cases died from HCC [2]. More seriously, estimated new HCC cases achieved 343,700 in males and 122,300 in females in China in 2015 [3], which is mainly attributed to the prevalence of hepatitis B virus (HBV) persistent infection and HBV-induced cirrhosis. Due to the absence of specific symptoms in early stages, the lack of early diagnostic markers, and the low percentage (10–20%) of radical resectable HCC on diagnosis, most HCC patients are often diagnosed in an advanced stage with poor prognosis (the overall ratio of mortality to incidence is 0.95) [4]. Although liver transplantation (LT) has been considered the most effective therapy for HCC [5], organ shortage significantly limits the application of LT. Even if sorafenib and regorafenib are applied in HCC, the overall outcome of HCC remains unsatisfactory with the median survival in early and advanced HCC of about 6–9 months and 1–2 months, respectively. Thus, it is very important to explore the novel diagnosis tools, therapy strategy, and prognosis markers for HCC.

In this special issue, we present a delicate collection of high-quality reviews and original articles that contains the latest thinking and exploration for the mechanisms of HCC

development, the biomarkers of HCC diagnosis and prognosis, and the therapeutic strategy of HCC. Full acquaintance with the diagnosis, therapy, and prognosis for HCC can be acquired through fundamental investigations and clinical research. The purpose of this editorial is to provide a brief introduction for each published or accepted paper and highlight their major findings and discoveries. We believe that these achievements will help to find a better way to deal with HCC, so as to conquer it eventually.

As HCC is a highly vascularized tumor, new vessel formation in the tumor plays an important role on HCC progression, metastasis, and recurrence. S. Hu et al. investigated the function of ginsenoside Rg3 on angiogenesis and explored the possible mechanism in an orthotopic murine model. The experiment results showed that ginsenoside Rg3 initialized the tumor apoptotic progress, which then weakened the tumor volume and its capability to produce the vascularized network for tumor growth and further metastasis. This study indicates clinical potential of using ginsenoside Rg3 in the angiogenesis therapy against HCC.

Instead of Rg3, M. N. Hasan et al. studied a novel Strigolactone (SL) analogue, TIT3. To reveal the mechanisms of TIT3-induced anticancer activity in HepG2, they performed RNA sequencing and the differential expression of genes was analyzed by different tools. Through the analysis of the experiment results, researchers demonstrated that the inhibition of HepG2 cancer cell growth was attributed to the

interplay of genes, wherein the treatment of TIT3 significantly altered their expression levels. These altered gene expressions affected cell proliferation, cell cycle, metastasis, and apoptosis.

Locoregional therapies are increasingly available and gradually benefit many patients of HCC. Z. Xu et al. reviewed the characteristics and advantages of transarterial chemoembolization (TACE), radiofrequency ablation (RFA), microwave ablation (MWA), and TACE combined with RFA or MWA in order to provide the physician a better background on decision. The authors concluded that TACE combined with either RFA or MWA was effective and promising in treating larger HCC lesions. Most of the interventional operations needed local anesthesia combined with intravenous sedation. Q. Jin et al. summarized and analyzed multiple anesthesia methods and their characters while being applied in interventional therapy for HCC. These results suggested that different percutaneous ablations should be performed by selecting the appropriate anesthesia method to obtain the best therapeutic effect. For instance, as the prevalence of TACE, increasing clinical cases about post-TACE pulmonary complication had been reported. L. Fang et al. retrospectively analyzed 14 HCC patients who were diagnosed with TACE-associated acute lung injury (ALI). Pulmonary Lipiodol embolism was one of the main causes of TACE-associated ALI. Hence, precise evaluation, early recognition, and management are critically important during TACE.

Recently, the long noncoding RNAs (lncRNAs) are involved in many human cancers, including liver cancer. H. Shi et al. summarized the differences in the expression of lncRNAs in HCC and reviewed the participation of lncRNAs in HCC cell proliferation, apoptosis, and migration. The lncRNA might be a candidate biomarker for the diagnosis, prognosis, and recurrence prediction, as well as the therapeutic target of liver cancer. Analogously, M. Elfar and A. Amleh explored miR-590-3p and its potential downstream target genes in HCC cell lines and discovered that SOX2 could be a direct downstream target gene of hsa-miR-590-3p in HCC, signifying its role in epithelial-mesenchymal transition. They also indicated that the hsa-miR-590-3p downstream targets had huge research potential.

Another interesting research was reported in detail by V. G. Bychkov et al., who explored the patterns of the intensity of the invasion and egg production of *Opisthorchis felinus* in the carcinogenesis of various organs and partial hepatectomy in the setting of superinvasive opisthorchiasis. When modeling tumors with various carcinogens in the setting of superinvasive opisthorchiasis, the intensity of invasion was reduced. On the contrary, a partial hepatectomy in the setting of opisthorchiasis did not affect the number of parasites in the ecological niche (liver). This finding implied the potential impact of liver cancer on the body.

In view of the above review and discussion, we believe that the present special issue explores the latest research on the diagnosis, therapy, and prognosis for HCC. Indeed, we need to further explore advanced and effective diagnostic tools, safe and minimally invasive treatments, and convenient and sensitive prognosis assessment for HCC.

## Conflicts of Interest

The guest editors declare that this work was conducted in the absence of any commercial or financial relationships that could be construed as a potential conflict of interest.

## Authors' Contributions

All the guest editors wrote the editorial and contributed to and approved the final editorial.

Zhigang Ren  
Xiaochao Ma  
Zhenfeng Duan  
Xinhua Chen

## References

- [1] L. X. Yu and R. F. Schwabe, "The gut microbiome and liver cancer: mechanisms and clinical translation," *Nature Reviews Gastroenterology & Hepatology*, vol. 14, no. 9, pp. 527–539, 2017.
- [2] R. L. Siegel, K. D. Miller, and A. Jemal, "Cancer statistics, 2017," *CA: A Cancer Journal for Clinicians*, vol. 67, no. 1, pp. 7–30, 2017.
- [3] W. Chen, R. Zheng, P. D. Baade et al., "Cancer statistics in China, 2015," *CA: A Cancer Journal for Clinicians*, vol. 66, no. 2, pp. 115–132, 2016.
- [4] T. Kobayashi, H. Aikata, T. Kobayashi, H. Ohdan, K. Arihiro, and K. Chayama, "Patients with early recurrence of hepatocellular carcinoma have poor prognosis," *Hepatobiliary & Pancreatic Diseases International*, vol. 16, no. 3, pp. 279–288, 2017.
- [5] S. G. Hubscher, "What is the long-term outcome of the liver allograft?," *Journal of Hepatology*, vol. 55, no. 3, pp. 702–717, 2011.

## Research Article

# Clinical Characteristics and Outcomes of Acute Lung Injury Caused by Transcatheter Arterial Chemoembolization for Hepatocellular Carcinoma: A Retrospective Cohort Study from a Single Institution in China

Liang-jie Fang,<sup>1</sup> Lu-yan Chen,<sup>2</sup> Jun-hui Sun,<sup>2</sup> and Jian-ying Zhou <sup>1</sup>

<sup>1</sup>Department of Respiratory Medicine, First Affiliated Hospital, School of Medicine, Zhejiang University, Hangzhou 310003, China

<sup>2</sup>Department of Surgery, First Affiliated Hospital, School of Medicine, Zhejiang University, Hangzhou 310003, China

Correspondence should be addressed to Jian-ying Zhou; [zjyhz@zju.edu.cn](mailto:zjyhz@zju.edu.cn)

Received 1 March 2019; Accepted 25 September 2019; Published 26 November 2019

Academic Editor: Alfredo Procino

Copyright © 2019 Liang-jie Fang et al. This is an open access article distributed under the Creative Commons Attribution License, which permits unrestricted use, distribution, and reproduction in any medium, provided the original work is properly cited.

**Background.** Acute lung injury (ALI) is a rare but life-threatening pulmonary complication of transcatheter arterial chemoembolization (TACE) for hepatocellular carcinoma (HCC). The aim of this study was to characterize the common risk factors, clinical features, imaging findings, treatments, and outcomes of acute lung injury caused by TACE. **Methods.** A retrospective study was performed on all TACE-associated ALI cases that were diagnosed at authors' hospital from January 2015 to June 2018. **Results.** The study included 14 ALI cases where the mean age of patients was  $60.9 \pm 11.7$  years (range 41-82 years), with a mean onset time of  $2.4 \pm 1.6$  d after TACE. Of the 14 patients, 8 patients (57.1%) developed acute respiratory distress syndrome (ARDS). 7 patients (50%) had underlying chronic respiratory disease and hepatic arteriovenous fistula was detected in 6 patients (42.6%), both of which were significantly higher than control group ( $P < 0.05$ ). Dyspnea (92.9%) was the most common symptoms. Pleural effusion (64.3%), diffuse pulmonary infiltration (42.9%), and accumulation of Lipiodol in lung field (42.9%) were frequent radiologic abnormalities. 11 patients (78.6%) achieved remission after treatment, and the 30-day mortality rate was approximately 21.4%. Patient's median survival time after the development of ALI was merely 4.3 months, which was obviously worse than control group (4.3 months vs. 13.5 months,  $P < 0.05$ ). **Conclusion.** This study illustrates that TACE-associated ALI is a rare pulmonary complication with a high mortality rate. We infer that pulmonary Lipiodol embolization might be one of the main causes of TACE-associated ALI. Thus, HCC patients who are at high risk should be closely evaluated and monitored during TACE to avoid such potentially fatal complication.

## 1. Introduction

Hepatocellular carcinoma (HCC), the most common primary hepatic malignancy, is a leading cause of cancer-related death in the world, and more than 80% of the cases occur in Asia due to the prevalence of chronic hepatitis [1, 2]. Transcatheter arterial chemoembolization (TACE), a palliative therapy, first reported in the 1970s, has been widely used in treatment of HCC to prolong survival time, especially when tumors are not surgically respectable [3]. The rationale for TACE is based on the embolization of tumor vessels which predominantly supplied by hepatic arterial blood.

Conventional TACE uses an emulsion of Lipiodol-chemotherapeutic agent, whereas TACE with drug-eluting beads (DEB-TACE) uses beads loaded with a chemotherapeutic agent such as doxorubicin. Both two regimens have been shown to achieve a significant survival benefit according to previous researches [4, 5].

Acute lung injury (ALI)/acute respiratory distress syndrome (ARDS) is a type of respiratory failure characterized as the acutely development, bilateral pulmonary infiltrates and severe hypoxemia. ALI/ARDS could be caused by varied etiology, including sepsis, pancreatitis, trauma, pneumonia, and aspiration. Its death rate can reach to 35-50% [6].

Recently, as the prevalence of TACE, increasing clinical cases about post-TACE pulmonary complication had been reported and vast majority resulted in disastrous consequences [7–11]. Now, it is gradually accepted that ALI/ARDS caused by TACE is a rare but fatal complication, mainly thought to be related to chemical injury subsequent to the migration of the infused Lipiodol or chemotherapeutic agent to the lung vasculature. However, so far, most of our knowledge about this complication is based on case reports. Its clinical characteristics and outcomes have not been fully investigated by researchers.

Thus, this study aimed at retrospectively analyzing the common risk factors, clinical features, imaging findings, treatments, and outcomes of TACE-associated ALI. This information will be useful for precise evaluation, early recognition, and management in clinical practice.

## 2. Materials and Methods

**2.1. Ethics Statement.** The institutional ethical committee approved our research protocol. All the patients or their relatives provided written informed consent and understood that their hospital data would be used for research.

**2.2. Study Patients and Diagnostic Criteria.** This study was a retrospective analysis conducted at the First Affiliated Hospital of Zhejiang University. 14 HCC patients with TACE-associated ALI, diagnosed from January 2015 to June 2018, were retrospectively analyzed. Patients, who developed pulmonary complication but no evidence of ALI, were selected as control group. Information was obtained regarding the following clinical parameters: demographic data, symptom, laboratory examination, radiographic presentation, treatment, follow-up, and outcome.

Diagnosis of HCC was made by pathological confirmation (postoperative pathological test or needle biopsy) and typical radiographic evidence (significantly enhanced tumor in the arterial phase and rapidly cleared contrast agents in the portal venous phase). Pulmonary complication defined as the presence of respiratory symptoms (such as cough, sputum, and dyspnea) and abnormalities in chest imaging after TACE. ALI was confirmed according to the standard American-European Consensus Conference (AECC) definition as the development of acute, bilateral pulmonary infiltrates and hypoxemia (ALI:  $\text{SpO}_2/\text{FiO}_2 < 300$ ; ADRS:  $\text{SpO}_2/\text{FiO}_2 < 200$ ) in the absence of clinical signs of the left atrial hypertension as the main explanation for pulmonary edema.

**2.3. TACE Therapy.** Puncture with the Seldinger technique was routinely performed with a 5 F catheter being placed into the celiac aorta. Further catheterization was performed in the feeding artery of the intrahepatic tumor after angiography. Next, the intrahepatic tumor was treated with TACE therapy in which iodized oil emulsion or drug-eluting beads loaded with a chemotherapeutic agent were injected into the tumor artery before 300–500  $\mu\text{m}$  particles to completely embolize the tumor feeding artery.

**2.4. Laboratory Parameters, Treatments, and Outcome Assessments.** Once acute respiratory symptom developed

after TACE, patient's laboratory examinations including blood gas analysis, CRP, D-dimer, myocardium zymogram level, and sputum or blood culture were tested according to the manufacturer's instructions. Chest computed tomography (CT) was performed using 16-slice or 64-slice systems (Toshiba Aquilion 16 CT Scanner; Brilliance iCT and 64-channel systems). Two experienced radiologists evaluated the CT images, and consensus was achieved by negotiation.

Patients, diagnosed with TACE-associated ALI, were treated with oxygen therapy, antibiotic therapy, systemic corticosteroids, and respiratory support with mechanical ventilation depending on their etiology and the severity of disease.

**2.5. Statistical Analysis.** Continuous variables were presented as mean  $\pm$  standard deviation and were performed by Student's *t*-test. Categorical variables were presented as frequencies and percentages (*n* (%)). Fisher's exact test was used to compare categorical variables. The survival curves were calculated by the Kaplan-Meier method. Survival differences were evaluated using log-rank test. *P* values  $< 0.05$  were considered statistically significant. All statistical analyses were performed with SPSS v19.0 for Windows (IBM, USA).

## 3. Results

**3.1. General Clinical Characteristics.** During the study period (January 2015 to June 2018), we identified 32 patients with pulmonary complication after TACE and 14 patients (10 female and 4 male) met the diagnostic criteria of ALI were included. The remaining 18 patients served as control group. The demographic features for those 14 patients were presented in Table 1. Briefly, the mean age of those 14 patients was  $60.9 \pm 11.7$  years (range 41–82 years). Cirrhosis was the most common underlying disease ( $n = 10$ , 71.4%), followed by respiratory disease ( $n = 7$ , 50%), diabetes ( $n = 1$ , 7.1%), and hypertension ( $n = 1$ , 7.1%). The mean tumor diameter was  $8.9 \pm 3.6$  cm. 10 patients (71.4%) were found to have portal vein tumor thrombus, and hepatic arteriovenous fistula was detected in 6 patients (42.9%). Among the 14 cases, 12 patients received conventional TACE therapy with mean dose of  $9.6 \pm 4.2$  mL infused Lipiodol and another 2 patients received DEB-TACE therapy. Compared to control group, the combination of chronic respiratory disease or hepatic arteriovenous fistula were significantly common in patients with ALI ( $P < 0.05$ ), which could be considered as risk factors for the development of ALI following TACE.

**3.2. Clinical Features.** The clinical features of TACE-associated ALI were presented in Table 2. The mean time of ALI onset after TACE was  $2.4 \pm 1.6$  d. Of the 14 patients, 8 patients (57.1%) developed ARDS. Dyspnea was the most common presenting symptom, occurring in 13 patients (92.9%), followed by cough ( $n = 10$ , 71.4%), fever ( $n = 4$ , 28.6%), hemoptysis ( $n = 2$ , 14.3%), and chest pain ( $n = 1$ , 7.1%). An increase in D-dimer was observed in most of the patients. Blood culture was performed in 4 febrile patients. *Klebsiella pneumoniae* was isolated from blood culture in 2 patients with an obvious increase in inflammatory markers

TABLE 1: Demographic and baseline characteristics of patients with HCC.

Clinical characteristics	ALI (n = 14)	Non-ALI <sup>#</sup> (n = 18)	P value*
Mean age (years)	60.9 ± 11.7	55.7 ± 5.9	0.1112
Sex, n (%)			0.7035
Male	10 (71.4)	14 (77.8)	
Female	4 (28.6)	4 (22.2)	
Cause of HCC, n (%)			1.000
Hepatitis B virus	13 (92.9)	16 (88.9)	
Alcoholic liver disease	1 (7.1)	2 (11.1)	
Underlying disease, n (%)			
Cirrhosis	10 (71.4)	12 (66.7)	0.4192
Chronic respiratory disease	7 (50)	2 (11.1)	0.0225
Diabetes	1 (7.1)	2 (11.1)	
Hypertension	1 (7.1)	3 (16.7)	
Child-Pugh classification, n (%)			1.000
Child class A	8 (57.1)	11 (61.1)	
Child class B	6 (42.9)	7 (38.9)	
Mean tumor diameter (cm)	8.9 ± 3.6	8.0 ± 3.3	0.4677
Portal vein tumor thrombus, n (%)			1.000
Presence	10 (71.4)	13 (72.2)	
Absence	4 (28.6)	5 (27.8)	
Hepatic arteriovenous fistula, n (%)			0.0265
Presence	6 (42.9)	1 (5.6)	
Absence	8 (57.1)	17 (94.4)	
Therapeutic regimen			1.000
Conventional TACE	13	16	
DEB-TACE	1	2	
Mean Lipiodol dose (mL)	9.6 ± 4.2	8.5 ± 3.6	0.4651

<sup>#</sup>Patients with pulmonary complication but no evidence of ALI; \* significance level set at  $P < 0.05$ .

such as C-reactive protein and white blood cell. The sputum and blood culture in other patients were negative.

All patients received chest CT scans after the onset of respiratory symptom. Pleural effusion was a frequent finding, which was detected in 9 cases (64.3%). The diffuse pulmonary infiltration (Figures 1(a), 1(b), 2(a), and 2(b)) and accumulation of Lipiodol in lung field (Figures 1(c), 1(d), 2(c), and 2(d)) were regarded as relatively specific findings, which are observed in 6 patients (42.9%). Other associated findings included multiple pulmonary consolidations and ground-glass opacity occurred in 35.7% and 21.4% of the patients, respectively.

**3.3. Etiology, Treatments, and Outcomes.** In current research, we concluded that pulmonary Lipiodol embolization might be one of the main causes of TACE-induced ALI since 6 patients (42.9%) presented with diffuse pulmonary infiltration and obvious accumulation of Lipiodol on chest CT with

TABLE 2: The clinical characteristics of HCC patients with TACE-associated ALI.

Clinical characteristics	No. of patients	Proportion (%)
Mean time to onset (days)	2.4 ± 1.6	
Clinical symptom		
Dyspnea	13	92.9
Cough	10	71.4
Fever	4	28.4
Hemoptysis	2	14.3
Chest pain	1	7.1
Laboratory examination		
ALI (SpO <sub>2</sub> /FiO <sub>2</sub> : 200-300)	6	42.9
ARDS (SpO <sub>2</sub> /FiO <sub>2</sub> : <200)	8	57.1
CRP (mg/L)	79.8 ± 54.2	
D-dimer (μg/mL)	8032 ± 4631	
Positive blood culture	2	14.3
Radiographic finding		
Pleural effusion	9	64.3
Diffuse pulmonary infiltration	6	42.9
Accumulation of Lipiodol in lung field	6	42.9
Multiple pulmonary consolidations	5	35.7
Multiple ground-glass opacity	3	21.4
Possible etiology		
Pulmonary Lipiodol embolization	6	42.9
Sepsis	2	14.3
Unknown	6	42.9
Treatment		
Oxygenation	14	100
Empirical antibiotic therapy	12	85.7
Systemic corticosteroids	6	42.9
Mechanical ventilation	2	14.3

a negative result in sputum or blood culture. In addition, patients whose blood culture detected *Klebsiella pneumoniae* were finally diagnosed as having liver abscess and bloodstream infection. Hence, sepsis induced by TACE ought to be another important reason for ALI. However, causes for the remaining 6 cases were unclear.

After a diagnosis of TACE-associated ALI was established, all the patients received oxygen therapy immediately. Other combined treatments including empirical antibiotic therapy (85.7%) and corticosteroids (42.9%) were listed in Table 2. Due to exacerbation of severe hypoxemia, 2 patients were referred to intensive care unit (ICU) for mechanical ventilation and finally died of multiple organ failure or bloodstream infection two weeks later. Another patient with ARDS refused to invasive ventilation and transferred to local hospital, resulting in a death of respiratory failure. Overall, 11 patients achieved remission after treatment and the 30-day mortality rate of TACE-associated ALI was approximately 21.4%.

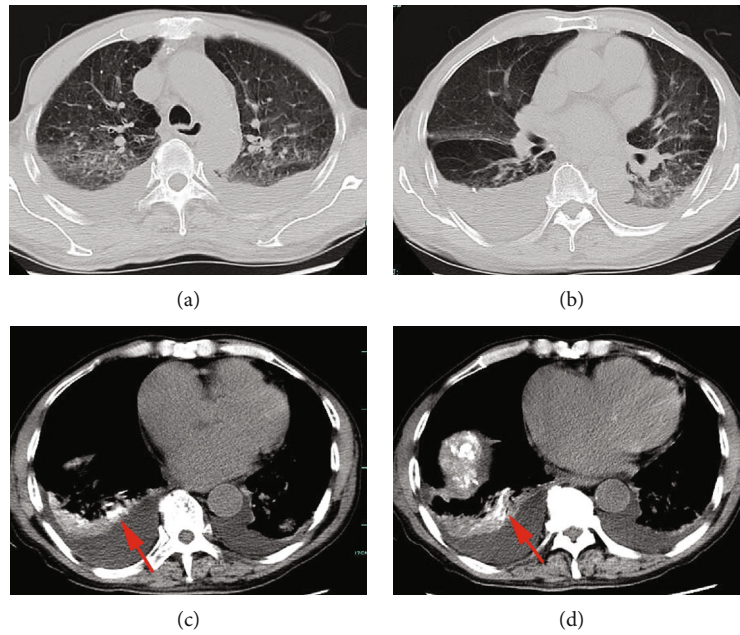


FIGURE 1: An 82-year-old man with HCC developed ARDS 24 h after the performance of TACE. The chest CT demonstrated diffuse pulmonary infiltration and bilateral pleural effusion (a, b). In addition, an obvious accumulation of Lipiodol (red arrows) was observed in the right lung lobe (c, d).

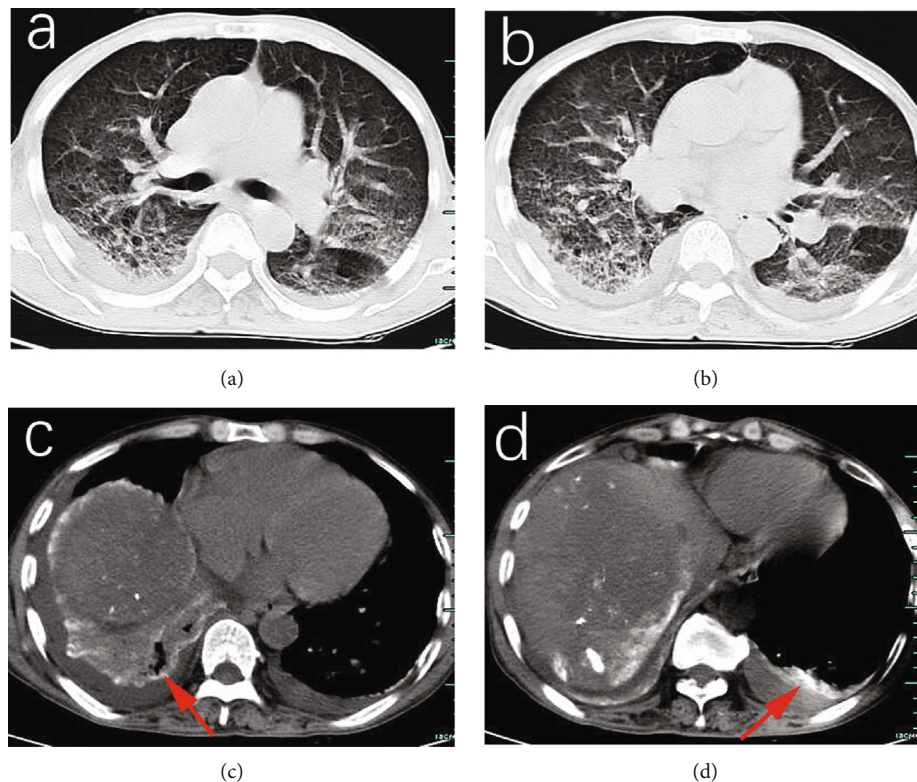


FIGURE 2: Chest CT findings in a 60-year-old man with an underlying disease of COPD. He suffered from dyspnea and hemoptysis 10 h after TACE for HCC. Chest CT showed diffuse pulmonary infiltration in bilateral lung fields (a, b) and accumulation of Lipiodol (red arrows) located in bilateral lung lower lobes (c, d).

Long-term follow-up was available for survivors (Table 3). Due to deterioration of physical condition, merely 4 patients (36.4%) were able to withstand further antitumor

therapy including TACE or surgery, while other 7 patients (63.6%) were given best supportive care. The proportion of antitumor therapy in ALI group was significantly lower than

TABLE 3: The outcomes of HCC patients with TACE-associated ALI.

	ALI (n = 14)	Non-ALI (n = 18)	P value*
30-day mortality rate, n (%)	3 (21.4)	0 (0)	
Cause of death			
Multiple organ failure	1 (7.1)		
Bloodstream infection	1 (7.1)		
Respiratory failure	1 (7.1)		
Antitumor treatment after remission, n (%)			0.0169
TACE and surgery	4 (36.4)	15 (83.3)	
Best supportive care	7 (63.6)	3 (16.7)	
Median survival time after ALI (months)	4.3	13.5	0.0215

\*Significance level set at  $P < 0.05$ .

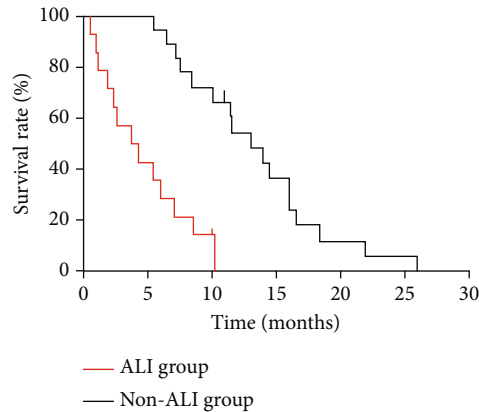


FIGURE 3: Survival curve of hepatocellular carcinoma patients with TACE-associated pulmonary complications. In ALI group, patient's median survival time was 4.3 months, which was obviously worse than non-ALI group (4.3 months vs. 13.5 months,  $P < 0.05$ ).

that in control group (36.4% vs. 83.3%,  $P < 0.05$ ). Accordingly, the patient's median survival time after the development of ALI was only 4.3 months, which was obviously worse than non-ALI group (4.3 months vs. 13.5 months,  $P < 0.05$ ) (Figure 3). It suggested that the development of ALI could significantly impair the long-term survival of the patients with HCC.

#### 4. Discussion

TACE is a widely accepted palliative treatment for patients with advanced HCC. Despite the great advantages of being less invasive and relatively safe, TACE still has multiple side effects [12, 13]. In the present research, we retrospectively analyzed 14 HCC patients who were diagnosed with TACE-associated ALI, revealing a high mortality rate (21.4%) and severe impairment of patient's long-term survival. We found that HCC patients with combined chronic respiratory disease or hepatic arteriovenous fistula were more prone to develop

ALI after TACE. Vast majority of patients presented dyspnea, elevated D-dimer, diffuse pulmonary infiltration, and accumulation of Lipiodol on chest CT. Hence, we considered that pulmonary Lipiodol embolism was one of the main causes of TACE-associated ALI. Nevertheless, this study still had some potential limitations. It was a retrospective analysis conducted in a single medical center. The number of ALI cases was relatively small, so the result required further confirmation by large sample clinical studies. In addition, etiological conclusions mainly based on the clinical data analysis, lacking of pathological support.

To date, the mechanisms underlying symptomatic pulmonary injury associated with TACE are not well understood. The most likely mechanism is chemical injury caused by infused Lipiodol or administered medicine. Generally, the procedure of TACE involves mechanical occlusion of selective hepatic artery, supplying HCC with emulsion of Lipiodol-chemotherapeutic agent or beads loaded with a chemotherapeutic agent such as doxorubicin. Early studies had observed that  $^{131}\text{I}$ -labeled Lipiodol could be detected in the lung when delivered to the hepatic artery of patients with hepatic cancer [14, 15]. Now, increasing evidence supports that pulmonary oil embolism is closely related to the development of ALI/ARDS [16, 17]. Hatamaru et al. reported a case of TACE-associated ARDS due to pulmonary Lipiodol embolism, which confirmed the presence of fat droplets in the pulmonary arteriolar lumen via pathological autopsy [16]. In current study, nearly half of the cases presented diffuse pulmonary infiltration and accumulation of Lipiodol on chest CT but without evidence of infection, which were consistent with findings from other studies [18]. Concerning the underlying molecular mechanisms, it attributed to enzymatic digestion of Lipiodol by lipase and formation of free fatty acid, which is toxic to alveolar-capillary membrane. To date, several risk factors including a large hypervascular HCC (>10 cm) with AV shunts, large-volume Lipiodol infusion (>14.5 mL), and transinferior phrenic artery embolization have been identified for pulmonary Lipiodol embolism after TACE [13, 19, 20]. Thus, recommendations suggest that the maximum safe Lipiodol dose is about 15 to 20 mL or approximately 0.25 mL/kg total body weight.

Although extremely rare, other chemotherapeutic agent may also possess potential for induction of ALI/ARDS when applies in TACE. Recently, acute lung injury following TACE of doxorubicin-loaded LC beads was reported by Khan et al. [8]. Kumasawa et al. described a TACE case using miriplatin with agents developed ARDS 5 days following therapy, presenting as cough, dyspnea, and pulmonary infiltration in chest imaging [7]. In our study, the definite causes of 6 cases were still unclear. We speculated that the etiology of some cases was implicated to chemotherapeutic drug-induced lung injury. In addition, our study revealed 2 ALI patients caused by bloodstream infection, indicating that sepsis secondary to TACE should not be completely ignored, especially in patient with fever and an obvious increase of inflammatory markers.

The optimal management strategy for TACE-associated ALI remains unknown. Oxygenation, systemic corticosteroids, and lung protective ventilation are the primary options and treatments varied according to etiological analysis and

the severity of symptoms. Intravenous methylprednisolone might be effective to reduce the inflammatory response, oxidative stress involved in ARDS, and chemical pneumonitis induced by chemotherapeutic agent. It achieved success in 6 cases presented in our research. Nevertheless, the 30-day mortality rate of TACE-associated ALI was still as high as 21.4%. For there are no proven effective therapies, its prevention is quite essential. Precise evaluation, early recognition, and management are critically important during TACE.

In this study, patient's median survival time after the development of ALI was merely 4.3 months, which was significantly worse than non-ALI group. We believed that it closely related to lack of effective antineoplastic therapy since only 36.4% of the patients in ALI group were able to continue further antitumor therapy while the proportion in control group can reach to 83.3%. We inferred that the development of ALI accelerated deterioration of physical condition, leading to a great difficulty for achievement of further antitumor treatment, finally resulting in a poor prognosis.

In summary, this study characterized clinical features and outcomes of ALI caused by TACE, presenting as a lower occurrence rate but a higher mortality. Moreover, the development of ALI could significantly impair the long-term survival of the patients with HCC. Thus, physicians should be fully aware of and avoid this potential fatal complication during TACE.

### Data Availability

The data used to support the findings of this study are included within the article.

### Conflicts of Interest

None of the authors have a conflict of interests regarding this paper.

### Acknowledgments

This work was supported by grants from the Medical and Health Technology Program of Zhejiang Province, China (no. 2016RCA013).

### References

- [1] F. Bray, J. Ferlay, I. Soerjomataram, R. L. Siegel, L. A. Torre, and A. Jemal, "Global cancer statistics 2018: GLOBOCAN estimates of incidence and mortality worldwide for 36 cancers in 185 countries," *CA: a Cancer Journal for Clinicians*, vol. 68, no. 6, pp. 394–424, 2018.
- [2] R. X. Zhu, W. K. Seto, C. L. Lai, and M. F. Yuen, "Epidemiology of hepatocellular carcinoma in the Asia-pacific region," *Gut Liver*, vol. 10, no. 3, pp. 332–339, 2016.
- [3] K. Takayasu, "Transarterial chemoembolization for hepatocellular carcinoma over three decades: current progress and perspective," *Japanese Journal of Clinical Oncology*, vol. 42, no. 4, pp. 247–255, 2012.
- [4] C. M. Lo, H. Ngan, W. K. Tso et al., "Randomized controlled trial of transarterial Lipiodol chemoembolization for unresectable hepatocellular carcinoma," *Hepatology*, vol. 35, no. 5, pp. 1164–1171, 2002.
- [5] A. Facciorusso, M. Di Maso, and N. Muscatiello, "Drug-eluting beads versus conventional chemoembolization for the treatment of unresectable hepatocellular carcinoma: a meta-analysis," *Digestive and Liver Disease*, vol. 48, no. 6, pp. 571–577, 2016.
- [6] H. El Kenz and P. Van der Linden, "Transfusion-related acute lung injury," *European Journal of Anaesthesiology*, vol. 31, no. 7, pp. 345–350, 2014.
- [7] F. Kumasawa, T. Miura, T. Takahashi et al., "A case of miriplatin-induced lung injury," *Journal of Infection and Chemotherapy*, vol. 22, no. 7, pp. 486–489, 2016.
- [8] I. Khan, V. Vasudevan, S. Nallagatla, F. Arjomand, and R. Ali, "Acute lung injury following transcatheter hepatic arterial chemoembolization of doxorubicin-loaded LC beads in a patient with hepatocellular carcinoma," *Lung India*, vol. 29, no. 2, pp. 169–172, 2012.
- [9] G. C. Wu, W. C. Perng, C. W. Chen, C. F. Chian, C. K. Peng, and W. L. Su, "Acute respiratory distress syndrome after transcatheter arterial chemoembolization of hepatocellular carcinomas," *The American Journal of the Medical Sciences*, vol. 338, no. 5, pp. 357–360, 2009.
- [10] Q. M. Nhu, H. Knowles, P. J. Pockros, and C. T. Frenette, "An unexpected pulmonary complication following transcatheter arterial chemoembolization of a small hepatocellular carcinoma," *Journal of Clinical Gastroenterology*, vol. 50, no. 6, pp. 524–525, 2016.
- [11] T. Naorungroj, T. Naksanguan, and Y. Chinthammitr, "Pulmonary Lipiodol embolism after transcatheter arterial chemoembolization for hepatocellular carcinoma: a case report and literature review," *Journal of the Medical Association of Thailand*, vol. 96, no. 2, pp. 270–275, 2013.
- [12] I. Sakamoto, N. Aso, K. Nagaoki et al., "Complications associated with transcatheter arterial embolization for hepatic tumors," *Radiographics*, vol. 18, no. 3, pp. 605–619, 1998.
- [13] Q. M. Nhu, H. Knowles, P. J. Pockros, and C. T. Frenette, "Pulmonary complications of transcatheter arterial chemoembolization for hepatocellular carcinoma," *World Journal of Respiriology*, vol. 6, no. 3, pp. 69–75, 2016.
- [14] J. L. Raoul, P. Bourguet, J. F. Bretagne et al., "Hepatic artery injection of I-131-labeled Lipiodol. Part I. Biodistribution study results in patients with hepatocellular carcinoma and liver metastases," *Radiology*, vol. 168, no. 2, pp. 541–545, 1988.
- [15] M. Nakajo, H. Kobayashi, K. Shimabukuro et al., "Biodistribution and in vivo kinetics of iodine-131 Lipiodol infused via the hepatic artery of patients with hepatic cancer," *Journal of Nuclear Medicine*, vol. 29, no. 3, pp. 1066–1077, 1988.
- [16] K. Hatamaru, S. Azuma, T. Akamatsu et al., "Pulmonary embolism after arterial chemoembolization for hepatocellular carcinoma: an autopsy case report," *World Journal of Gastroenterology*, vol. 21, no. 4, pp. 1344–1348, 2015.
- [17] R. C. Silvestri, J. S. Huseby, I. Rughani, D. Thorning, and B. H. Culver, "Respiratory distress syndrome from lymphangiography contrast medium," *The American Review of Respiratory Disease*, vol. 122, no. 5, pp. 543–549, 1980.
- [18] Y. Watanabe, H. Tokue, A. Taketomi-Takahashi, and Y. Tsushima, "Imaging findings and complications of transcatheter interventional treatments via the inferior phrenic arteries in patients with hepatocellular carcinoma," *European Journal of Radiology Open*, vol. 5, no. 5, pp. 171–176, 2018.

- [19] G. C. Wu, E. D. Chan, Y. C. Chou et al., "Risk factors for the development of pulmonary oil embolism after transcatheter arterial chemoembolization of hepatic tumors," *Anti-Cancer Drugs*, vol. 25, no. 8, pp. 976–981, 2014.
- [20] M. T. Lin and P. H. Kuo, "Pulmonary Lipiodol embolism after transcatheter arterial chemoembolization for hepatocellular carcinoma," *JRSM Short Reports*, vol. 8, no. 3, pp. 1–6, 2010.

## Research Article

# miR-590-3p and Its Downstream Target Genes in HCC Cell Lines

Mennatallah Elfar <sup>1</sup> and Asma Amleh <sup>1,2</sup>

<sup>1</sup>Biotechnology Program, The American University in Cairo, Cairo, Egypt

<sup>2</sup>Biology Department, The American University in Cairo, Cairo, Egypt

Correspondence should be addressed to Asma Amleh; [aamleh@aucegypt.edu](mailto:aamleh@aucegypt.edu)

Received 25 February 2019; Accepted 17 September 2019; Published 3 November 2019

Guest Editor: Zhigang Ren

Copyright © 2019 Mennatallah Elfar and Asma Amleh. This is an open access article distributed under the Creative Commons Attribution License, which permits unrestricted use, distribution, and reproduction in any medium, provided the original work is properly cited.

miRNAs are small non-coding RNA sequences of 18-25 nucleotides. They can regulate different cellular pathways by acting on tumor suppressors, oncogenes, or both. miRNAs are mostly tissue-specific, and their expression varies depending on the cancer or the tissue in which they are found. hsa-miR-590-3p was found to be involved in several types of cancers. In this study, we identified potential downstream target genes of hsa-miR-590-3p computationally. Several bioinformatics tools and more than one approach were used to identify potential downstream target genes of hsa-miR-590-3p. CX3CL1, SOX2, N-cadherin, E-cadherin, and FOXA2 were utilized as potential downstream target genes of hsa-miR-590-3p. SNU449 and HepG2, hepatocellular carcinoma cell lines, were used to carry out various molecular techniques to further validate our *in silico* results. mRNA and protein expression levels of these genes were detected using RT-PCR and western blotting, respectively. Co-localization of hsa-miR-590-3p and its candidate downstream target gene, SOX2, was carried out using a miRNA in situ hybridization combined with immunohistochemistry staining through anti-SOX2. The results show that there is an inverse correlation between hsa-miR-590-3p expression and SOX2 protein expression in SNU449. Subsequently, we suggest that SOX2 can be a direct downstream target of hsa-miR-590-3p indicating that it may have a role in the self-renewal and self-maintenance of cancer cells. We also suggest that CX3CL1, E-cadherin, N-cadherin, and FOXA2 show a lot of potential as downstream target genes of hsa-miR-590-3p signifying its role in epithelial-mesenchymal transition. Studying the expression of hsa-miR-590-3p downstream targets can enrich our understanding of the cancer pathogenesis and how it can be used as a therapeutic tool.

## 1. Introduction

Cancer is considered a worldwide epidemic, as it is the second leading cause of death worldwide. According to the World Health Organization, cancer is responsible for around 9.6 million deaths in 2018 only [1]. Liver cancer is the second leading cause of cancer deaths worldwide [2]. According to the American Cancer Society, since 1980, liver cancer incidence has more than tripled. Every year, approximately 700,000 new cases of liver cancer are diagnosed. According to GLOBOCAN, the less developed countries account for 83% of these cases. Liver cancer is male predominant [3].

Hepatocellular carcinoma (HCC), also known as malignant hepatoma, is the most common primary tumor of liver cancer cases [4]. It usually occurs secondary to liver cirrhosis

due to viral hepatitis infection (HBV and HCV), alcoholism, or exposure to high levels of aflatoxin-b1 (AFB). HCC is heterogeneous and a number of factors contribute to the disease progression, starting from tumor initiation to metastasis [5]. These factors include the tumor's microenvironment, hypoxia, inflammation, and oxidative stress [6]. Cytokines and reactive oxygen species released in the organ's microenvironment due to chronic inflammation and oxidative stresses, respectively, result in gradual accumulation of mutations that change the hepatocytes genetically, altering gene expression and affecting various signaling pathways causing liver damage and eventually cancer development [7].

Small non-coding RNA sequences, known as microRNAs (miRNAs), are 18-25 nucleotides. miRNAs can posttranscriptionally regulate different cellular pathways including

cellular differentiation, growth, proliferation, metabolism, angiogenesis, regeneration, survival, apoptosis, and tumorigenesis [8].

Most miRNA genes are located on intergenic regions (non-coding regions) of the nuclear DNA and are expressed in the cytoplasm through the following process. In the nucleus, RNA polymerase II transcribes a long primary miRNA (pri-miRNA) with a hairpin-like structure. Drosha then converts it to precursor miRNA (pre-miRNA), a 70-nucleotide stem loop, followed by its transport to the cytoplasm through the action of Exportin 5, where it meets Dicer and is cleaved into 22-nucleotide double-stranded miRNAs. Then, it is separated into two single-stranded miRNAs. The sense (passenger) strand is degraded while the antisense (guide) strand binds to RNA-induced silencing complex (RISC). The interaction between the 5' seed sequence of the miRNA and the 3'-untranslated region of the mRNA determines the effect of the miRNA, whether degradation of the mRNA or the inhibition of its translation [9].

According to miRBase, there are 1917 precursor and 2654 mature human miRNAs [10]. Various miRNAs can act as tumor suppressors, oncogenes, or both through the regulation of their target genes. They are tissue-specific, meaning they can be upregulated or downregulated, depending on the cancer or the tissue in which they are found [11]. hsa-miR-590-3p is a good example of one miRNA that is upregulated in a specific cancer and downregulated in another.

In this study, we focused on hsa-miR-590-3p's downstream target genes. We used various bioinformatics analyses to identify the potential downstream target genes of hsa-miR-590-3p and to predict their function in relation to HCC. Then, we employed various molecular techniques to access the levels of the potential downstream target genes. The main aim of the study is to assess the levels of hsa-miR-590-3p and the role of its downstream target genes in HCC.

## 2. Material and Methods

**2.1. In Silico Analysis.** Several bioinformatics tools were used to predict the potential downstream target genes of hsa-miR-590-3p. For the primary screening, five databases were used (TargetScan [12] (<http://www.targetscan.org>), miRanda-mirSVR [13] (<http://www.microrna.org>), miRDB [14] (<http://mirdb.org/>), miRTarBase [15] (<http://mirtarbase.mbc.nctu.edu.tw/php/index.php>), and Diana Tools [16] (<http://diana.imis.athena-innovation.gr>)) to achieve a dataset of potential downstream target genes of hsa-miR-590-3p from each database. For the function prediction, we used the Functional Assignment of MicroRNAs via Enrichment (FAME) software [17] (<http://acgt.cs.tau.ac.il/fame/index.html>) to predict the potential functions of hsa-miR-590-3p through the prediction of the potential functions of its potential downstream target genes. Alignment of the mRNA of potential downstream target genes against hsa-miR-590-3p was carried out using miRanda-mirSVR [13] (<http://www.microrna.org>). The mRNA and protein expression of these genes were assessed computationally using The Human Protein Atlas

[18] (<http://www.proteinatlas.org/>) and Expression Atlas [19] (<http://www.ebi.ac.uk/gxa>), respectively.

**2.2. Cell Lines and Cell Culture.** The human hepatocellular carcinoma cell lines, HepG2 and SNU449, were used. HepG2 is an early-stage liver cancer cell line while SNU449 is an HBV-infected intermediate stage liver cancer cell line. Both cell lines were a kind gift from Dr. Mehmet Ozuturk at the Department of Molecular Biology and Genetics, Bilkent University, Turkey. Cells were cultured in RPMI 1640 (Lonza, USA) media supplemented with 10% FBS (Gibco, USA) and 5% penicillin-streptomycin antibiotic (Lonza, USA). They were maintained at 37°C and 5% CO<sub>2</sub> in a humidified atmosphere. Cells were passaged and used for experiments during their logarithmic growth phase.

**2.3. Semiquantitative Reverse Transcription-Polymerase Chain Reaction (RT-PCR).** Total RNA was extracted from HepG2 and SNU449 cells using TRizol Reagent (Invitrogen, USA) following the manufacturer's protocol. 0.5 µg RNA was used to synthesize cDNA using the RevertAid First Strand cDNA Synthesis Kit (Thermo Scientific, USA) according to the manufacturer's protocol. mRNA expression was determined using semiquantitative RT-PCR. MyTaq Red DNA Polymerase (Bioline, UK) was used to perform the PCR reactions using GAPDH as an endogenous control. Specific primers (Invitrogen, USA) were designed using Primer3 [20] (<http://primer3.ut.ee>) for each gene. PCR conditions used were the same among the genes except for the annealing temperatures and the number of cycles. PCR conditions are as follows: Step 1: initiation at 94°C for 3 minutes. Step 2: denaturation at 94°C for 30 seconds, annealing at specific temperatures for each primer for 30 seconds, and extension at 72°C for 45 seconds; Step 2 is repeated for a specific number of cycles for each primer. Step 3: final extension at 72°C for 10 minutes. Primer sequences, annealing temperatures, number of cycles, and PCR amplicon sizes are listed in Supplementary A.

**2.4. Western Blotting Analysis.** Total protein was extracted from HepG2 and SNU449 cells using 1x Laemmli lysis buffer (50 mM Tris/HCl, pH 6.8, 2% SDS, and 10% glycerol) supplemented with 1x Halt Protease Inhibitor Cocktail (Thermo Scientific, USA). The Pierce BCA Protein Assay Kit (Thermo Scientific, USA) was used to quantify the total extracted protein according to the manufacturer's protocol. 30 µg protein was used to perform western blotting. Protein was separated on a 10% SDS-polyacrylamide gel and electrotransferred onto a nitrocellulose membrane (Thermo Scientific, USA). The membrane was blocked using 5% non-fat dry milk in 1x TBST (0.01% Tween 20 in 1x TBS buffer) and then incubated with specific primary antibodies followed by the secondary antibodies. The BCIP/NBT phosphatase colorimetric substrate (KPL, USA) was used for detection. GAPDH and β-tubulin were used as endogenous controls.

Antibodies were diluted in 5% non-fat dry milk in 1x TBST. Primary antibodies used were as follows: anti-GAPDH (1:10,000, ab8245, Abcam, UK), anti-β-tubulin (1:20,000, T7816, Sigma, USA), anti-SOX2 (1:2000, PA1-

16968, Thermo Scientific, USA), and anti-Vimentin (1 : 1000, ab8978, Abcam, UK). Secondary antibodies used were as follows: ReverseAP Phosphatase labeled Goat anti-Mouse IgG (H+L) Conjugate (1 : 20,000, 4751-1806, KPL, USA) and ReverseAP Phosphatase labeled Goat anti-Rabbit IgG (H+L) Conjugate (1 : 10,000, 4751-1516, KPL, USA).

**2.5. In Situ Hybridization-Immunocytochemistry (ISH-ICC).** For the codetection of hsa-miR-590-3p and one of its downstream target genes (SOX2), ISH-ICC was carried out on SNU449 cells. Cells were seeded into 24-well cell culture plates and incubated till 70% confluency was reached. Fixation of the cells was carried out using 100% methanol. For the ISH, the cells were incubated with DIG-labeled probes for miR-590-3p (hsa-miR-590-3p miRCURY LNA Detection probe, Exiqon, Denmark), U6 (as a positive control probe), and scrambled probes (as a negative control) (miRCURY LNA microRNA Detection ISH Buffer and Controls kits, Exiqon, Denmark) for 1 hour at 54°C. Blocking was done using a blocking solution rich in 7.5% BSA Fraction V (Gibco, USA), and then, the cells were incubated with anti-DIG phosphatase labeled antibody (1 : 800, 11 093 274 910, Roche, Germany). The BCIP/NBT phosphatase colorimetric substrate (KPL, USA) was used for hsa-miR-590-3p detection. For ICC, blocking was performed again and the cells were incubated with anti-SOX2 (1 : 250, PA1-16968, Thermo Scientific, USA), followed by the secondary antibody, Goat anti-rabbit IgG (H+L) DyLight 488 Conjugated (1 : 250, 35552, Thermo Scientific, USA). The nuclei were stained with DAPI (1 : 1000 in PBS, KPL, USA).

**2.6. Statistical Analysis.** PCR and western blotting analysis results were quantified and normalized against an endogenous control using ImageJ Software [21] (<https://imagej.nih.gov/ij/>). Data is presented as mean  $\pm$  standard deviation (SD) from three independent experiments. All statistical comparisons were done using Prism GraphPad 7.0 [22] (<http://www.graphpad.com/>). For the analysis of the difference between multiple experimental groups with a single variable, one-way ANOVA (with a Bonferroni posttest) was used. *P* values less than 0.05 are considered significant (\**P* value < 0.05, \*\**P* value < 0.01, and \*\*\**P* value < 0.001).

### 3. Results

**3.1. Prediction of Potential Downstream Target Genes of hsa-miR-590-3p.** Prediction of the potential downstream target genes of hsa-miR-590-3p was carried out using five databases (TargetScan, miRanda-mirSVR, miRDB, miRTarBase, and Diana Tools). Each database uses a different scoring system based on different molecular and bioinformatics techniques. TargetScan uses the conserved sites of the target genes that match miRNA's seed region to predict the miRNA's target genes [23]. Through TargetScan, 8611 potential target genes of hsa-miR-590-3p were obtained (Supplementary B). miRanda-mirSVR uses a two-step strategy to predict potential target genes of miRNAs. Primarily, the program aligns the miRNA sequence against mRNA sequences and produces a score based on the complementarity through A:U and

G:C matches, followed by the usage of high-scoring alignments, meaning they passed a certain threshold, to calculate their thermodynamic stability [13]. Through miRanda-mirSVR, 21,123 potential downstream target genes of hsa-miR-590-3p were obtained. miRDB uses MirTarget, a bioinformatics tool, to predict potential target genes. MirTarget was developed by the analysis of thousands of miRNA-target interactions obtained from high-throughput sequencing experiments [24]. Through miRDB, 1590 potential target genes of hsa-miR-590-3p were obtained (Supplementary C). miRTarBase was established on the collection of miRNA-target interactions (MTIs) from the previous literature and validating them experimentally using next-generation sequencing (NGS), microarray, western blotting, and reporter assay [15]. Through miRTarBase, 447 potential target genes of hsa-miR-590-3p were obtained (Supplementary D). Diana TarBase was established using specific and high-throughput experiments to predict miRNA-gene interactions [16]. Through Diana TarBase, 4576 potential target genes of hsa-miR-590-3p were obtained (Supplementary E). All potential downstream target genes of hsa-miR-590-3p from all 5 databases were placed in a pivot table, and a list of 362 common genes (primary screening) was obtained (Supplementary F).

To get further insight on hsa-miR-590-3p's function, we performed the functional prediction analysis of its downstream target genes using FAME software. FAME analysis is founded on a collection of miRNA pathways and miRNA process association that has been verified experimentally [17]. FAME identified many functions and the downstream target genes of hsa-miR-590-3p that perform these functions. We chose cancer pathogenesis-related functions to narrow down our study (Supplementary G). These functions include response to DNA damage stimulus, DNA repair, cell-cell adhesion, nucleotide excision repair, and DNA damage response and signal transduction. Using this approach (function prediction), thirty-four potential target genes of hsa-miR-590-3p were achieved.

Thirty-two genes of the thirty-four genes from the function prediction approach were found in the list from the primary screening approach. From these thirty-two genes, fourteen genes were chosen based on the results obtained from The Human Protein Atlas [18] (Figure 1) and previous literature. These genes are BRIP1, CX3CL1, DCLRE1A, DLG1, DYRK2, ERCC5, FANCF, HIPK2, MLH3, NPHP1, RAD21, SMC6, TMEM33, and UVRAG. The genes were categorized according to the functions they share from FAME software (Figure 2).

**3.2. mRNA Expression of Potential Downstream Target Genes of hsa-miR-590-3p.** The mRNA levels of the potential target genes of hsa-miR-590-3p were assessed in HepG2 and SNU449 using RT-PCR. mRNA expression levels of all genes showed no significant difference between HepG2 and SNU449 except for CX3CL1 (Supplementary H1). CX3CL1 mRNA expression was significantly higher in HepG2 compared to SNU449 (*P* < 0.01) (Figure 3, Supplementary H2).

**3.3. Alignment of Potential Targets of hsa-miR-590-3p Using miRanda-mirSVR.** Through the alignment of hsa-miR-590-

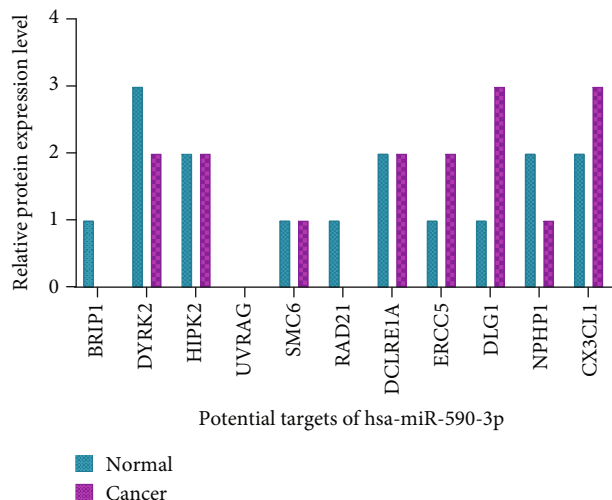


FIGURE 1: Protein expression of potential targets of hsa-miR-590-3p in normal versus cancerous liver tissue using The Human Protein Atlas. Diagram of the protein expression of the potential downstream target genes chosen for further analysis in normal liver tissue versus cancerous liver tissue. Scale: 0: not detected; 1: low; 2: medium; and 3: high.

3p against the mRNA of some genes using miRanda-mirSVR, more genes were identified as potential downstream target genes of hsa-miR-590-3p. These genes are E-cadherin, N-cadherin, SOX2, and FOXA2. Figure 4 illustrates the binding site(s) of hsa-miR-590-3p on all four genes. hsa-miR-590-3p has one binding site on E-cadherin mRNA (Figure 4(a)) and one binding site on N-cadherin mRNA (Figure 4(b)), three binding sites on SOX2 mRNA (Figure 4(c)), and one binding site on FOXA2 mRNA (Figure 4(d)).

**3.4. Protein Expression of Potential Targets of hsa-miR-590-3p Using Expression Atlas.** The protein expression of E-cadherin, N-cadherin, and FOXA2 was assessed computationally using the Expression Atlas (Figure 5). Also, Vimentin was assessed as an epithelial-mesenchymal transition (EMT) marker and VCAN as a downstream target gene of FOXA2 (Figure 5).

**3.5. E-Cadherin and N-Cadherin mRNA Expression as Potential Targets of hsa-miR-590-3p Using Vimentin mRNA Expression as a Mesenchymal Marker.** E-cadherin, N-cadherin, and Vimentin mRNA levels in HepG2 and SNU449 were analyzed using RT-PCR. E-cadherin mRNA expression was found to be elevated in HepG2 compared to SNU449 ( $P < 0.01$ ) (Figure 6, Supplementary H3). N-cadherin mRNA expression showed no statistically significant difference between HepG2 and SNU449 ( $P > 0.05$ ) (Figure 6, Supplementary H3). Vimentin mRNA expression was found to be elevated in SNU449 compared to HepG2 ( $P < 0.01$ ) (Figure 6, Supplementary H3).

**3.6. Vimentin Protein Expression as a Mesenchymal Marker.** Vimentin protein level in HepG2 and SNU449 was analyzed using western blotting. Vimentin protein is expressed in

SNU449 while it is not detected in HepG2 ( $P < 0.001$ ) (Figure 7, Supplementary H4).

**3.7. SOX2 mRNA and Protein Expression as a Potential Target of hsa-miR-590-3p.** SOX2 mRNA and protein levels in HepG2 and SNU449 were analyzed using RT-PCR and western blotting, respectively. On the mRNA level, SNU449 shows increased SOX2 expression compared to HepG2 ( $P < 0.01$ ) (Figure 8(a), Supplementary H5). On the protein level, HepG2 and SNU449 show comparable SOX2 expression ( $P > 0.05$ ) (Figure 8(b), Supplementary H5).

**3.8. FOXA2 mRNA Expression as a Potential Target of hsa-miR-590-3p and Its Downstream Target Gene VCAN mRNA Expression.** FOXA2 and VCAN mRNA levels in HepG2 and SNU449 were analyzed using RT-PCR. No statistically significant difference was observed between the FOXA2 and VCAN mRNA expression in HepG2 and SNU449 ( $P > 0.05$ ) (Figure 9, Supplementary H6).

**3.9. Expression and Localization of hsa-miR-590-3p and Its Potential Target, SOX2, in SNU449 Cells.** Expression and localization of hsa-miR-590-3p and SOX2 in SNU449 cells were assessed using ISH-ICC (Figures 10 and 11). hsa-miR-590-3p signal was detected in the cytoplasm of SNU449 cells. SOX2 fluorescence was detected mainly in the cytoplasm of the SNU449 cells. Cells that showed hsa-miR-590-3p signal showed minimal SOX2 fluorescence (red circles, Figure 10), and in cells that did not show hsa-miR-590-3p signal, SOX2 fluorescence was detected (white circles, Figure 10).

## 4. Discussion

Hepatocellular carcinoma is an aggressive malignant tumor with poor prognosis. It is usually diagnosed during the late stages of the cancer when most medications and surgical interventions are not efficient. Hence, understanding the cancer progression and pathogenesis is important.

miRNAs were discovered twenty years ago, broadening our understanding of cancer pathogenesis. Several miRNAs have been studied previously in relation to HCC and different liver disease including HCV, HBV, and non-alcoholic fatty liver disease. These miRNAs include miR-17, miR-21, miR-22, miR-26, miR-29b, miR-122, miR-135a, miR-146a, miR-151, miR-181b, miR-221/222, miR-224, miR-233, miR-338-3p, miR-491, and miR-500 [8, 9, 25–28]. They were found in the serum and liver tissues of HCC patients; some were found to be upregulated while others were found to be downregulated.

Several studies tested hsa-miR-590-3p in relation to various cancers. In glioblastoma multiforme (GBM), an aggressive brain cancer, hsa-miR-590-3p was significantly downregulated in cancer tissue compared to normal tissues [29], while in epithelial ovarian cancer (EOC) hsa-miR-590-3p was significantly upregulated in cancer tissue compared to that of the normal ovarian tissues [30]. This difference in expression in two different cancers suggests that hsa-miR-590-3p is tissue-specific and can regulate tumor suppressor genes and oncogenes in different tissues.

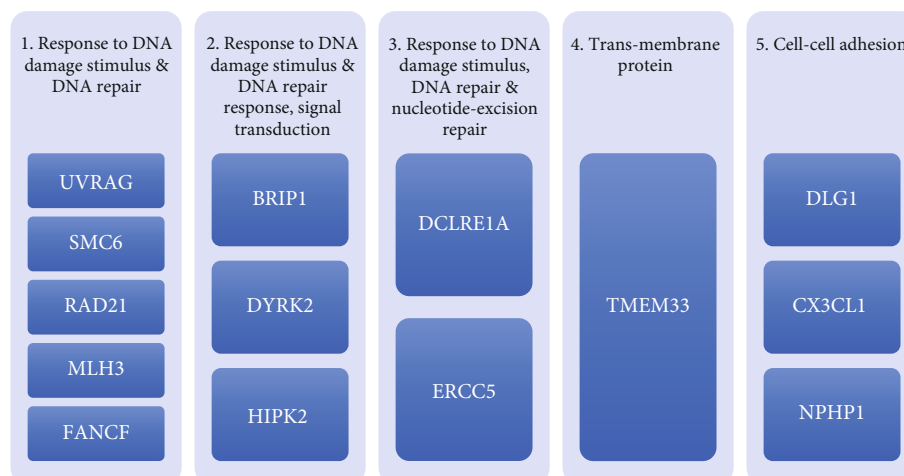


FIGURE 2: Classification of the fourteen genes. The fourteen genes chosen for further analysis categorized based on the functions they share according to the FAME software.

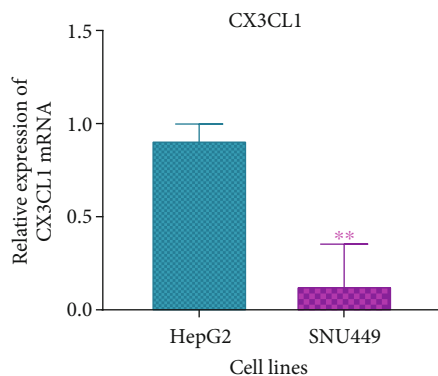


FIGURE 3: Graphical representation of CX3CL1 mRNA expression in HepG2 and SNU449. RT-PCR band intensities were measured using ImageJ and normalized against GAPDH and statistically analyzed using Prism GraphPad.  $P$  values were computed using one-way ANOVA (with a Bonferroni posttest).  $P$  values less than 0.05 are considered significant (\* $P$  value < 0.05, \*\* $P$  value < 0.01, and \*\*\* $P$  value < 0.001). Results are a representation of three independent experiments.

hsa-miR-590-3p was also reported to be expressed in HCC by two studies. In the first study, hsa-miR-590-3p was significantly downregulated in cancer tissue compared to normal tissues [31], while in the second study, it was reported to be significantly upregulated in three HCC cell lines (HepG2, Hep3B, and Huh7) [32]. The inconsistency of the reported findings may result from the fact that tissue specimens are heterogeneous and that cell lines may change their characteristics and in turn their gene expression when they are in culture for a long time.

**4.1. Prediction of Potential Downstream Target Genes of hsa-miR-590-3p.** In this study, several bioinformatics analyses were carried out to predict potential downstream target genes of hsa-miR-590-3p. First, preliminary screening of five databases (TargetScan, miRanda-mirSVR, miRDB, miRTarBase, and Diana Tools) was carried out (Supplementary B, C, D,

E, and F), giving rise to a list of potential downstream target genes. Second, the FAME software was used for the function prediction approach (Supplementary G), giving rise to a list of potential downstream target genes based on function. Thirty-two genes from the first approach were found in the list from the second approach. Through the usage of previous literature and The Human Protein Atlas to assess protein levels of the potential targets of hsa-miR-590-3p in normal liver tissue versus cancerous liver tissue, fourteen genes were chosen for further validation using molecular techniques (Figure 1).

**4.2. Potential Downstream Target Genes of hsa-miR-590-3p.** The fourteen genes are BRIP1, CX3CL1, DCLRE1A, DLG1, DYRK2, ERCC5, FANCF, HIPK2, MLH3, NPHP1, RAD21, SMC6, TMEM33, and UVRAG. Figure 2 categorizes the genes according to the functions they share.

UVRAG, SMC6, MLH3, FANCF, and RAD21 belong to the first category: response to DNA damage stimulus and DNA repair. UVRAG encodes the UV radiation resistance-associated protein, which activates the Beclin1-PI(3)KC3 complex that promotes autophagy and inhibits the proliferation and tumorigenicity of human colon cancer cells [33]. SMC6 encodes the structural maintenance of chromosome 6 protein and is mostly involved in DNA repair [34]. MLH3 is a member of the MutL-homolog family that is involved with DNA mismatch repair genes [35]. FANCF, known as Fanconi anemia complementation group F, are essential in DNA repair [36]. The RAD21 cohesin complex component is important for mitotic growth and has a role in the repair of DNA double-strand breaks [37].

BRIP1, DYRK2, and HIPK2 belong to the second category: response to DNA damage stimulus and DNA damage response and signal transduction. BRIP1, known as BRCA1-interacting protein C-terminal helicase 1, forms a complex with BRCA1 that is essential in the repair of double-strand breaks [38]. DYRK2, known as dual specificity tyrosine phosphorylation-regulated kinase 2, is part of a protein kinase family which is involved in cellular growth and development

hsa-miR-590-3p/CDH1 alignment	
3' ugAUCGAAUAUGUA-UUUUAAu 5' hsa-miR-590-3p          :         1432:5' ucUACCUCAUCUCUGAAAAUuc 3' CDH1	mirSVR score: -0.1176 PhastCons score: 0.5450
(a)	
hsa-miR-590-3p/CDH2 alignment	
3' ugaUCGAAUAUGUAUUUUAAu 5' hsa-miR-590-3p   :  :    :       586:5' accAAUUUGUA-GCAAAUug 3' CDH2	mirSVR score: -0.1913 PhastCons score: 0.7068
(b)	
hsa-miR-590-3p/SOX2 alignment	
3' ugaucgaaauauguaUUUUAAu 5' hsa-miR-590-3p       606:5' aacgugaaaagaagAAAAUu 3' SOX2	mirSVR score: -0.3046 PhastCons score: 0.6364
3' ugaucgaaauauguaUUUUAAu 5' hsa-miR-590-3p       640:5' auuuuuuuuguuuuAAAAUg 3' SOX2	mirSVR score: -0.2036 PhastCons score: 0.6364
3' ugaucgaaauauguaUUUUAAu 5' hsa-miR-590-3p       658:5' uuguacaaaaggaaAAAAUu 3' SOX2	mirSVR score: -0.1449 PhastCons score: 0.6364
(c)	
hsa-miR-590-3p/FOXA2 alignment	
3' ugaUCGAAUAUGUAUUUUAAu 5' hsa-miR-590-3p   :            817:5' aacAUUUUUAUUAUAAAAUu 3' FOXA2	mirSVR score: -0.7704 PhastCons score: 0.5034
(d)	

FIGURE 4: Alignment of hsa-miR-590-3p against the mRNA of E-cadherin, N-cadherin, SOX2, and FOXA2 using miRanda-mirSVR. (a) Binding site of hsa-miR-590-3p on E-cadherin mRNA at position 1432. (b) Binding site of hsa-miR-590-3p on N-cadherin mRNA at position 586. (c) Binding sites of hsa-miR-590-3p on SOX2 mRNA at positions 606, 640, and 658. (d) Binding site of hsa-miR-590-3p on FOXA2 mRNA at position 817.

[39]. HIPK2, known as homeodomain-interacting protein kinase 2, is a cell growth and apoptosis regulator [40].

ERCC5 and DCLRE1A belong to the third category: response to DNA damage stimulus, DNA repair, and nucleotide excision repair. ERCC5, or excision repair cross-complementing 5, encodes a single-strand-specific DNA endonuclease that creates a 3' incision following UV-induced damage in the DNA excision repair [41]. DCLRE1A, or DNA cross-link repair 1A, encodes a conserved protein that has a role in the DNA interstrand cross-link repair [42].

TMEM33, or transmembrane protein 33, is a transmembrane protein involved in endoplasmic reticulum stress-

responsive events in cancer cells [43]. CX3CL1, DLG1, and NPHP1 are involved in cell-cell adhesion. DLG1, or human discs large tumor suppressor, regulates cell polarity and proliferation suggesting a connection between epithelial organization and cellular growth control [44]. NPHP1, nephrocystin 1, encodes a protein that interacts with a Crk-associated substrate, and it is involved in cell division and cell-cell and cell-matrix adhesion [45]. CX3CL1, or C-X3-C motif chemokine ligand 1 or chemokine fractalkine, has been reported in many epithelial tissues and facilitates strong cell adhesion [46].

The mRNA expression of all these genes was assessed in the HCC cell lines, HepG2 and SNU449. All the genes

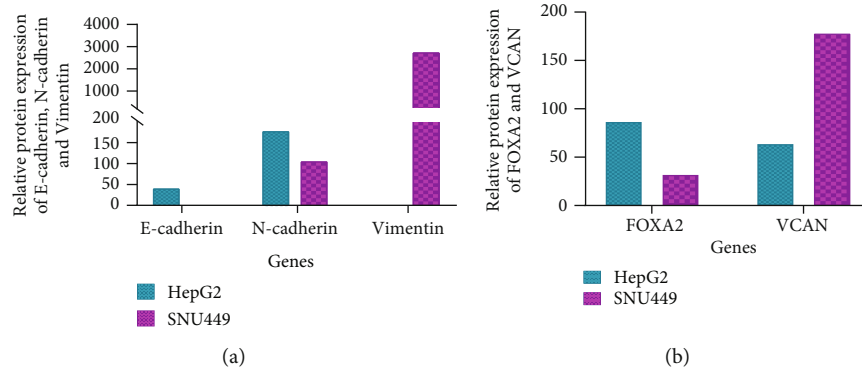


FIGURE 5: Relative protein expression of potential targets of hsa-miR-590-3p in HCC cell lines using the Expression Atlas. (a) Graphical representation of the relative protein expression of E-cadherin, N-cadherin, and Vimentin in HepG2 and SNU449. (b) Graphical representation of the relative protein expression of FOXA2 and VCAN in HepG2 and SNU449.

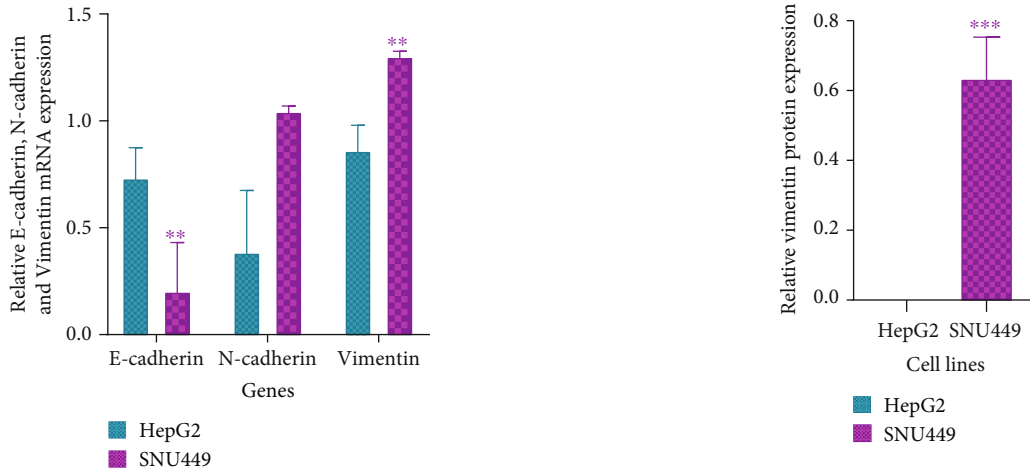


FIGURE 6: Graphical representation of E-cadherin, N-cadherin, and Vimentin relative mRNA expression in HepG2 and SNU449. RT-PCR band intensities were measured using ImageJ and normalized against GAPDH and statistically analyzed using Prism GraphPad. *P* values were computed using one-way ANOVA (with a Bonferroni posttest). *P* values less than 0.05 are considered significant (\**P* value < 0.05, \*\**P* value < 0.01, and \*\*\**P* value < 0.001). Results are a representation of three independent experiments.

FIGURE 7: Graphical representation of Vimentin protein expression in HepG2 and SNU449 using western blotting. Western blotting band intensities were measured using ImageJ and normalized against GAPDH and statistically analyzed using Prism GraphPad. *P* values were computed using one-way ANOVA (with a Bonferroni posttest). *P* values less than 0.05 are considered significant (\**P* value < 0.05, \*\**P* value < 0.01, and \*\*\**P* value < 0.001). Results are a representation of three independent experiments.

showed comparable expression between both cell lines except CX3CL1 (Supplementary H1). HepG2 showed high CX3CL1 mRNA expression compared to SNU449 (Figure 3, Supplementary H2). HepG2 is an early-stage well-differentiated human HCC cell line while SNU449 is an intermediate stage hepatitis B virus- (HBV-) infected HCC cell line. This explains the obtained results as high expression of CX3CL1 indicates tighter cell adhesion, thus no metastasis.

Since CX3CL1 is the only gene that showed differential expression between the tested HCC cell lines and it is involved in cell-cell adhesion, we decided to choose genes related to that function and validate them as potential downstream target genes of hsa-miR-590-3p but using miRanda-

mirSVR. E-cadherin and N-cadherin mRNA were aligned against hsa-miR-590-3p to assess the binding sites of our miRNA on the mRNA of these genes (Figures 4(a) and 4(b)).

4.3. *Potential Targets of hsa-miR-590-3p and Cell-Cell Adhesion.* Calcium-dependent cell adhesion molecules known as cadherins are mainly involved in cell-cell adhesion and cell migration [47]. There are several types of cadherins, but in our study, we are focusing on E-cadherin (CDH1) and N-cadherin (CDH2). E-cadherin, or epithelial cadherin, is the protein that holds epithelial cells together. As cancer progresses, cells start to lose E-cadherin expression and start producing N-cadherin. N-cadherin, or neural cadherin, increases with the cell's increased invasiveness potential [48]. These molecular changes take place through a well-

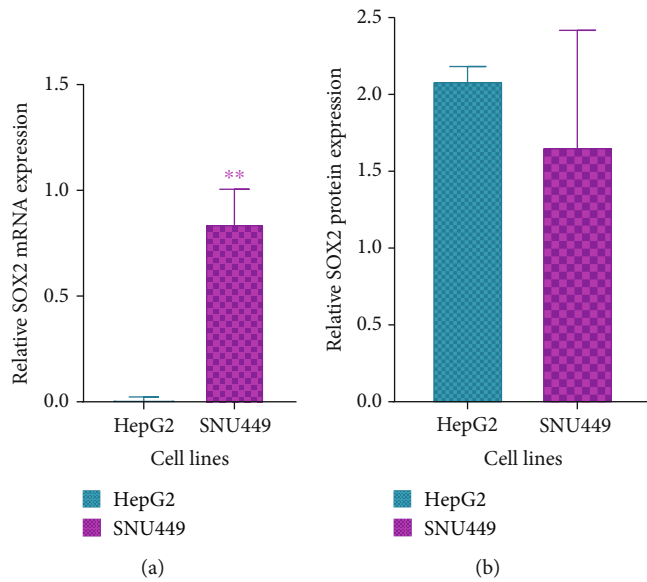


FIGURE 8: SOX2 mRNA and protein expression in HepG2 and SNU449 using RT-PCR and western blotting, respectively. (a) Graphical representation of SOX2 mRNA expression in HepG2 and SNU449 using RT-PCR. (b) Graphical representation of SOX2 protein expression using western blotting. RT-PCR and western blotting band intensities were measured using ImageJ and normalized against GAPDH and  $\beta$ -tubulin, respectively, and statistically analyzed using Prism GraphPad.  $P$  values were computed using one-way ANOVA (with a Bonferroni posttest).  $P$  values less than 0.05 are considered significant (\* $P$  value < 0.05, \*\* $P$  value < 0.01, and \*\*\* $P$  value < 0.001). Negatives were carried out for RT-PCR experiments. Results are a representation of three independent experiments.

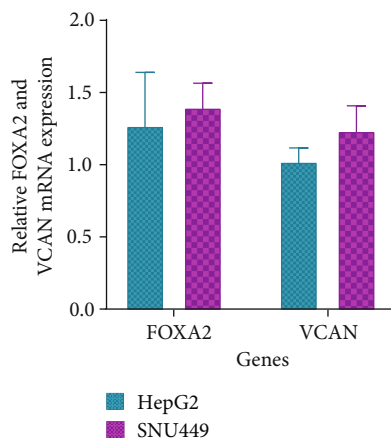


FIGURE 9: Graphical representation of FOXA2 and VCAN relative mRNA expression in HepG2 and SNU449 using RT-PCR. RT-PCR band intensities were measured using ImageJ and normalized against GAPDH and statistically analyzed using Prism GraphPad.  $P$  values were computed using one-way ANOVA (with a Bonferroni posttest).  $P$  values less than 0.05 are considered significant (\* $P$  value < 0.05, \*\* $P$  value < 0.01, and \*\*\* $P$  value < 0.001). Negatives were carried out for all experiments. Results are a representation of three independent experiments.

studied phenomenon known as epithelial-mesenchymal transition (EMT). EMT is a process in which epithelial cells lose their adherent nature and acquire mesenchymal traits, including migration and invasion abilities hence the ability to metastasize to other organs [49]. These molecular changes include alteration in Vimentin expression (a mesenchymal marker), which increases as the cancer progresses and the cells become more invasive [47].

E-cadherin, N-cadherin, and Vimentin protein expression in HepG2 and SNU449 were assessed computationally using the Expression Atlas. E-cadherin and N-cadherin protein expression is higher in HepG2 compared to SNU449 while Vimentin protein is expressed in SNU449 and not detected in HepG2 (Figure 5).

E-cadherin, N-cadherin, and Vimentin mRNA expression was assessed in HepG2 and SNU449 using RT-PCR (Figure 6, Supplementary H3). HepG2 showed high E-cadherin expression, low N-cadherin expression, and low Vimentin expression compared to SNU449. Since HepG2 is of epithelial origin, it is retaining its epithelial characteristics, hence the increase in E-cadherin, an epithelial marker, and the decrease in N-cadherin and Vimentin, mesenchymal markers. SNU449 showed low E-cadherin expression, high N-cadherin expression, and high Vimentin expression compared to HepG2. Since SNU449 is at a more advanced stage of the cancer, it acquired some mesenchymal characteristics, hence the decrease in the epithelial marker, E-cadherin, and the increase in the mesenchymal markers, N-cadherin and Vimentin.

Vimentin protein expression was assessed in HepG2 and SNU449 using western blotting (Figure 7, Supplementary H4). Vimentin protein expression was highly expressed in SNU449 while it was not detected in HepG2. Two bands were observed in SNU449; the second band could be a result of alternative splicing or posttranslational modification [50, 51]. As for HepG2, the protein is not detected while the mRNA is expressed. This can be attributed to the degradation of the mRNA or inhibition of translation. Our Vimentin protein expression results of both cell lines match our computational results via the Expression Atlas.

**4.4. Potential Targets of hsa-miR-590-3p and the FOXA2-VCAN Pathway.** In a previous study, FOXA2 was identified as a potential downstream target gene of miR-590-3p in epithelial ovarian cancer (EOC) [30]. Forkhead box A2 (FOXA2) is part of the FOXA family. It is a transcription factor that is associated with embryo development regulation and metabolism and homeostasis during the adult stage. Its involvement in hepatic specification and its importance for hepatic glucose and lipid homeostasis were previously reported in a study [52]. FOXA2's dual role in cancer development as a tumor suppressor and a tumor promoter in various cancers has been reported by several studies [30, 52]. Interestingly, it was also found to be sexually dimorphic in HCC; meaning it is tumor suppressing in females and tumor promoting in males [52].

A recent study proposes that VCAN is a downstream target gene of FOXA2 and shows that there is a negative correlation between their mRNA expression in EOC [30].

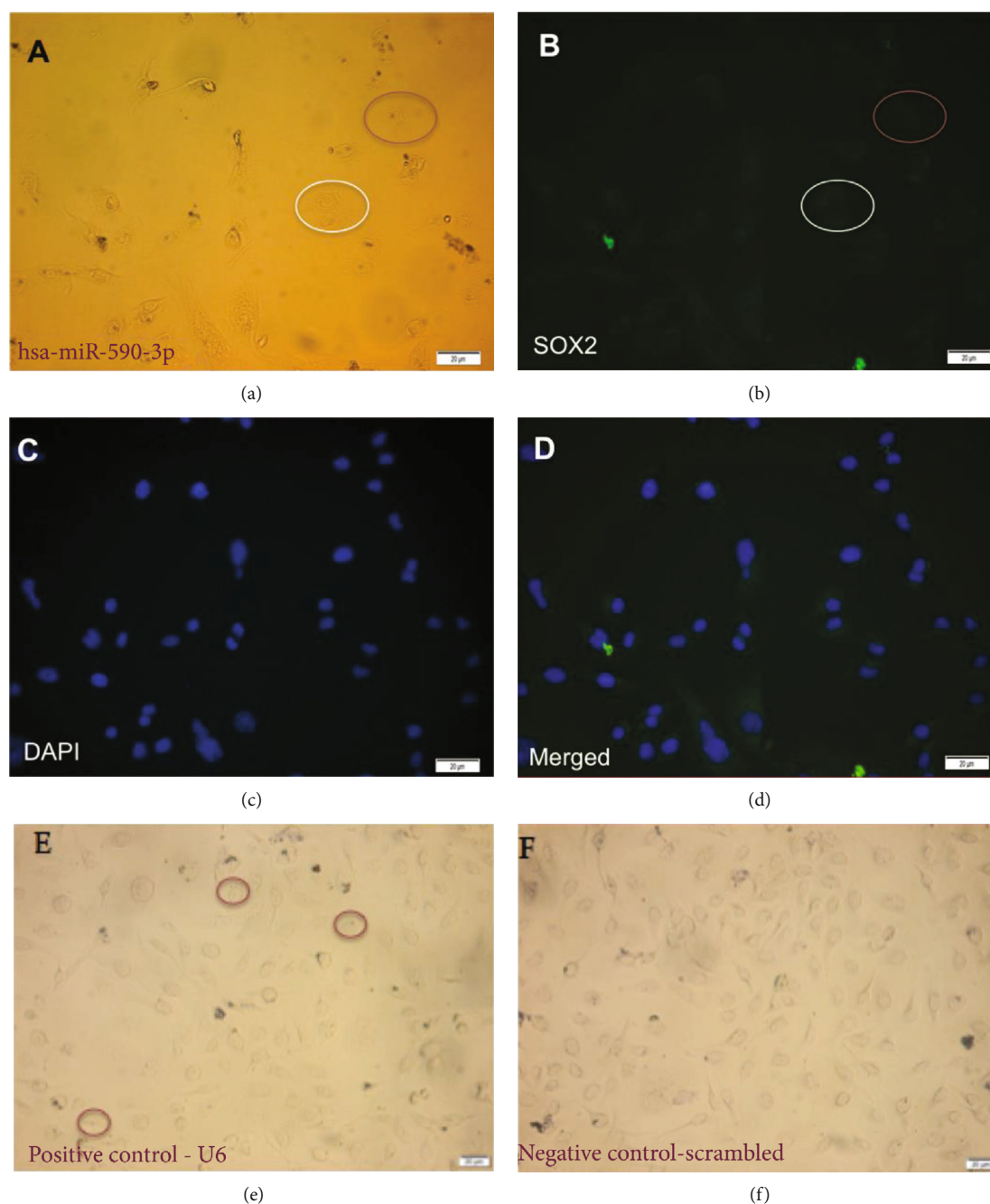


FIGURE 10: Expression and localization of hsa-miR-590-3p and SOX2 in SNU449 cells. (a) hsa-miR-590-3p signal in SNU449 cells under 20x magnification using ISH (red circle). (b) SOX2 fluorescent signal in SNU449 cells under 20x magnification using ICC (white circle). (c) DAPI staining of the nucleus. (d) Merged image of (b) and (c). (e) U6 signal SNU449 cells under 20x magnification using ISH as a positive control (red circles). (f) Negative control in SNU449 cells under 20x magnification using ISH using scrambled probes. Scale for (a)–(f): 20  $\mu\text{m}$ .

Versican (VCAN) is part of the aggrecan/versican proteoglycan family and a main component of the extracellular matrix. Its important role in tumor development through cell adhesion, proliferation, migration, invasion, and angiogenesis has been reported in several studies [30, 53].

Alignment of the mRNA of FOXA2 against hsa-miR-590-3p to assess the binding sites of our miRNA on its mRNA was carried out using miRanda-mirSVR (Figure 4(d)). FOXA2

and VCAN protein expression in HepG2 and SNU449 was assessed computationally using the Expression Atlas. FOXA2 protein expression is higher in HepG2 compared to SNU449 while VCAN protein expression is higher in SNU449 compared to HepG2 (Figure 5).

FOXA2 and VCAN mRNA expression were assessed in HepG2 and SNU449 using RT-PCR (Figure 9, Supplementary H6). No statistically significant change was observed

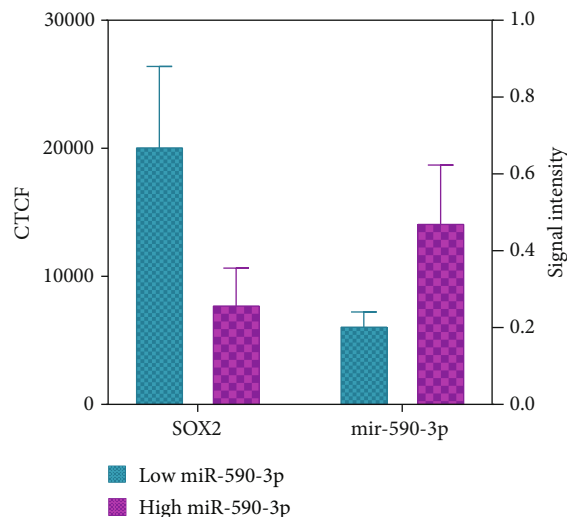


FIGURE 11: Graphical representation of the expression of hsa-miR-590-3p and SOX2 in SNU449 cells. The cell fluorescence of SOX2 and the signal intensity of hsa-miR-590-3p were assessed using ImageJ and compared using Prism GraphPad. Low-expressing hsa-miR-590-3p cells show increased SOX2-corrected total cell fluorescence (CTCF) compared to high-expressing hsa-miR-590-3p cells, which show low SOX2 CTCF. Results are a representation of three independent experiments.

among the mRNA levels of FOXA2 and VCAN in both cell lines.

**4.5. Potential Downstream Target Genes of miR-590-3p and Cell Stemness.** SOX2 also has been previously reported as a target of hsa-miR-590-3p in EOC [54]. SOX2, known as SRY (sex-determining region on the Y chromosome) box 2, is part of the SOX family and is important in reprogramming differentiated cells into induced pluripotent stem cells and maintaining cell self-renewal [55]. It was also reported to participate in oncogenesis and tumor progression of several cancers.

Alignment of the mRNA of SOX2 against hsa-miR-590-3p to assess the binding sites of our miRNA on its mRNA was carried out using miRanda-mirSVR (Figure 4(c)). SOX2 mRNA and protein expression were assessed in HepG2 and SNU449 using RT-PCR and western blotting, respectively (Figure 8, Supplementary H5). SNU449 showed higher mRNA expression than HepG2. Surprisingly, HepG2 and SNU449 showed comparable protein expression. Since HepG2 is an early-stage well-differentiated cell line, we expected that SOX2 protein levels in HepG2 would be lower than SNU449.

**4.6. Expression and Localization of hsa-miR-590-3p and SOX2.** The co-expression and co-localization of hsa-miR-590-3p in relation to one of its downstream target genes, SOX2, in SNU449 were carried out using ISH-ICC. A negative correlation between the hsa-miR-590-3p expression and the SOX2 expression was observed. Cells that showed hsa-miR-590-3p signal showed minimal SOX2 fluorescence (red circles, Figures 10 and 11), and in cells that did not show

hsa-miR-590-3p signal, SOX2 fluorescence was detected (white circles, Figures 10 and 11). These findings strongly suggest that SOX2 can be a direct downstream target gene of hsa-miR-590-3p in HCC. However, it remains to be determined whether the consequences of overexpressing hsa-miR-590-3p suppresses the expression of the 3'UTR of SOX2, utilizing the dual-luciferase reporter assay.

## 5. Conclusion

In conclusion, our study suggests that SOX2 can be a direct downstream target gene of hsa-miR-590-3p in HCC implying that hsa-miR-590-3p can directly affect the self-renewal and self-maintenance of cancer cells. We propose that CX3CL1, E-cadherin, N-cadherin, and FOXA2 show a lot of potential as downstream target genes of hsa-miR-590-3p signifying hsa-miR-590-3p's indirect effect on EMT and in turn cancer progression. Nevertheless, more studies are needed to further prove our work.

## Data Availability

The data used to support the findings of this study are included within the article and within the supplementary files.

## Conflicts of Interest

The authors declare that there is no conflict of interest regarding the publication of this paper.

## Acknowledgments

This research was funded by a research support grant received from the American University in Cairo.

## Supplementary Materials

Supplementary A: primers used in semiquantitative RT-PCR. Supplementary B: downstream target genes of hsa-miR-590-3p obtained from TargetScan. Supplementary C: downstream target genes of hsa-miR-590-3p obtained from miRDB. Supplementary D: downstream target genes of hsa-miR-590-3p obtained from miRTarBase. Supplementary E: downstream target genes of hsa-miR-590-3p obtained from Diana Tools. Supplementary F: pivot table. Supplementary G: the chosen functions of the potential downstream target genes of hsa-miR-590-3p obtained from FAME Software. Supplementary H1: mRNA expression of potential targets of hsa-miR-590-3p in HepG2 and SNU449 using RT-PCR. Supplementary H2: RT-PCR analysis for CX3CL1 mRNA expression in HepG2 and SNU449. Supplementary H3: RT-PCR analysis for E-cadherin, N-cadherin, and Vimentin mRNA expression in HepG2 and SNU449. Supplementary H4: membrane image for Vimentin protein expression in HepG2 and SNU449. Supplementary H5: SOX2 mRNA and protein expression in HepG2 and SNU449 using RT-PCR and western blotting. Supplementary H6: RT-PCR analysis for FOXA2 and VCAN mRNA expression in HepG2 and SNU449. (*Supplementary Materials*)

## References

- [1] World Health Organization, *Cancer*, 2018, January 20, 2019 <https://www.who.int/news-room/fact-sheets/detail/cancer>.
- [2] W. Ma, A. S. Soliman, W. A. Anwar et al., “Forecasted impacts of a sofosbuvir-based national hepatitis C treatment programme on Egypt’s hepatocellular cancer epidemic: simulation of alternatives,” *BMJ Global Health*, vol. 3, no. 2, p. e000572, 2018.
- [3] American Cancer Society, *Liver Cancer*, 2018, <https://www.cancer.org>.
- [4] Y. Ghouri, I. Mian, and J. Rowe, “Review of hepatocellular carcinoma: epidemiology, etiology, and carcinogenesis,” *Journal of Carcinogenesis*, vol. 16, 2017.
- [5] J. A. Marrero, M. Kudo, and J.-P. Bronowicki, “The challenge of prognosis and staging for hepatocellular carcinoma,” *Oncologist*, vol. 15, Supplement 4, pp. 23–33, 2010.
- [6] R. N. Aravalli, E. N. K. Cressman, and C. J. Steer, “Cellular and molecular mechanisms of hepatocellular carcinoma: an update,” *Archives of Toxicology*, vol. 87, no. 2, pp. 227–247, 2013.
- [7] M. Kumar, X. Zhao, and X. W. Wang, “Molecular carcinogenesis of hepatocellular carcinoma and intrahepatic cholangiocarcinoma: one step closer to personalized medicine?,” *Cell & Bioscience*, vol. 1, no. 1, pp. 1–13, 2011.
- [8] S. Patrick Nana-Sinkam and CMC, “MicroRNAs as therapeutic targets in cancer,” *Translational Research*, vol. 157, no. 4, pp. 216–225, 2011.
- [9] M. Abba, N. Patil, and H. Allgayer, “MicroRNAs in the regulation of MMPs and metastasis,” *Cancers*, vol. 6, no. 2, pp. 625–645, 2014.
- [10] A. Kozomara and S. Griffiths-Jones, “MiRBase: annotating high confidence microRNAs using deep sequencing data,” *Nucleic Acids Research*, vol. 42, no. D1, pp. D68–D73, 2014.
- [11] A. L. Gartel and E. S. Kandel, “miRNAs: little known mediators of oncogenesis,” *Seminars in Cancer Biology*, vol. 18, no. 2, pp. 103–110, 2008.
- [12] V. Agarwal, G. W. Bell, J. W. Nam, and D. P. Bartel, “Predicting effective microRNA target sites in mammalian mRNAs,” *eLife*, vol. 4, 2015.
- [13] D. Betel, A. Koppal, P. Agius, C. Sander, and C. Leslie, “Comprehensive modeling of microRNA targets predicts functional non-conserved and non-canonical sites,” *Genome Biology*, vol. 11, no. 8, 2010.
- [14] N. Wong and X. Wang, “miRDB: an online resource for microRNA target prediction and functional annotations,” *Nucleic Acids Research*, vol. 43, no. D1, pp. D146–D152, 2015.
- [15] C.-H. Chou, S. Shrestha, C.-D. Yang et al., “MiRTarBase update 2018: a resource for experimentally validated microRNA-target interactions,” *Nucleic Acids Research*, vol. 46, no. D1, pp. D296–D302, 2018.
- [16] M. D. Paraskevopoulou, G. Georgakilas, N. Kostoulas et al., “DIANA-LncBase: experimentally verified and computationally predicted microRNA targets on long non-coding RNAs,” *Nucleic Acids Research*, vol. 41, no. D1, pp. D239–D245, 2013.
- [17] I. Ulitsky, L. C. Laurent, and R. Shamir, “Towards computational prediction of microRNA function and activity,” *Nucleic Acids Research*, vol. 38, no. 15, pp. e160–e160, 2010.
- [18] P. J. Thul, L. Åkesson, M. Wiking et al., “A subcellular map of the human proteome,” *Science*, vol. 356, no. 6340, p. eaal3321, 2017.
- [19] I. Papatheodorou, N. A. Fonseca, M. Keays et al., “Expression atlas: gene and protein expression across multiple studies and organisms,” *Nucleic Acids Research*, vol. 46, no. D1, pp. D246–D251, 2018.
- [20] A. Untergasser, I. Cutcutache, T. Koressaar et al., “Primer3—new capabilities and interfaces,” *Nucleic Acids Research*, vol. 40, no. 15, pp. e115–e115, 2012.
- [21] J. Schindelin, I. Arganda-Carreras, E. Frise et al., “Fiji: an open-source platform for biological-image analysis,” *Nature Methods*, vol. 9, no. 7, pp. 676–682, 2012.
- [22] H. Motulsky, *Analyzing Data with GraphPad Prism*, GraphPad Software Incorporated, 1999.
- [23] B. P. Lewis, C. B. Burge, and D. P. Bartel, “Conserved seed pairing, often flanked by adenosines, indicates that thousands of human genes are microRNA targets,” *Cell*, vol. 120, no. 1, pp. 15–20, 2005.
- [24] X. Wang, “Improving microRNA target prediction by modeling with unambiguously identified microRNA-target pairs from CLIP-ligation studies,” *Bioinformatics*, vol. 32, no. 9, pp. 1316–1322, 2016.
- [25] J. Wittmann and H. M. Jäck, “Serum microRNAs as powerful cancer biomarkers,” *Biochimica et Biophysica Acta (BBA) - Reviews on Cancer*, vol. 1806, no. 2, pp. 200–207, 2010.
- [26] T. A. Kerr, K. M. Korenblat, and N. O. Davidson, “MicroRNAs and liver disease,” *Translational Research*, vol. 157, no. 4, pp. 241–252, 2011.
- [27] Y. Yamamoto, N. Kosaka, M. Tanaka et al., “MicroRNA-500 as a potential diagnostic marker for hepatocellular carcinoma,” *Biomarkers*, vol. 14, no. 7, pp. 529–538, 2009.
- [28] K. Takahashi, I. Yan, H. J. Wen, and T. Patel, “MicroRNAs in liver disease: from diagnostics to therapeutics,” *Clinical Biochemistry*, vol. 46, no. 10–11, pp. 946–952, 2013.
- [29] H. Pang, Y. Zheng, Y. Zhao, X. Xiu, and J. Wang, “miR-590-3p suppresses cancer cell migration, invasion and epithelial–mesenchymal transition in glioblastoma multiforme by targeting ZEB1 and ZEB2,” *Biochemical and Biophysical Research Communications*, vol. 468, no. 4, pp. 739–745, 2015.
- [30] M. Salem, J. A. O’Brien, S. Bernaudo et al., “miR-590-3p promotes ovarian cancer growth and metastasis via a novel FOXA2–versican pathway,” *Cancer Research*, vol. 78, no. 15, pp. 4175–4190, 2018.
- [31] X. Ge and L. Gong, “MiR-590-3p suppresses hepatocellular carcinoma growth by targeting TEAD1,” *Tumor Biology*, vol. 39, no. 3, p. 101042831769594, 2017.
- [32] Y. Hongfei, Z. Wenhong, Z. Wentao, G. Chunyan, and A. Jing, “Roles of miR-590-5p and miR-590-3p in the development of hepatocellular carcinoma,” *Journal of Southern Medical University*, vol. 33, no. 6, pp. 804–811, 2013.
- [33] M. S. Kim, E. G. Jeong, C. H. Ahn, S. S. Kim, S. H. Lee, and N. J. Yoo, “Frameshift mutation of UVRAG, an autophagy-related gene, in gastric carcinomas with microsatellite instability,” *Human Pathology*, vol. 39, no. 7, pp. 1059–1063, 2008.
- [34] J. Torres-Rosell, F. Machín, S. Farmer et al., “SMC5 and SMC6 genes are required for the segregation of repetitive chromosome regions,” *Nature Cell Biology*, vol. 7, no. 4, pp. 412–419, 2005.
- [35] N. P. Taylor, M. A. Powell, R. K. Gibb et al., “MLH3 mutation in endometrial cancer,” *Cancer Research*, vol. 66, no. 15, pp. 7502–7508, 2006.
- [36] G. Narayan, H. Arias-Pulido, S. V. Nandula et al., “Promoter hypermethylation of FANCF: disruption of Fanconi anemia-

- BRCA pathway in cervical cancer,” *Cancer Research*, vol. 64, no. 9, pp. 2994–2997, 2004.
- [37] G. Yamamoto, T. Irie, T. Aida, Y. Nagoshi, R. Tsuchiya, and T. Tachikawa, “Correlation of invasion and metastasis of cancer cells, and expression of the RAD21 gene in oral squamous cell carcinoma,” *Virchows Archiv*, vol. 448, no. 4, pp. 435–441, 2006.
- [38] L. J. Monteiro, P. Khongkow, M. Kongsema et al., “The Forkhead box M1 protein regulates BRIP1 expression and DNA damage repair in epirubicin treatment,” *Oncogene*, vol. 32, no. 39, pp. 4634–4645, 2013.
- [39] H. Yan, K. Hu, W. Wu et al., “Low expression of DYRK2 (dual specificity tyrosine phosphorylation regulated kinase 2) correlates with poor prognosis in colorectal cancer,” *PLoS One*, vol. 11, no. 8, pp. 1–19, 2016.
- [40] D. Sombroek and T. G. Hofmann, “How cells switch HIPK2 on and off,” *Cell Death and Differentiation*, vol. 16, no. 2, pp. 187–194, 2009.
- [41] H. Wang, T. Wang, H. Guo et al., “Association analysis of ERCC5 gene polymorphisms with risk of breast cancer in Han women of Northwest China,” *Breast Cancer*, vol. 23, no. 3, pp. 479–485, 2016.
- [42] S. Ma, J. Huang, and M. S. Moran, “Identification of genes associated with multiple cancers via integrative analysis,” *BMC Genomics*, vol. 10, pp. 1–11, 2009.
- [43] I. Sakabe, R. Hu, L. Jin, R. Clarke, and U. N. Kasid, “TMEM33: a new stress-inducible endoplasmic reticulum transmembrane protein and modulator of the unfolded protein response signaling,” *Breast Cancer Research and Treatment*, vol. 153, no. 2, pp. 285–297, 2015.
- [44] A. L. Cavatorta, A. Di Gregorio, M. B. Valdano et al., “DLG1 polarity protein expression associates with the disease progress of low-grade cervical intraepithelial lesions,” *Experimental and Molecular Pathology*, vol. 102, no. 1, pp. 65–69, 2017.
- [45] R. Snoek, J. van Setten, B. J. Keating et al., “NPHP1 (nephrocystin-1) gene deletions cause adult-onset ESRD,” *Journal of the American Society of Nephrology*, vol. 29, no. 6, pp. 1772–1779, 2018.
- [46] F. Gaudin, S. Nasreddine, A.-C. Donnadieu et al., “Identification of the chemokine CX3CL1 as a new regulator of malignant cell proliferation in epithelial ovarian cancer,” *PLoS One*, vol. 6, no. 7, 2011.
- [47] S. Nakajima, R. Doi, and E. Toyoda, “N-cadherin expression and epithelial-mesenchymal transition in pancreatic carcinoma,” *Clinical Cancer Research*, vol. 10, pp. 4125–4133, 2004.
- [48] A. Khorram-Manesh, H. Ahlman, S. Jansson, and O. Nilsson, “N-cadherin expression in adrenal tumors: upregulation in malignant pheochromocytoma and downregulation in adrenocortical carcinoma,” *Endocrine Pathology*, vol. 13, pp. 99–110, 2002.
- [49] L. Zheng, M. Xu, J. Xu et al., “ELF3 promotes epithelial–mesenchymal transition by protecting ZEB1 from miR-141-3p-mediated silencing in hepatocellular carcinoma,” *Cell Death & Disease*, vol. 9, no. 3, 2018.
- [50] S. E. Harvey and C. Cheng, “Long non-coding RNAs,” in *Methods in Molecular Biology*, vol. 1402, pp. 229–241, 2016.
- [51] D. D. O. Martin, C. Kay, J. A. Collins, Y. T. Nguyen, R. A. Slama, and M. R. Hayden, “A human huntingtin SNP alters post-translational modification and pathogenic proteolysis of the protein causing Huntington disease,” *Scientific Reports*, vol. 8, no. 1, pp. 1–8, 2018.
- [52] J. Wang, C.-P. Zhu, P.-F. Hu et al., “FOXA2 suppresses the metastasis of hepatocellular carcinoma partially through matrix metalloproteinase-9 inhibition,” *Carcinogenesis*, vol. 35, no. 11, pp. 2576–2583, 2014.
- [53] Z. Sun, H. Gao, G. Junjie, Y. Cheng, and C. B. Yuanjia Chen, “The expression of versican and its role in pancreatic neuroendocrine tumors,” *J Clin Oncol*, vol. 36, no. 4, pp. 254–254, 2018.
- [54] H. Shawer, *The Expression Pattern of Circulating miR-590-3p as a Promising Diagnostic Biomarker for Early Detection of Epithelial Ovarian Cancer*, The American University in Cairo, Digital Archive and Research Repository (AUC DAR), 2016, <http://dar.aucegypt.edu/handle/10526/4631>.
- [55] C. Sun, L. Sun, Y. Li, X. Kang, S. Zhang, and Y. Liu, “Sox2 expression predicts poor survival of hepatocellular carcinoma patients and it promotes liver cancer cell invasion by activating Slug,” *Medical Oncology*, vol. 30, no. 2, 2013.

## Review Article

# The Combination Strategy of Transarterial Chemoembolization and Radiofrequency Ablation or Microwave Ablation against Hepatocellular Carcinoma

Zhentian Xu <sup>1,2</sup>, Haiyang Xie <sup>1,2</sup>, Lin Zhou <sup>1,2</sup>, Xinhua Chen <sup>1,2</sup>  
and Shusen Zheng <sup>1,2</sup>

<sup>1</sup>Division of Hepatobiliary and Pancreatic Surgery, Department of Surgery First Affiliated Hospital, School of Medicine, Zhejiang University, NHFPC Key Laboratory of Combined Multi-Organ Transplantation, Key Laboratory of the Diagnosis and Treatment of Organ Transplantation, CAMS, Key Laboratory of Organ Transplantation, Zhejiang Province, Hangzhou 310003, China

<sup>2</sup>Collaborative Innovation Center for Diagnosis Treatment of Infectious Diseases, China

Correspondence should be addressed to Shusen Zheng; [shusenzheng@zju.edu.cn](mailto:shusenzheng@zju.edu.cn)

Received 19 December 2018; Revised 23 June 2019; Accepted 7 August 2019; Published 26 August 2019

Academic Editor: Consuelo Amantini

Copyright © 2019 Zhentian Xu et al. This is an open access article distributed under the Creative Commons Attribution License, which permits unrestricted use, distribution, and reproduction in any medium, provided the original work is properly cited.

Hepatocellular carcinoma (HCC) is the most common primary cancer of the liver. Hepatectomy and liver transplantation (LT) are regarded as the radical treatment, but great majority of patients are already in advanced stage on the first diagnosis and lose the surgery opportunity. Multifarious image-guided interventional therapies, termed as locoregional ablations, are recommended by various HCC guidelines for the clinical practice. Transarterial chemoembolization (TACE) is firstly recommended for intermediate-stage (Barcelona Clinic Liver Cancer (BCLC) B class) HCC but has lower necrosis rates. Radiofrequency ablation (RFA) is effective in treating HCCs smaller than 3 cm in size. Microwave ablation (MWA) can ablate larger tumor within a shorter time. Combination of TACE with RFA or MWA is effective and promising in treating larger HCC lesions but needs more clinical data to confirm its long-term outcome. The combination of TACE and RFA or MWA against hepatocellular carcinoma needs more clinical data for a better strategy. The characters and advantages of TACE, RFA, MWA, and TACE combined with RFA or MWA are reviewed to provide physician a better background on decision.

## 1. Introduction

Liver cancer is estimated to be ranked sixth on most currently diagnosed cancer as well as the fourth main reason of cancer death with about 841,000 new cases and 782,000 deaths occurred in 2018 worldwide [1]. Hepatocellular carcinoma (HCC) is the most common type of primary liver neoplasm and also one of the most common malignant tumors in the world [2, 3].

Surgeries including hepatectomy along with liver transplantation are curative potential treatments [4]. Unfortunately, less than 20% of patients are appropriate candidates for surgical resection and liver transplantation [4]. Systemic chemotherapy has not revealed beneficial on the survival rates of advanced HCC in the event of no valid treatment

options until sorafenib was used as the targeted molecular remedy [5].

Locoregional therapies include transarterial chemoembolization (TACE), percutaneous ethanol injection (PEI), radiofrequency ablation (RFA), microwave ablation (MWA), cryoablation (CA), laser ablation, high-intensity focused ultrasound (HIFU), and irreversible electroporation (IRE) [2, 6]. Multifarious image-guided interventions now play a key role in treating HCC [7]. TACE is recommended as the first-line therapy for BCLC stage B HCC based on the Barcelona Clinic Liver Cancer (BCLC) guidelines. However, the necrosis rate of tumor cells is low and the intrahepatic recurrence rate of HCC is high using TACE alone [8]. Percutaneous thermal ablation is regarded as the optimum locoregional therapy choice for focal unresectable early-

Reference: Lurje et al. [2]

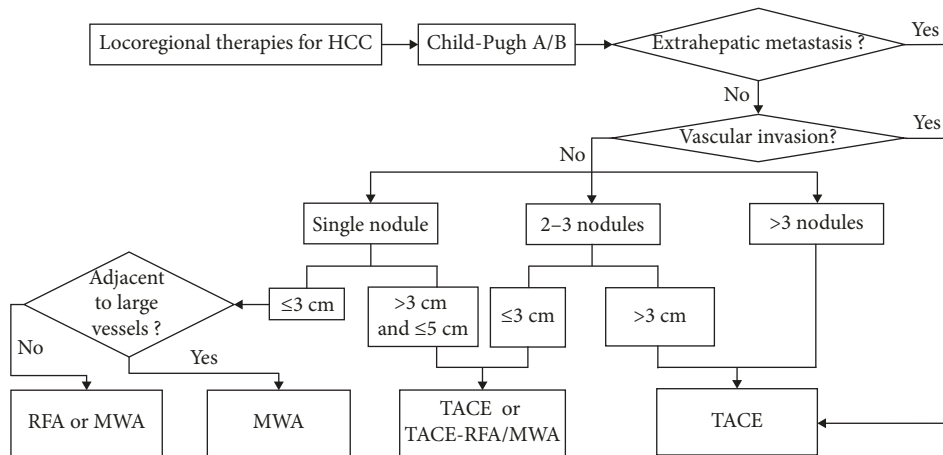


FIGURE 1: Locoregional therapies for HCC.

stage HCC [7]. Radiofrequency ablation and microwave ablation are important two types of ablative treatments. Furthermore, researchers have revealed that combined therapy was an effective selection on the therapy of patients with early or intermediate HCC at the moment of resection not being viable [9]. In this article, the profiles of TACE, RFA, MWA, and combination of TACE with RFA or MWA are reviewed based on the clinical data. Moreover, we provide some suggestions for locoregional therapies for HCC in Figure 1 on the basis of clinical data.

## 2. Transarterial Chemoembolization

Transarterial chemoembolization (TACE) is one kind of the arterially directed treatment methods currently besides transarterial embolization (TAE) and TACE with drug-eluting beads (DEB-TACE) [10]. It is the first-line applied therapy for patients with HCC in intermediate stage including unresectable, large, or multiple focal nodules without vascular involvement or extrahepatic metastasis [11]. TACE is confirmed effective by clinical trials and a meta-analysis [12]. Camma et al. [13] revealed that the overall 2-year mortality rate was obviously reduced in the TACE group than in the untreated group (OR, 0.54; 95% CI: 0.33, 0.89;  $P = 0.015$ ) in a meta-analysis of 18 RCTs. TACE, a standard minimally invasive therapy, is aimed at delivering specific chemical with lipiodol mainly into the tumor area to result in necrosis and controlling the growth of tumor cells and to reduce the toxicity of chemotherapy of normal tissues [14]. The common regimens of TACE are cisplatin, mitomycin, doxorubicin, and epirubicin [15, 16]. The investigation conducted by Liu et al. [17] found that combination of chemotherapeutic regimens might improve survival rates as well as tumor response rates; gemcitabine seemed to be helpful to ameliorate the prognosis of HCC patients. However, at the moment of causing necrosis of tumor tissues by TACE, angiogenic factors like EGF and insulin-like growth factor 2 also increase; antiangiogenic drugs may be suggested in TACE-treated HCC [18].

Doxorubicin-eluting bead TACE (DEB-TACE) is a newly developed method based on conventional TACE (cTACE). A meta-analysis of seven studies (693 patients in total) compared DEB-TACE with cTACE [19]. It discovered that the pooled estimates for tumor response of DEB-TACE showed no difference compared with cTACE. Therefore, it indicated that DEB-TACE accomplishes the same as cTACE in tumor response. Interestingly, Zou et al. [20] concluded that DEB-TACE was superior to cTACE for higher complete response rates and overall survival rates for HCC patients.

As we have mentioned above, TACE used only leads to a low necrosis rate but a high intrahepatic recurrence rate of HCC. TACE can increase the risk of liver function failure especially in patients with Child-Pugh B cirrhosis because it can damage the liver parenchyma and the hepatic artery. Thus, Child-Pugh C liver function is mainly regarded as a contraindication for TACE [21, 22].

## 3. Radiofrequency Ablation

Radiofrequency ablation (RFA) was firstly applied for HCC patient in 1993 based on electromagnetic energy [23, 24]. An electrical current within the radiofrequency range is released through a needle electrode guided by imaging methods resulting in heat-based thermal cytotoxicity in RFA [25]. The creation and completion of an integrated electrical circuit are by means of finding the ground, generally a foil pad adhered to the thighs or back of patients [24]. Resistance encircling the electrodes produces heat with the temperatures ranging between 60°C and 100°C; the heat can cause almost instantaneous coagulation necrosis [24]. HCC tends to occur in the cirrhotic liver and often has its pseudocapsule; the cirrhotic liver along with pseudocapsule can serve as thermal insulators that lead to higher peak temperatures and prolong the time of cytotoxic temperatures. This is the so-called “oven effect” that makes RFA better efficiency in HCC than in hepatic metastases [26].

Usually, RFA can eliminate nodules no more than 3 cm in size, but if larger than 4 cm, it is not considered much effective [27]. In RFA, a solitary inserted electrode can cause

necrosis of an area with the diameter equal to or less than 3.0 cm therefore ablating a 2 cm tumor completely [28]. A 0.5-1.0 cm safety margin of nontumor liver tissue is ablated to make sure that not only the peripheral tumor but also any microscopic extension are included [29]. According to the analysis conducted by Livraghi et al. [28], a complete necrosis of lesions up to 2 cm was achieved 90% with a locoregional recurrence rate of 1% and the estimable 3-year and 5-year survival rates were 76% and 55%, respectively, whereas another trial conducted by Livraghi et al. [30] included 80 HCCs with the tumors 3.1-5 cm in diameter (medium-sized tumors) and 46 HCCs with the tumors 5.1-9.5 cm in diameter (large-sized tumors) found that the complete necrosis (defined as 100% necrosis) was 61% in the medium-sized tumor group and 24% in the large-sized tumor group ( $P = 0.001$ ). It reveals that RFA is perhaps an effective method in treating HCC lesions 3.1 cm or larger in diameter.

The efficacy of RFA is confined due to the diameter and location of tumor. RFA may cause inadequate ablation of perivascular tumor tissues because of the “heat-sink effect.” It is a phenomenon occurring as the energy disperses from the target lesion because of the blood flow. Thus, these tumor nodules near large vessels (>3 mm) should take modified treatment strategies to increase the success rate of therapy [31].

#### 4. Microwave Ablation

Microwave ablation (MWA) is another type of ablation methodology using electromagnetic energy [24]. It was originated in the 1980s and 1990s [32]. MWA has become increasingly popular for its low cost and high ablation rate [33]. The high frequency electromagnetic energy (>900 MHz, generally 2450 MHz) is applied in MWA, leading dipole molecules, mainly water molecules, to continuous rotation in the oscillating electric field of microwave [34]. The drastic motion of dipoles produce frictional heat and cause coagulation necrosis in the target ablation zone [35].

MWA has several theoretical advantages in contrast of RFA. MWA can be applied for treating HCC in the patients with materials such as pacemaker or surgical clips in the body because complete electrical circuit is not requisite and grounding pads are not necessary [4]. Microwaves can reach a higher temperature in a shorter time and can generate a larger ablation area; MWA allows synergistic tissue heating of large or multifocal tumors because the machine can activate multiple antennae simultaneously [36]. Shorter treating time reducing the pain for patients is thought to be beneficial [37]. In addition, the heat-sink effect is attenuated, making MWA feasible in ablating the tumors that are adjacent to large vessels [37].

With the improvement of antennae and therapy strategies, MWA expands the ablation zone and can treat tumor of 5-8 cm in diameter [38]. MWA is now regarded as a curative treatment for the patients with very early stage HCC defined by the BCLC stage system with limited metastases. MWA is also a palliative therapy for HCC patients in BCLC

B or C stage or inappropriate for other methods [38]. A multicenter study from China reported that 1-, 3-, and 5-year survival rates of 1007 patients with primary hepatic cancer treated by MWA were 91.2%, 72.5%, and 59.8%, respectively [39]. Another study conducted by Dong et al. [40] analyzed 234 HCC patients treated by MWA (mean tumor size,  $4.1 \pm 1.9$  cm) and found that the 1-, 3-, and 5-year cumulative survival rates of patients were 92.70%, 72.85%, and 56.70%, respectively.

However, MWA may cause thermal injury [4]. Multiple antennae activated simultaneously may increase the range of treating zone whereas the interantenna distance may not be wholly covered and lead to incomplete ablation of the large tumor [4]. And a defect of MWA is high local development of tumor which may be caused by a larger applicator (5 mm in diameter) applied for tumor puncture increasing the risk of bleeding and subsequent tumor seeding [41].

#### 5. Combination of Transarterial Chemoembolization and Radiofrequency Ablation

As mentioned above, RFA is feasible for small HCC because of its high complete ablation rate, but it is not recommended for larger lesions. Lesions adjacent to a large vessel (>3 mm) may not perform a complete necrosis owing to the so-called “heat-sink effect” [31]. Lessening or dispelling blood flow to restrain heat loss was confirmed to be capable of increasing the ablation volume [42]. In most studies, TACE has only achieved the complete necrosis rate of 10%-20% with the 1-, 3-, and 5-year overall survival rates at 49%-71.9%, 23%-62.5%, and 9%-17% [43]. Both of them have their own limitations. TACE followed by RFA has been more widely applied in recent years. The heat-sink effect of blood flow is reduced by lessening liver arterial flow after TACE procedure; meanwhile, the necrotizing effect of RFA treatment is increased in a tumor level. In addition, the zone of tumor necrosis in the treatment process of RFA is anticipated to be enlarged for the reason that ischemia and inflammation after TACE inducing the oedematous change [9].

Current clinical data reveal that TACE combined with RFA is superior to the single use of RFA or TACE alone in inducing higher complete necrosis and increasing overall survival rates [9]. The study conducted by Liu et al. [44] divided 88 patients into two groups (TACE group, TACE-RFA group); they found that the complete necrosis rates (CR) of the single TACE group and the TACE-RFA group were 27.9% (12/43) and 83.2% (37/45), respectively. Cao et al. [45] found that TACE-RFA was better than TACE used alone in 1-, 2-, and 3-year overall survival rates ( $OR_{1-year} = 3.98$ , 95% CI: 2.87-5.51,  $P < 0.00001$ ;  $OR_{2-year} = 3.03$ , 95% CI: 2.10-4.38,  $P < 0.00001$ ;  $OR_{3-year} = 7.02$ , 95% CI: 4.14-11.92,  $P < 0.00001$ ). A meta-analysis conducted by Ni et al. [43] suggested that combination of RFA and TACE had apparently higher overall survival rates and recurrence-free survival rates than RFA alone. Furthermore, Peng et al. [46] found that TACE-RFA treatment is superior to RFA used alone

TABLE 1: Comparison of clinical studies in patients with HCC for radiofrequency ablation or microwave ablation.

References	Methods	Patients	Lesions	Mean age (years)	Size (cm)	Complete ablation rates (%)	Local recurrence rates (%)	Overall survival rates		
								1 yr (%)	3 yr (%)	5 yr (%)
Livraghi et al. [28]	RFA	218	—	68	$\leq 2.0$	98.1	0.9	—	76	55
Livraghi et al. [30]	RFA	114	126	64.4	5.4 (mean)	47.6	—	—	—	—
Liang et al. [39]	MWA	1007	1363	56.3	1.0-18.5 2.1 $\pm$ 1.8 (mean)	97.1 <sup>a</sup>	5.9	91.2	72.5	59.8
Dong et al. [40]	MWA	234	339	54.8 $\pm$ 11.4	1.2-8.0 4.1 $\pm$ 1.9 (mean)	92.0 (US) <sup>b</sup>	7.3	92.7 <sup>c</sup>	72.85 <sup>c</sup>	56.7 <sup>c</sup>

<sup>a</sup>Technique effectiveness; <sup>b</sup>color Doppler flow signals disappeared in 92.0% (263/286) of the lesions; <sup>c</sup>cumulative survival rates.

TABLE 2: The efficacy of combination of TACE with RFA or MWA vs. monotherapy.

References	Methods	Patients	Age (years)	Size (cm)	Response rates (%)	Overall survival (OS) rates (%)				OS P value
						0.5 yr	1 yr	1.5 yr	2 yr	
Liu et al. [44]	TACE	43	44-78	5-14	67.4	—	—	—	—	0.081
	TACE-RFA	45	45-75	4-15	91.1	—	—	—	—	
Peng et al. [46]	RFA	95	55.3 $\pm$ 13.3	3.39 $\pm$ 1.35	96.8	—	66.6	—	—	0.002
	TACE-RFA	94	53.3 $\pm$ 11.0	3.47 $\pm$ 1.44	96.8	—	92.6	—	—	
Liu et al. [50]	TACE	18	51.9 $\pm$ 13.6	6.7 $\pm$ 1.5	38.9	50	11.1	0	0	0.003
	TACE-MWA	16	52.1 $\pm$ 14.5	6.8 $\pm$ 1.5	87.5	75	33.3	18.7	6.25	
Chen et al. [51]	TACE	96	59.7 $\pm$ 10.5	2.88 $\pm$ 1.25	46.3	96.9	87.2	81.1	77	0.317
	TACE-MWA	48	58.8 $\pm$ 9.6	2.74 $\pm$ 1.09	92.1	100	91.7	88.5	88.5	
Zheng et al. [52]	TACE	166	54.6 $\pm$ 10.5	8.5 $\pm$ 2.5	55.4	—	59	—	40.4	<0.001
	TACE-MWA	92	53.3 $\pm$ 8.2	9.1 $\pm$ 2.8	81.5	—	85.9	—	59.8	

in overall survival and recurrence-free survival. TACE combined with RFA is considered a secure and efficient choice treating HCC patients despite not all the studies draw the same conclusion. However, TACE combined with RFA has no advantage for small lesions less than 3 cm, perhaps for the reason that RFA can reach complete necrosis alone making the TACE adding to RFA a superfluous way [9].

## 6. Combination of Transarterial Chemoembolization and Microwave Ablation

MWA has the advantage over RFA in ablating larger HCC lesions; nevertheless, it is also affected by the cooling effect more or less. Just like combining with RFA, TACE has its special superiority in attenuating heat loss by convection and leading to tissue necrosis and inflammatory edema by reducing local blood supply of tumor lesion [47, 48]. TACE selectively deliver the chemotherapeutics to targeted tumor, and the precaution of ischemic necrosis of the rest liver is realized [49]. Many factors confine the applying of TACE like size of tumors, incomplete ability eliminating tumor cells, local recurrence, and distant metastasis of remaining viable HCC cells [50].

Combination of TACE and MWA is another popular choice of interventional therapy and is confirmed effective.

Many studies adopt MWA performed 2-4 weeks after TACE [50, 51]. Chen et al. [51] analyzed the data of 244 patients with HCC treated by TACE-MWA or TACE alone and found that the complete ablative rate in the TACE-MWA group was 92.1% and the TACE only group was 46.3% ( $P < 0.001$ ), and they concluded that TACE-MWA led to better responses for HCC tumors  $\leq 5$  cm compared with the TACE group. Liu et al. [50] came into a conclusion that combination of MWA and TACE seemed to be a valid and potential modality in treating larger unresectable hepatocellular carcinoma based on their study. They chose 34 consecutive patients with large unresectable HCCs ( $>5$  cm) and divided them into the TACE group and the TACE-MWA group. The reduction in tumor size was 61.7%, and the survival rate in the TACE-MWA group was observably higher than the TACE group ( $P < 0.003$ ). A retrospective study conducted by Zheng et al. [52] involves 258 patients with a large solitary nodule or multinodular HCCs ( $\leq 10$  nodules). They were treated by TACE-MWA ( $n = 92$ ) or TACE alone ( $n = 166$ ). The 1-, 2-, and 3-year overall survival (OS) rates were 85.9%, 59.8%, and 32.6% in the TACE-MWA group and 59.0%, 40.4%, and 11.4% in the TACE group, respectively ( $P < 0.001$ ). The corresponding recurrence rates were 47.8%, 78.3%, and 94.6% in the TACE-MWA group and 74.7%, 96.4%, and 97.6% of that in the TACE group, respectively ( $P < 0.001$ ).

## 7. Conclusion

Interventional therapies are appealing and confirmed to be beneficial for patients with HCCs. TACE combines with RFA or MWA is a better choice because of the specialty of TACE in reducing or preventing blood flow. As shown in Table 1, RFA and MWA present their advantages. RFA ablates HCC nodules in small sizes with lower local recurrence rates. Meanwhile, MWA does better on ablating whether small or large nodules but has higher local recurrence rates than RFA. Combination of RFA and TACE makes up the drawbacks using RFA alone. Many studies also reveal the efficacy of MWA combined with TACE, but more clinical data should be analyzed. Preliminary data in Table 2 has told us that combination therapy tend to be more effective than monotherapy. The study conducted by Abdelaziz et al. [49] showed that TACE-MWA tended to be higher complete response rates than TACE-RFA compared with TACE-RFA ( $P = 0.06$ ) and resulted in better complete response rates with lesions 3-5 cm ( $P = 0.01$ ) but had no difference in survival rates in treating HCC tumors.

## 8. Summary

RFA and MWA play a critical role for HCC. It is worth mentioning that TACE combined with either RFA or MWA is effective and promising in treating larger HCC lesions as preliminary data have proved. More clinical data need to be well analyzed to provide clinician better strategies in treating HCC.

## Abbreviations

BCLC:	Barcelona Clinic Liver Cancer
CA:	Cryoablation
cTACE:	Conventional transarterial chemoembolization
DEB-TACE:	Doxorubicin-eluting bead transarterial chemoembolization
HCC:	Hepatocellular carcinoma
HIFU:	High-intensity focused ultrasound
IRE:	Irreversible electroporation
LT:	Liver transplantation
MELD:	Mayor model for end stage liver disease
MWA:	Microwave ablation
RFA:	Radiofrequency ablation
TACE:	Transarterial chemoembolization
TAE:	Transarterial embolization.

## Conflicts of Interest

The authors declare no competing interests.

## Acknowledgments

The study was supported by the National S&T Major Project of China (2018ZX10301201), Innovative Research Groups of the National Natural Science Foundation of China (No. 81721091), Major Program of National Natural Science Foundation of China (No. 91542205), National S&T Major Project (No. 2017ZX10203205), and Zhejiang

International Science and Technology Cooperation Project (No. 2016C04003).

## References

- [1] F. Bray, J. Ferlay, I. Soerjomataram, R. L. Siegel, L. A. Torre, and A. Jemal, "Global cancer statistics 2018: GLOBOCAN estimates of incidence and mortality worldwide for 36 cancers in 185 countries," *CA: A Cancer Journal for Clinicians*, vol. 68, no. 6, pp. 394–424, 2018.
- [2] I. Lurje, Z. Czigany, J. Bednarsch et al., "Treatment strategies for hepatocellular carcinoma—a multidisciplinary approach," *International Journal of Molecular Sciences*, vol. 20, no. 6, p. 1465, 2019.
- [3] C. Bosetti, F. Turati, and C. La Vecchia, "Hepatocellular carcinoma epidemiology," *Best Practice & Research Clinical Gastroenterology*, vol. 28, no. 5, pp. 753–770, 2014.
- [4] L. S. Poulou, E. Botsa, I. Thanou, P. D. Ziakas, and L. Thanos, "Percutaneous microwave ablation vs radiofrequency ablation in the treatment of hepatocellular carcinoma," *World Journal of Hepatology*, vol. 7, no. 8, pp. 1054–1063, 2015.
- [5] K. W. Kim, J. M. Lee, and B. I. Choi, "Assessment of the treatment response of HCC," *Abdominal Imaging*, vol. 36, no. 3, pp. 300–314, 2011.
- [6] C. W. Bailey and M. K. Sydnor Jr., "Current state of tumor ablation therapies," *Digestive Diseases and Sciences*, vol. 64, no. 4, pp. 951–958, 2019.
- [7] N. Molla, N. Almenieir, E. Simoneau et al., "The role of interventional radiology in the management of hepatocellular carcinoma," *Current Oncology*, vol. 21, no. 3, pp. 480–492, 2014.
- [8] W. Li and C. F. Ni, "Current status of the combination therapy of transarterial chemoembolization and local ablation for hepatocellular carcinoma," *Abdominal Radiology*, vol. 44, no. 6, pp. 2268–2275, 2019.
- [9] R. Iezzi, M. Pompili, A. Posa, G. Coppola, A. Gasbarrini, and L. Bonomo, "Combined locoregional treatment of patients with hepatocellular carcinoma: state of the art," *World Journal of Gastroenterology*, vol. 22, no. 6, pp. 1935–1942, 2016.
- [10] A. B. Benson III, M. I. D'Angelica, D. E. Abbott et al., "NCCN guidelines insights: hepatobiliary cancers, version 1.2017," *Journal of the National Comprehensive Cancer Network*, vol. 15, no. 5, pp. 563–573, 2017.
- [11] J. F. Geschwind, M. Kudo, J. A. Marrero et al., "TACE treatment in patients with sorafenib-treated unresectable hepatocellular carcinoma in clinical practice: final analysis of GIDEON," *Radiology*, vol. 279, no. 2, pp. 630–640, 2016.
- [12] M. Tsurusaki and T. Murakami, "Surgical and locoregional therapy of HCC: TACE," *Liver Cancer*, vol. 4, no. 3, pp. 165–175, 2015.
- [13] C. Cammà, F. Schepis, A. Orlando et al., "Transarterial chemoembolization for unresectable hepatocellular carcinoma: meta-analysis of randomized controlled trials," *Radiology*, vol. 224, no. 1, pp. 47–54, 2002.
- [14] D. E. Ramsey, L. Y. Kernagis, M. C. Soulen, and J. F. H. Geschwind, "Chemoembolization of hepatocellular carcinoma," *Journal of Vascular and Interventional Radiology*, vol. 13, no. 9, pp. S211–S221, 2002.
- [15] R. Sacco, G. Tapete, N. Simonetti et al., "Transarterial chemoembolization for the treatment of hepatocellular carcinoma: a review," *Journal of Hepatocellular Carcinoma*, vol. 4, pp. 105–110, 2017.

- [16] X. Ma, R. S. Li, J. Wang et al., "The therapeutic efficacy and safety of compound Kushen injection combined with transarterial chemoembolization in unresectable hepatocellular carcinoma: an update systematic review and meta-analysis," *Frontiers in Pharmacology*, vol. 7, no. 70, 2016.
- [17] B. Liu, J. W. Huang, Y. Li et al., "Single-agent versus combination doxorubicin-based transarterial chemoembolization in the treatment of hepatocellular carcinoma: a single-blind, randomized, phase II trial," *Oncology*, vol. 89, no. 1, pp. 23–30, 2015.
- [18] A. Sergio, C. Cristofori, R. Cardin et al., "Transcatheter arterial chemoembolization (TACE) in hepatocellular carcinoma (HCC): the role of angiogenesis and invasiveness," *The American Journal of Gastroenterology*, vol. 103, no. 4, pp. 914–921, 2008.
- [19] S. Gao, Z. Yang, Z. Zheng et al., "Doxorubicin-eluting bead versus conventional TACE for unresectable hepatocellular carcinoma: a meta-analysis," *Hepatogastroenterology*, vol. 60, no. 124, pp. 813–820, 2013.
- [20] J. H. Zou, L. Zhang, Z. G. Ren, and S. L. Ye, "Efficacy and safety of cTACE versus DEB-TACE in patients with hepatocellular carcinoma: a meta-analysis," *Journal of Digestive Diseases*, vol. 17, no. 8, pp. 510–517, 2016.
- [21] S. Miyayama, "Ultrasensitive conventional transarterial chemoembolization: when and how?," *Clinical and Molecular Hepatology*, 2019.
- [22] I. F. Hsin, C. Y. Hsu, H. C. Huang et al., "Liver failure after transarterial chemoembolization for patients with hepatocellular carcinoma and ascites: incidence, risk factors, and prognostic prediction," *Journal of Clinical Gastroenterology*, vol. 45, no. 6, pp. 556–562, 2011.
- [23] Z. X. Zhu, J. W. Huang, M. H. Liao, and Y. Zeng, "Treatment strategy for hepatocellular carcinoma in China: radiofrequency ablation versus liver resection," *Japanese Journal of Clinical Oncology*, vol. 46, no. 12, pp. 1075–1080, 2016.
- [24] S. N. Goldberg, G. S. Gazelle, and P. R. Mueller, "Thermal ablation therapy for focal malignancy: a unified approach to underlying principles, techniques, and diagnostic imaging guidance," *American Journal of Roentgenology*, vol. 174, no. 2, pp. 323–331, 2000.
- [25] D. A. Gervais and R. S. Arellano, "Percutaneous tumor ablation for hepatocellular carcinoma," *American Journal of Roentgenology*, vol. 197, no. 4, pp. 789–794, 2011.
- [26] T. Livraghi, S. N. Goldberg, S. Lazzaroni, F. Meloni, L. Solbiati, and G. S. Gazelle, "Small hepatocellular carcinoma: treatment with radio-frequency ablation versus ethanol injection," *Radiology*, vol. 210, no. 3, pp. 655–661, 1999.
- [27] M. Dhir, A. A. Melin, J. Douaiher et al., "A review and update of treatment options and controversies in the management of hepatocellular carcinoma," *Annals of Surgery*, vol. 263, no. 6, pp. 1112–1125, 2016.
- [28] T. Livraghi, F. Meloni, M. Di Stasi et al., "Sustained complete response and complications rates after radiofrequency ablation of very early hepatocellular carcinoma in cirrhosis: is resection still the treatment of choice?," *Hepatology*, vol. 47, no. 1, pp. 82–89, 2008.
- [29] L. Crocetti, T. de Baere, and R. Lencioni, "Quality improvement guidelines for radiofrequency ablation of liver tumours," *Cardiovascular and Interventional Radiology*, vol. 33, no. 1, pp. 11–17, 2010.
- [30] T. Livraghi, S. N. Goldberg, S. Lazzaroni et al., "Hepatocellular carcinoma: radio-frequency ablation of medium and large lesions," *Radiology*, vol. 214, no. 3, pp. 761–768, 2000.
- [31] D. S. K. Lu, S. S. Raman, P. Limanond et al., "Influence of large peritumoral vessels on outcome of radiofrequency ablation of liver tumors," *Journal of Vascular and Interventional Radiology*, vol. 14, no. 10, pp. 1267–1274, 2003.
- [32] T. Matsukawa, Y. Yamashita, A. Arakawa et al., "Percutaneous microwave coagulation therapy in liver tumors. A 3-year experience," *Acta Radiologica*, vol. 38, no. 3, pp. 410–415, 1997.
- [33] S. Thamtorawat, R. M. Hicks, J. Yu et al., "Preliminary outcome of microwave ablation of hepatocellular carcinoma: breaking the 3-cm barrier?," *Journal of Vascular and Interventional Radiology*, vol. 27, no. 5, pp. 623–630, 2016.
- [34] A. Facciorusso, G. Serviddio, and N. Muscatiello, "Local ablative treatments for hepatocellular carcinoma: an updated review," *World Journal of Gastrointestinal Pharmacology and Therapeutics*, vol. 7, no. 4, pp. 477–489, 2016.
- [35] P. Liang and Y. Wang, "Microwave ablation of hepatocellular carcinoma," *Oncology*, vol. 72, no. 1, pp. 124–131, 2007.
- [36] M. G. Lubner, C. L. Brace, J. L. Hinshaw, and F. T. Lee Jr., "Microwave tumor ablation: mechanism of action, clinical results, and devices," *Journal of Vascular and Interventional Radiology*, vol. 21, no. 8, Supplement 8, pp. S192–S203, 2010.
- [37] T. Vogl, N.-E. Nour-Eldin, R. Hammerstingl, B. Panahi, and N. Naguib, "Microwave ablation (MWA): basics, technique and results in primary and metastatic liver neoplasms - review article," *RöFo - Fortschritte auf dem Gebiet der Röntgenstrahlen und der bildgebenden Verfahren*, vol. 189, no. 11, pp. 1055–1066, 2017.
- [38] P. Liang, J. Yu, M. D. Lu et al., "Practice guidelines for ultrasound-guided percutaneous microwave ablation for hepatic malignancy," *World Journal of Gastroenterology*, vol. 19, no. 33, pp. 5430–5438, 2013.
- [39] P. Liang, J. Yu, X. L. Yu et al., "Percutaneous cooled-tip microwave ablation under ultrasound guidance for primary liver cancer: a multicentre analysis of 1363 treatment-naive lesions in 1007 patients in China," *Gut*, vol. 61, no. 7, pp. 1100–1101, 2012.
- [40] B. Dong, P. Liang, X. Yu et al., "Percutaneous sonographically guided microwave coagulation therapy for hepatocellular carcinoma: results in 234 patients," *American Journal of Roentgenology*, vol. 180, no. 6, pp. 1547–1555, 2003.
- [41] K. F. Lee, J. W. Hui, Y. S. Cheung et al., "Surgical ablation of hepatocellular carcinoma with 2.45-GHz microwave: a critical appraisal of treatment outcomes," *Hong Kong Medical Journal*, vol. 18, no. 2, pp. 85–91, 2012.
- [42] S. Rossi, F. Garbagnati, I. De Francesco et al., "Relationship between the shape and size of radiofrequency induced thermal lesions and hepatic vascularization," *Tumori*, vol. 85, no. 2, pp. 128–132, 1999.
- [43] J. Y. Ni, S. S. Liu, L. F. Xu, H. L. Sun, and Y. T. Chen, "Meta-analysis of radiofrequency ablation in combination with transarterial chemoembolization for hepatocellular carcinoma," *World Journal of Gastroenterology*, vol. 19, no. 24, pp. 3872–3882, 2013.
- [44] H. C. Liu, E. B. Shan, L. Zhou et al., "Combination of percutaneous radiofrequency ablation with transarterial chemoembolization for hepatocellular carcinoma: observation of clinical effects," *Chinese Journal of Cancer Research*, vol. 26, no. 4, pp. 471–477, 2014.

- [45] J. H. Cao, J. Zhou, X. L. Zhang, X. Ding, and Q. Y. Long, "Meta-analysis on radiofrequency ablation in combination with transarterial chemoembolization for the treatment of hepatocellular carcinoma," *Journal of Huazhong University of Science and Technology Medical Sciences*, vol. 34, no. 5, pp. 692–700, 2014.
- [46] Z. W. Peng, Y. J. Zhang, M. S. Chen et al., "Radiofrequency ablation with or without transcatheter arterial chemoembolization in the treatment of hepatocellular carcinoma: a prospective randomized trial," *Journal of Clinical Oncology*, vol. 31, no. 4, pp. 426–432, 2013.
- [47] W. Z. Yang, N. Jiang, N. Huang, J. Y. Huang, Q. B. Zheng, and Q. Shen, "Combined therapy with transcatheter arterial chemoembolization and percutaneous microwave coagulation for small hepatocellular carcinoma," *World Journal of Gastroenterology*, vol. 15, no. 6, pp. 748–752, 2009.
- [48] J. W. Sturm and M. Keese, "Multimodal treatment of hepatocellular carcinoma (HCC)," *Onkologie*, vol. 27, no. 3, pp. 294–303, 2004.
- [49] A. O. Abdelaziz, A. H. Abdelmaksoud, M. M. Nabeel et al., "Transarterial chemoembolization combined with either radiofrequency or microwave ablation in management of hepatocellular carcinoma," *Asian Pacific Journal of Cancer Prevention*, vol. 18, no. 1, pp. 189–194, 2017.
- [50] C. Liu, P. Liang, F. Liu et al., "MWA combined with TACE as a combined therapy for unresectable large-sized hepatocellular carcinoma," *International Journal of Hyperthermia*, vol. 27, no. 7, pp. 654–662, 2011.
- [51] Q. F. Chen, Z. Y. Jia, Z. Q. Yang, W. L. Fan, and H. B. Shi, "Transarterial chemoembolization monotherapy versus combined transarterial chemoembolization-microwave ablation therapy for hepatocellular carcinoma tumors  $\leq 5$  cm: a propensity analysis at a single center," *Cardiovascular and Interventional Radiology*, vol. 40, no. 11, pp. 1748–1755, 2017.
- [52] L. Zheng, H. L. Li, C. Y. Guo, and S. X. Luo, "Comparison of the efficacy and prognostic factors of transarterial chemoembolization plus microwave ablation versus transarterial chemoembolization alone in patients with a large solitary or multinodular hepatocellular carcinomas," *Korean Journal of Radiology*, vol. 19, no. 2, pp. 237–246, 2018.

## Research Article

# Ginsenoside Rg3 Prolongs Survival of the Orthotopic Hepatocellular Carcinoma Model by Inducing Apoptosis and Inhibiting Angiogenesis

Shen Hu <sup>1</sup>, Yan Zhu,<sup>2</sup> Xiangyang Xia <sup>3</sup>, Xiaobo Xu <sup>4</sup>, Fen Chen <sup>4</sup>, Xudong Miao <sup>5</sup>,  
and Xinmei Chen <sup>6</sup>

<sup>1</sup>Department of Obstetrics, The Second Affiliated Hospital of Zhejiang University School of Medicine, Hangzhou 310000, China

<sup>2</sup>Department of Respiratory Hangzhou Shulan Hospital, Hangzhou 310009, China

<sup>3</sup>Department of Ultrasound, The Second Affiliated Hospital of Zhejiang University School of Medicine, Hangzhou 310000, China

<sup>4</sup>Department of Hepatobiliary and Pancreatic Surgery, Key Laboratory of Combined Multi-Organ Transplantation, Ministry of Public Health, The First Affiliated Hospital, School of Medicine, Zhejiang University, Hangzhou, 310003 Zhejiang Province, China

<sup>5</sup>The Department of Orthopedics, The Second Affiliated Hospital, Zhejiang University, Hangzhou, Zhejiang 310003, China

<sup>6</sup>The Department of Pharmacy, Shandong University of Traditional Chinese Medicine, Jinan, 250014 Shandong Province, China

Correspondence should be addressed to Xudong Miao; [zrmxd@zju.edu.cn](mailto:zrmxd@zju.edu.cn) and Xinmei Chen; [chenxinmei@sducm.edu.cn](mailto:chenxinmei@sducm.edu.cn)

Received 1 December 2018; Accepted 28 April 2019; Published 26 August 2019

Academic Editor: Maryou Lambros

Copyright © 2019 Shen Hu et al. This is an open access article distributed under the Creative Commons Attribution License, which permits unrestricted use, distribution, and reproduction in any medium, provided the original work is properly cited.

**Aim.** Microvessel density is a marker of tumor angiogenesis activity for development and metastasis. Our preliminary study showed that ginsenoside Rg3 (Rg3) induces apoptosis in hepatocellular carcinoma (HCC) *in vitro*. The aim of this study was to investigate the cross-link for apoptosis induction and antiangiogenesis effect of Rg3 on orthotopic HCC *in vivo*. **Methods.** The murine HCC cells Hep1-6 were implanted in the liver of mouse. With oral feeding of Rg3 (10 mg/kg once a day for 30 days), the quantitative analysis of apoptosis was performed by using pathology and a transmission electron microscope and microvessel density was quantitatively measured by immunohistochemical staining of the CD105 antibody. The mice treated with Rg3 ( $n = 10$ ) were compared with the control ( $n = 10$ ) using Kaplan-Meier analysis. Animal weight and tumor weight were measured to determine the toxicity of Rg3 and antitumor effect on an orthotopic HCC tumor model. **Results.** With oral feeding of Rg3 daily in the first 30 days on tumor implantation, Rg3 significantly decreased the orthotopic tumor growth and increased the survival of animals ( $P < 0.05$ ). Rg3-treated mice showed a longer survival than the control ( $P < 0.05$ ). Rg3 treatment induced apoptosis and inhibited angiogenesis. They contributed to the tumor shrinkage. Rg3 initialized the tumor apoptotic progress, which then weakened the tumor volume and its capability to produce the vascularized network for further growth of the tumor and remote metastasis. **Conclusion.** Rg3 inhibited the activation of microtumor vessel formation *in vivo* besides its apoptosis induction. Rg3 may be used as an adjuvant agent in the clinical HCC treatment regimen.

## 1. Introduction

Hepatocellular carcinoma (HCC) is one of the fifth most common cancers worldwide and the third most common cause of cancer death [1–3]. HCC is a highly vascularized tumor, and thus, the antiangiogenesis treatments such as arterializations and embolization have been applied; the overall clinical effect is not satisfying [4]. The metastasis

and recurrence of hepatocellular carcinoma are still very challenging [5, 6].

HCC is especially highly prevalent in China, mainly attributed to the prevalence of hepatitis B virus (HBV) persistent infection and HBV-induced cirrhosis [7, 8]. The majority of HCC patients are already in advanced stage on the first diagnosis; on diagnosis, the majority of patients have already lose the opportunity for radical surgery or liver

transplantation; the median survival is usually less than one year due to the absence of effective target medicine [8, 9]. Because HCC is generally originated from chronic hepatitis and many patients suffer from cirrhosis, the treatment is even more challenging than other malignancies. The underlying liver disease hinders the liver function and limits the application of the aggressive treatments. The effect and the toxicity are two sides that must be conjointly balanced.

Sorafenib is the only approved medicine, but it can only cure part of patients [10]. The local-regional ablation is recommended as the first-line treatment, but ablation currently works for the early stage HCC but fails for the advanced HCC cases [11]. Transarterial chemoembolization (TACE) is now accepted by many centers as a palliative treatment for HCC larger than 5 cm or multinodular lesions [4, 12]. It can increase the chemotherapeutic concentration in the tumor, but it can cause vessel obstruction and reduce hepatic ischemia. Even for the target therapy like Y90 microspheres, immune therapy has been tested but its long-term outcome is still uncertain for treating HCC by bioelectric ablation with microsecond pulsed electric fields ( $\mu$ sPEFs) which is in the experimental period [13]. In fact, the therapeutic options in advanced HCC are still very limited, so the novel treatment with high target but low toxicity is in great need. Ginseng is a Chinese tradition herbal medicine; ginsenoside Rg3 is a chemical compound isolated from ginseng. Ginseng has a wide spectrum of pharmacological effects such as antihyperglycemia, antioxidant status, and antioxidative stress in type 2 diabetes [14]; anti-inflammatory effects of ginsenoside Rg3 in A549 cells and human asthmatic lung tissue [15]; and induction of nitric oxide synthase of ginsenoside Rg3 to relax vessels [16]. Researchers have found that ginsenoside Rg3 can inhibit the growth of such kinds of tumors as colorectal cancer [17], lung cancer [18], breast cancer [19], pancreatic cancer [20], and acute leukemia [21].

HCC is a highly vascularized tumor, and thus, the antiangiogenesis treatments such as arterializations and embolization have been applied but the overall clinical effect is not satisfying [4, 12]. The destruction of the local HCC blood supply was expected to cause tumor starving and then necrosis, but for the orthotopic HCC *in vivo*, the absence of tumor blood supply also stimulates the endothelial cellular growth directly and indirectly. They stimulate even tinier new tumor vessels to grow up as a compensation. In HCC development, the tumor new vessel formation is an independent risk factor on HCC progression, metastasis, and recurrence. The hypothesis is that Rg3 might increase the HCC tumor-bearing animal survival by inhibiting new tumor vessel formation which has been raised in a rat model of endometriosis [22]. In a few *in vivo* studies, ginsenoside Rg3 combined with gemcitabine or cisplatin on angiogenesis had been tested on lung cancer in mice [23, 24]; ginsenoside Rg3 combined with metronomic temozolomide had been tested on glioma cancer in rat [25], combined with fiber for inhibiting scar hyperplasia of the skin [26] and prostate stromal cells [27], but the exact molecular mechanism is unclear.

We have previously demonstrated the antitumor potential of ginsenoside Rg3 (Rg3) against HCC *in vitro* and *in vivo* [28]. When applied in Hep1-6 and HepG2 HCC cells,

Rg3 induces HCC cell apoptosis via the intrinsic pathway by altering the expression of Bcl-2. The long-term follow-up study had showed that no matter the single use of Rg3 or the combination use with cyclophosphamide (CTX), Rg3 inhibited tumor growth in a subcutaneous HCC model, while its effect on vascular formation is kept unknown. In this study, benefit from a murine orthotopic HCC model in the liver, the function of Rg3 on angiogenesis was investigated and the possible mechanism was explored.

## 2. Materials and Methods

**2.1. Ginsenoside Rg3.** Ginsenoside Rg3 (Lot number HJ20110802-Rg3) was purchased from Hongjiu Biotechnology Co. Ltd. (Dalian, China). The purified Rg3 extract was dissolved, and 10 mg/kg dosage was orally fed to mice.

**2.2. Cell Lines and Cell Culture.** Hep1-6 HCC cells were purchased from the Institute of Shanghai Cell Bank, Academy of Science (Shanghai, China) and multiplied in DMEM (ATCC, Manassas, VA, United States) supplemented with 10% FBS (Shengong, Shanghai, China). The cells were incubated at 37°C in a mixture of 5% CO<sub>2</sub> and 95% air.

**2.3. Animal Ethics.** Animals received appropriate humane care from a certificated professional staff in compliance with both the Principles of Laboratory Animal Care (NIH publication NO 85-23, revised 1985) and the Guide for the Care and Use of Laboratory Animals approved by the Animal Care and Use Committees of Zhejiang University. All mice were housed in a clean-level animal house in the first affiliated hospital. The mice were caged in 22-24°C, 12 h light/dark cycle, and fed with standard mouse chow and water.

**2.4. Orthotopic HCC Tumor Model and HCC Animal Model.** Female C57BL/6 mice were purchased from Shanghai Experimental Animal Center (Shanghai, China). They were housed to 8-week-old and implanted HCC tumor in an orthotopic manner. Hepa1-6 cells in a log phase were collected and resuspended in 0.2 ml NS. The cells were subcutaneously injected into the back of one C57BL/6 mouse when mice were purchased. After 10 days, tumors were visible and then dissected; the dissected tumors were cut into small pieces immediately (1.0 mm<sup>3</sup>) and then implanted into the liver on the 8-week-old recipient C57BL/6 mouse with percutaneous approach by puncturing a tunnel in the left liver lobe. The anesthesia of mice was performed by intraperitoneal injection of ketamine hydrochloride (100 mg/kg) and atropine (1 mg/kg) (Shanghai No. 1 Biochemical and Pharmaceutical, China).

**2.5. The Experiment Design and Illustration.** After orthotopic implantation with HCC tumor (day 0), altogether, 20 HCC tumor-bearing mice were randomly divided into two groups: control group ( $n = 10$ ) and Rg3 treatment group ( $n = 10$ ). They were fed orally by normal saline (0.2 ml/mouse, once a day) or Rg3 (10 mg/kg) for 30 consecutive days (day 1 to day 30). After treatment, the survival study began. The animal technician, who was blind to the study, monitored the mouse weight and tumor size every day. The survival was

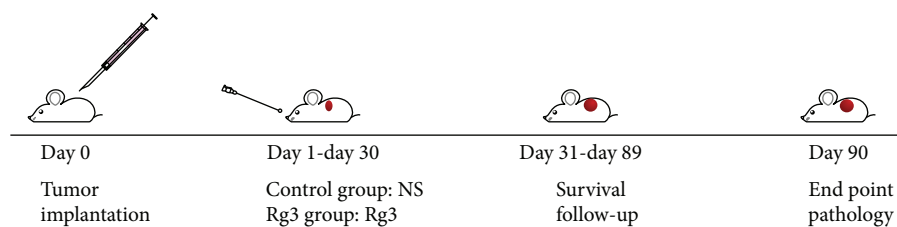


FIGURE 1: The experiment design and illustration. After implantation with Hep-1 HCC tumor cells (day 0), altogether, 20 HCC tumor-bearing mice were randomly divided into two groups: the control group ( $n = 10$ ) and the Rg3 treatment group ( $n = 10$ ). They were fed orally by normal saline (0.2 ml/mouse, once a day) or Rg3 (10 mg/kg) for 30 days (day 1-day 30). The experiment was investigated for three months.

followed up for three months. Whenever the animal showed the palpable tumor on the abdomen which the preliminary ultrasound study showed, the tumor volume was approximately  $2 \text{ cm}^3$ , the animals with the heavy tumor burden were sacrificed by inhaling ether for their welfare according to the animal experiment proposal, and the time was marked as the end. Otherwise, the tumor-bearing mice were kept to the cutoff till the 90th day posttumor implantation. On the 90th day, the end of survival study, when the rest of the animals were all euthanized, the tumor was dissected for weighing, pathology, transmission electron microscope (TEM), and microvessel density (MVD) analysis. The survival difference between two groups was compared by Kaplan-Meier survival analysis.  $P$  value of less than 0.05 was considered statistically significant. The experiment design is shown in the flow chart in Figure 1.

**2.6. The Mouse Survival by Kaplan-Meier Survival Analysis.** The Hep1-6 HCC tumor-bearing mice were followed up, and the survival time was decided based on the length of time after Hep1-6 HCC tumor was palpable (the volume is about  $2 \text{ cm}^3$ ). The rate of survival between two groups was compared by Kaplan-Meier survival analysis by SPSS software (version 17.0, SPSS, Chicago, United States).

**2.7. Tumor Histopathology.** When the tumor was as large as 20 mm in diameter, the animal was euthanized and the tumor was dissected and fixed in 40 g/l neutral formaldehyde. After 24 h, it was embedded in paraffin, cut into  $3 \mu\text{m}$  sections, stained with hematoxylin and eosin (HE), and examined under light microscopy.

**2.8. Apoptotic Cell Identification and Quantification.** The quantitative analysis of apoptosis was performed by using pathology and TEM. Apoptotic cells were recognized by the morphological character of condensed nuclear stain with pyknosis and fragmented nuclei. They were quantified as the average of 10 randomly selected fields under a microscope per tumor. All the identification and quantification were performed by software Image Processing and Analysis in Java, (NIH ImageJ, Version 1.42-2).

**2.9. Tumor MVD.** HCC tumor angiogenesis can be quantified by counting the number of new tumor blood vessels, termed as MVD, which is characterized as the highly vascularized area (hot spots) on pathological slides. In this study, the endothelial antibody CD105 was stained by immunohisto-

chemical assays in order to illustrate the active neovascularization in HCC. MVD counting was performed by experienced pathologists with digital camera image acquisition system (Olympus, Japan) and image analysis software ImageJ (NIH, Version 1.42-2, USA). In brief, the hot spots which represent the most vascularized tumor areas were selected under light microscope; then, the exact number of CD105-stained vessels was assessed by the built-in software. The brown color stained CD105-positive cells can be differentiated from the unstained tumor cells, while the preexisting big vessels ( $>20 \mu\text{m}$ ) were excluded.

**2.10. Immunohistochemistry.** Immunohistochemical staining was performed for CD105 antibody (1 : 50, Dako, CA, USA) in  $6 \mu\text{m}$  paraffin slide. After routine antibody incubation and PBS rinse, the stained sinusoidal spots were captured by Olympus microscope. MVD areas were quantitatively measured using immunopositively stained vessels vs. the total vessels in the field by a pathologist.

**2.11. Statistical Analysis.** Data were presented as mean  $\pm$  SD. Statistics was performed using SPSS (version 17.0; SPSS Inc., Chicago, IL, USA). Data were analyzed using Student's  $t$ -test for statistical significance. A  $P$  value of less than 0.05 was considered statistically significant.

### 3. Results

**3.1. Rg3 Prolonged the Survival of Hep1-6 HCC Tumor-Bearing Mice.** The median survival for the control group was 65 days and 86 days for Rg3-treated mice (log-rank test  $P < 0.05$ ). Kaplan-Meier analysis shows that mice with Rg3 treatment had a significantly higher survival rate than control without treatment ( $P < 0.05$ ) (Figure 2). As seen in Figure 2, survival curves of Hep1-6 HCC-bearing mice were treated with normal saline as control (blue curve) or Rg3 (red curve) at a dose of 10 mg/kg. The survival curve indicated that mice with Rg3 treatment had a significantly higher survival rate than control without Rg3 treatment ( $P < 0.05$ ).

**3.2. The Animal Weight Changed during 90-Day Follow-Up.** The mouse weight follow-up study was shown in Figure 3. The twenty newborn mice were divided into two groups, and their weight had no significant difference in the beginning of the experiment. After the tumor implantation on 8-week-old mice, the animals were weighted regularly to check the effect of the HCC tumor and Rg3 on body weight. Both

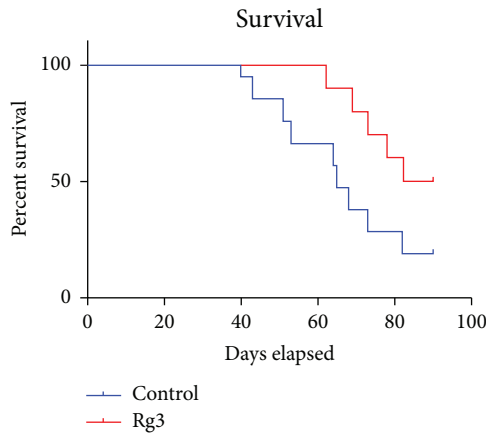


FIGURE 2: The mouse survival by Kaplan-Meier survival analysis. Hep1-6 HCC tumor-bearing mice were treated with normal saline, control (blue curve), or Rg3 (red curve). Survival was based on the length of time after the Hep1-6 HCC tumor volume reached  $2\text{ cm}^3$  (time when the animal was euthanized). The median survival for control was 65 days and 86 days for Rg3-treated mice (log-rank test  $P < 0.05$ ). Kaplan-Meier analysis shows that mice with Rg3 treatment had a significant higher survival rate than the control without Rg3 treatment ( $P < 0.05$ ).

control and Rg3 groups increased their weight in the first month after the Hep1-6 tumor cubes were initially implanted in the liver lobe. After 30 days when the tumor developed, the tumor-bearing mice began to stop gaining weight. Particularly in the control group without any treatment, the mouse weight curve even went down the baseline. As a comparison, the body weight kept above the baseline in the Rg3 group. While due to the limited range, the statistical analysis found no significant difference between two groups ( $P < 0.05$ ) suggesting that the Rg3 had no negative toxicity effect on the body weight of the hepatocellular carcinoma-bearing mice.

**3.3. The Tumor Weight at the End of the Experiment.** When the tumor was palpable in the abdomen, which has been confirmed by preliminary ultrasound study that the tumor size reached the upper limit of tumor burden as  $2\text{ cm}^3$ , the tumor-bearing mouse was euthanized by inhaling ether for the animals' welfare. No remote metastasis was found. The tumor lump in the liver was dissected for the weight scaling and further pathological exams. The tumor weight in the Rg3 group was significantly lower than those in the control group ( $P < 0.05$ ), suggesting Rg3 suppressed HCC tumor growth in the liver. The oral feeding with Rg3 significantly reduces HCC tumor growth without obvious poisonous effect ( $P < 0.05$ ) (Figure 4).

**3.4. Rg3 Induced Apoptosis In Vivo.** HE-stained pathological sections are shown in Figure 5. Apoptosis was detected in HCC to determine whether Rg3 reduces angiogenesis. Apoptotic cells were identified by pathology. Effect of Rg3 on apoptosis in HCC was identified by pathology. They demonstrate the pathological changes of posttumor implantation. The representative images in the Rg3 group showed the fragmented nuclei indicating apoptotic cells; in the control

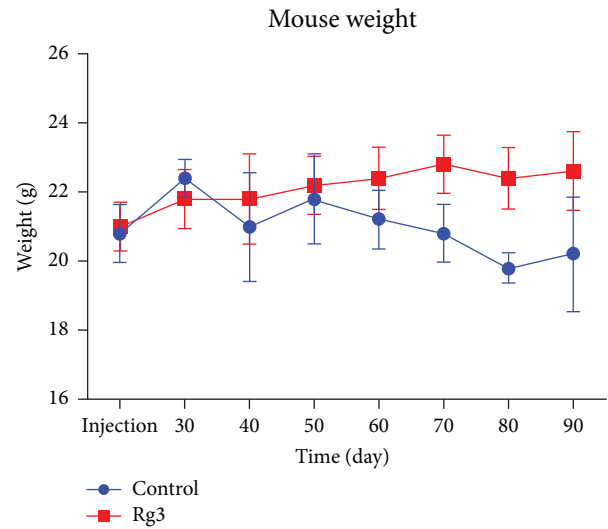


FIGURE 3: The mouse weight follow-up study. The animal weight in the control and Rg3 groups both increased in the first month after the Hep1-6 tumor cubes were implanted in the liver lobe. After the initial 30 days when the tumor developed, the tumor-bearing mice began to stop gaining weight. Statistical analysis showed that there was no significant difference between the average weights between the two groups, suggesting that the Rg3 had no negative effect on the body weight of the hepatocellular carcinoma-bearing mice.

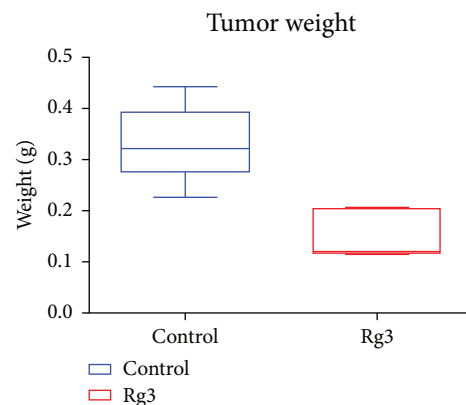


FIGURE 4: Rg3 inhibit on Hep-1 HCC tumor development *in vivo*. At the end of the experiment, mice were sacrificed to dissect the tumors. The weight of the tumor from mice was scaled.  $P < 0.05$  vs. the control group, suggesting Rg3 decreased the Hep1-6 HCC tumor growth in mice.

group, hepatic morphology exhibits the clear hepatic lobular structure and tumor nodules with rich vessels. In the Rg3 group, the tumor clusters showed extensive cell death without infectious neutrophil infiltration. No vessels appeared but there is a loss of endothelial integrity with extensive hepatocellular degeneration in the background.

**3.5. Rg3 Decreased MVD in HCC.** Angiogenesis quantification (MVD) in tumors is performed by counting vessels stained with CD105 (Figure 5). The CD105 is an endothelium marker that was found highly expressed in HCC. The

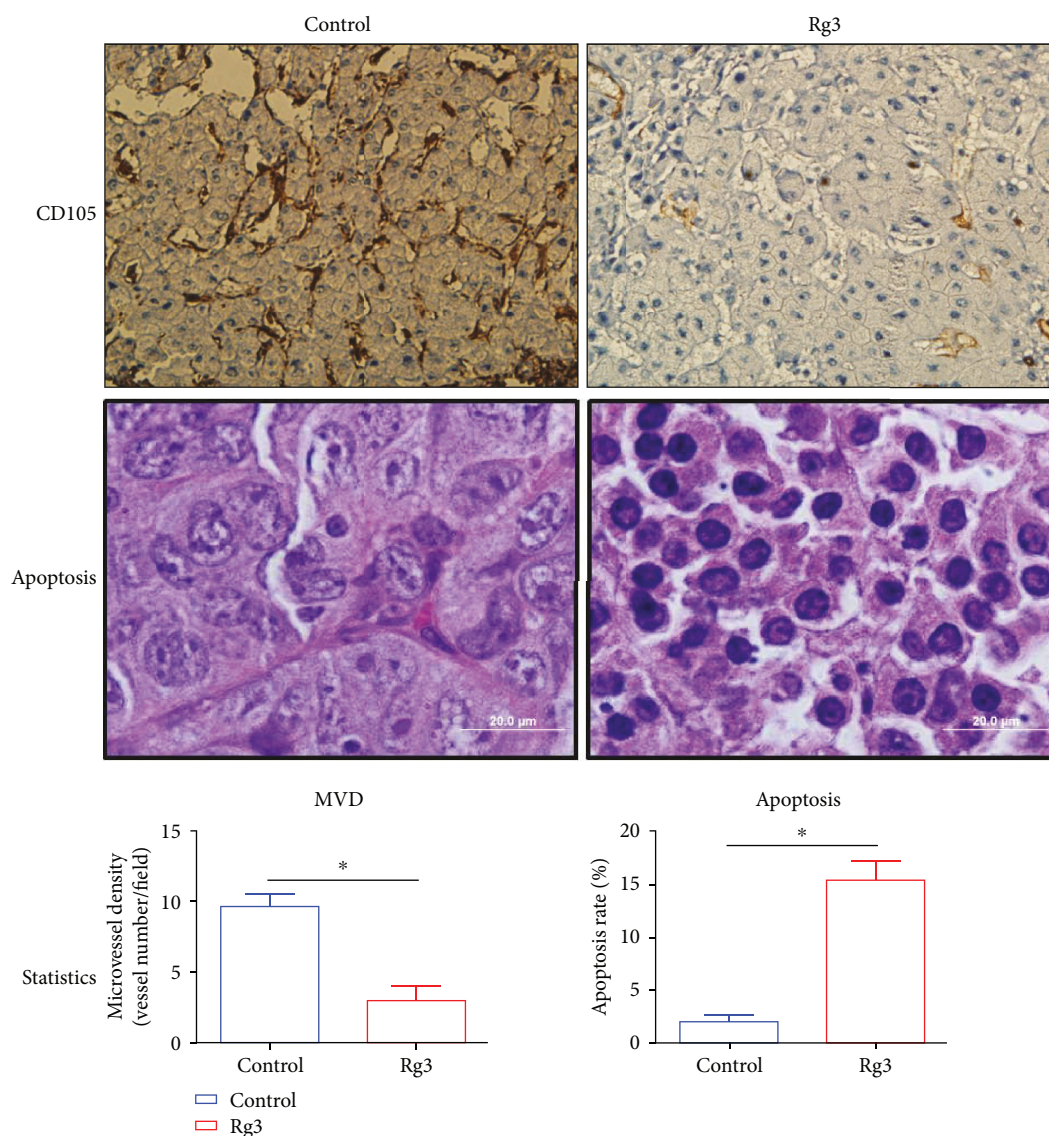


FIGURE 5: The quantities of apoptotic and microvessel density analysis. Apoptotic cells and microvessels were quantified as the average of 10 fields selected per tumor (magnification was shown as the bar). The CD105 is an endothelium marker that was found highly expressed in HCC. The MVD-CD105 positively stained tumor vessels were significantly less in the Rg3 group than in the control group ( $P < 0.05$ ). In addition, the apoptotic rate increased dramatically in the Rg3 group vs. the control group ( $P < 0.05$ ).

MVD-CD105 positively stained tumor vessels were significantly less in the Rg3 group than in the control group ( $P < 0.05$ ). In addition, the apoptotic rate increased dramatically in the Rg3 group vs. the control group ( $P < 0.05$ ), suggesting that the Rg3 initialized the tumor apoptotic progress, which then weakened the tumor volume and its capability to produce the vascularized network for tumor growth and further metastasis.

#### 4. Discussion

Our previous work has shown that Rg3 is a nonpoisonous herb extract that can induce apoptosis [28]. The programmed cell death controlled by caspase protease activation was also found in the in vitro HCC cells and other tumors

[23–27]. Apoptosis is cross-linked with multiple pathways associating with tumor development among which angiogenesis is critical for prognosis. In the hypoxia HCC microenvironment, Rg3 inhibited the activity of the implanted tumor cells and weakened the angiogenesis of tumor vascular system as well as the complicated network with immune system and microtumor environment [29–31].

In order to get closer to the clinical features, we assessed the inhibitory effects of Rg3 on tumor growth in an orthotopic murine model. The results showed that there is no difference in body weight found between the Rg3-treated and the control mice. During the first 30 days after the tumor implantation, HCC in both control and Rg3 groups continued to grow progressively, suggesting that the HCC tumor caused nutrition exhaustion whereas the oral administration of

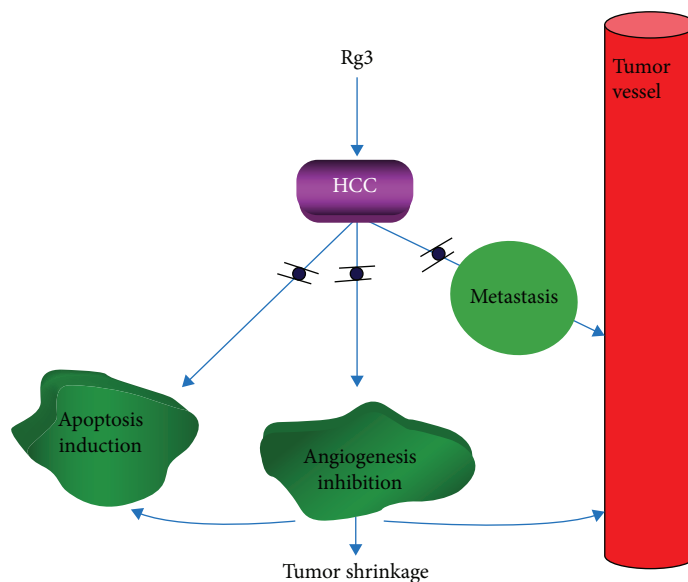


FIGURE 6: The molecular mechanical illustration. In order to further elucidate the mechanisms of the Rg3 antitumor effects, the orthotopic HCC tumor-bearing mouse was followed up to 3 months with the 30-day oral taking of Rg3 in the early stage of tumor development when the initial tumor was implanted in the liver. Results showed that apoptosis induction and angiogenesis was significantly detected in tumor tissue by Rg3 treatment, contributing to the tumor shrinkage and negative remote metastasis. Rg3 initialized the tumor apoptotic progress, which then weakened the tumor volume and its capability to produce the vascularized network for tumor growth and further metastasis.

Rg3 resulted in a significant reduction in tumor size. At the end of the experiment, tumors from mice in the control group were larger than those in the Rg3 group and were about double the weight of tumors from the Rg3-treated mice, demonstrating that without Rg3 intervention in the early tumor development stage, HCC will grow dramatically, while Rg3 treatment can significantly suppress the tumor growth.

In order to further elucidate the mechanisms of the Rg3 antitumor effects, the cross-link for antiangiogenesis and apoptosis induction effect of Rg3 on orthotopic HCC in vivo was investigated. A marked increase in pyknosis cells was observed in tumor tissue sections and TEM image from mice treated with Rg3 as compared to control, suggesting that Rg3 significantly induced cell apoptosis in HCC; at the same time, the CD105 positively stained tumor vessels were significantly less in the Rg3 group than that in the control group. These data showed that the continuous oral taking of Rg3 decreases neovascularization formation in the early stage of HCC development.

As illustrated in Figure 6, in view of the current data, Rg3 showed the potential of antineovascularization in HCC. The oral feeding of Rg3 in the HCC early stage showed the significant blockage of tumor new blood vessel mobilization. As a result, the use of Rg3 in the early stage slows down HCC development and improves the overall survival of the tumor-bearing animals. The current data showed that Rg3 initialized the tumor apoptotic progress, which then weakened the tumor volume and its capability to produce the vascularized network for tumor growth and further metastasis. Our study indicates the clinical potential of using Rg3 in the angiogenesis therapy against HCC.

## Data Availability

The research and result data type used to support the findings of this study are included within the article.

## Conflicts of Interest

All authors have no conflicts of interest to declare.

## Acknowledgments

This work was supported by the National S&T Major Project (2018ZX10301201) and Zhejiang Province Science Grants (No. 2016KYB092, No. 2017C37102, and LY17H160018).

## References

- [1] R. L. Siegel, K. D. Miller, and A. Jemal, "Cancer statistics, 2017," *CA: A Cancer Journal for Clinicians*, vol. 67, no. 1, pp. 7–30, 2017.
- [2] J. Ferlay, I. Soerjomataram, R. Dikshit et al., "Cancer incidence and mortality worldwide: sources, methods and major patterns in GLOBOCAN 2012," *International Journal of Cancer*, vol. 136, no. 5, pp. E359–E386, 2015.
- [3] P. Tabrizian, S. Roayaie, and M. E. Schwartz, "Current management of hepatocellular carcinoma," *World Journal of Gastroenterology*, vol. 20, no. 30, pp. 10223–10237, 2014.
- [4] K. Mumtaz, N. Patel, R. M. Modi et al., "Trends and outcomes of transarterial chemoembolization in hepatocellular carcinoma: a national survey," *Hepatobiliary & Pancreatic Diseases International*, vol. 16, no. 6, pp. 624–630, 2017.
- [5] V. Hernandez-Gea, S. Toffanin, S. L. Friedman, and J. M. Llovet, "Role of the microenvironment in the pathogenesis

- and treatment of hepatocellular carcinoma,” *Gastroenterology*, vol. 144, no. 3, pp. 512–527, 2013.
- [6] T. Kobayashi, H. Aikata, T. Kobayashi, H. Ohdan, K. Arihiro, and K. Chayama, “Patients with early recurrence of hepatocellular carcinoma have poor prognosis,” *Hepatobiliary & Pancreatic Diseases International*, vol. 16, no. 3, pp. 279–288, 2017.
  - [7] W. Chen, R. Zheng, P. D. Baade et al., “Cancer statistics in China, 2015,” *CA: A Cancer Journal for Clinicians*, vol. 66, no. 2, pp. 115–132, 2016.
  - [8] J. M. Llovet, C. Brú, and J. Bruix, “Prognosis of hepatocellular carcinoma: the BCLC staging classification,” *Seminars in Liver Disease*, vol. 19, no. 3, pp. 329–338, 1999.
  - [9] J. F. Zhang, Z. J. Shu, C. Y. Xie et al., “Prognosis of unresectable hepatocellular carcinoma: comparison of seven staging systems (TNM, Okuda, BCLC, CLIP, CUPI, JIS, CIS) in a Chinese cohort,” *PLoS One*, vol. 9, no. 3, article e88182, 2014.
  - [10] J. M. Llovet, S. Ricci, V. Mazzaferro et al., “Sorafenib in advanced hepatocellular carcinoma,” *The New England Journal of Medicine*, vol. 359, no. 4, pp. 378–390, 2008.
  - [11] X. Chen, H. P. Liu, M. Li, and L. Qiao, “Advances in non-surgical management of primary liver cancer,” *World Journal of Gastroenterology*, vol. 20, no. 44, pp. 16630–16638, 2014.
  - [12] S. Colagrande, A. L. Inghilesi, S. Aburas, G. G. Taliani, C. Nardi, and F. Marra, “Challenges of advanced hepatocellular carcinoma,” *World Journal of Gastroenterology*, vol. 22, no. 34, pp. 7645–7659, 2016.
  - [13] X. Chen, Z. Ren, C. Li et al., “Preclinical study of locoregional therapy of hepatocellular carcinoma by bioelectric ablation with microsecond pulsed electric fields ( $\mu$ sPEFs),” *Scientific Reports*, vol. 5, no. 1, article 9851, 2015.
  - [14] S. W. Ma, I. F. Benzie, T. T. Chu, B. S. Fok, B. Tomlinson, and L. A. Critchley, “Effect of *Panax ginseng* supplementation on biomarkers of glucose tolerance, antioxidant status and oxidative stress in type 2 diabetic subjects: results of a placebo-controlled human intervention trial,” *Diabetes, Obesity & Metabolism*, vol. 10, no. 11, pp. 1125–1127, 2008.
  - [15] I.-S. Lee, I. J. Uh, K.-S. Kim et al., “Anti-inflammatory effects of ginsenoside Rg3 via NF- $\kappa$ B pathway in A549 cells and human asthmatic lung tissue,” *Journal of Immunology Research*, vol. 2016, Article ID 7521601, 11 pages, 2016.
  - [16] N. D. Kim, E. M. Kim, K. W. Kang, M. K. Cho, S. Y. Choi, and S. G. Kim, “Ginsenoside Rg3 inhibits phenylephrine-induced vascular contraction through induction of nitric oxide synthase,” *British Journal of Pharmacology*, vol. 140, no. 4, pp. 661–670, 2003.
  - [17] Y. C. Tang, Y. Zhang, J. Zhou et al., “Ginsenoside Rg3 targets cancer stem cells and tumor angiogenesis to inhibit colorectal cancer progression in vivo,” *International Journal of Oncology*, vol. 52, no. 1, pp. 127–138, 2018.
  - [18] Q. Zhang, X. Kang, B. Yang, J. Wang, and F. Yang, “Antiangiogenic effect of capecitabine combined with ginsenoside Rg3 on breast cancer in mice,” *Cancer Biotherapy & Radiopharmaceuticals*, vol. 23, no. 5, pp. 647–654, 2008.
  - [19] T. Xu, Z. Jin, Y. Yuan et al., “Ginsenoside Rg3 serves as an adjuvant chemotherapeutic agent and VEGF inhibitor in the treatment of non-small cell lung cancer: a meta-analysis and systematic review,” *Evidence-Based Complementary and Alternative Medicine*, vol. 2016, Article ID 7826753, 14 pages, 2016.
  - [20] J. Q. Guo, Q. H. Zheng, H. Chen et al., “Ginsenoside Rg3 inhibition of vasculogenic mimicry in pancreatic cancer through downregulation of VE-cadherin/EphA2/MMP9/MMP2 expression,” *International Journal of Oncology*, vol. 45, no. 3, pp. 1065–1072, 2014.
  - [21] D. Zeng, J. Wang, P. Kong, C. Cheng, J. Li, and J. Li, “Ginsenoside Rg3 inhibits HIF-1 $\alpha$  and VEGF expression in patient with acute leukemia via inhibiting the activation of PI3K/Akt and ERK1/2 pathways,” *International Journal of Clinical and Experimental Pathology*, vol. 7, no. 5, pp. 2172–2178, 2014.
  - [22] Y. Cao, Q. Ye, M. Zhuang et al., “Ginsenoside Rg3 inhibits angiogenesis in a rat model of endometriosis through the VEGFR-2-mediated PI3K/Akt/mTOR signaling pathway,” *PLoS One*, vol. 12, no. 11, article e0186520, 2017.
  - [23] T.-G. Liu, Y. Huang, D.-D. Cui et al., “Inhibitory effect of ginsenoside Rg3 combined with gemcitabine on angiogenesis and growth of lung cancer in mice,” *BMC Cancer*, vol. 9, no. 1, p. 250, 2009.
  - [24] J. Wang, L. Tian, M. N. Khan et al., “Ginsenoside Rg3 sensitizes hypoxic lung cancer cells to cisplatin via blocking of NF- $\kappa$ B mediated epithelial-mesenchymal transition and stemness,” *Cancer Letters*, vol. 415, pp. 73–85, 2018.
  - [25] C. Sun, Y. Yu, L. Wang et al., “Additive antiangiogenesis effect of ginsenoside Rg3 with low-dose metronomic temozolomide on rat glioma cells both in vivo and in vitro,” *Journal of Experimental & Clinical Cancer Research*, vol. 35, no. 1, p. 32, 2016.
  - [26] W. Cui, L. Cheng, C. Hu, H. Li, Y. Zhang, and J. Chang, “Electrospun poly(L-lactide) fiber with ginsenoside Rg3 for inhibiting scar hyperplasia of skin,” *PLoS One*, vol. 8, no. 7, article e68771, 2013.
  - [27] Y. Peng, R. Zhang, L. Kong et al., “Ginsenoside Rg3 inhibits the senescence of prostate stromal cells through down-regulation of interleukin 8 expression,” *Oncotarget*, vol. 8, no. 39, pp. 64779–64792, 2017.
  - [28] J.-W. Jiang, X.-M. Chen, X.-H. Chen, and S.-S. Zheng, “Ginsenoside Rg3 inhibit hepatocellular carcinoma growth via intrinsic apoptotic pathway,” *World Journal of Gastroenterology*, vol. 17, no. 31, pp. 3605–3613, 2011.
  - [29] K.-S. Kim, H. Jung Yang, I.-S. Lee et al., “The aglycone of ginsenoside Rg3 enables glucagon-like peptide-1 secretion in enteroendocrine cells and alleviates hyperglycemia in type 2 diabetic mice,” *Scientific Reports*, vol. 5, no. 1, article 18325, 2015.
  - [30] X. Shan, Y.-S. Fu, F. Aziz, X.-Q. Wang, Q. Yan, and J.-W. Liu, “Ginsenoside Rg3 inhibits melanoma cell proliferation through down-regulation of histone deacetylase 3 (HDAC3) and increase of p53 acetylation,” *PLoS One*, vol. 9, no. 12, article e115401, 2014.
  - [31] S. I. Gum and M. K. Cho, “The amelioration of N-acetyl-p-benzoquinone imine toxicity by ginsenoside Rg3: the role of Nrf2-mediated detoxification and Mrp1/Mrp3 transports,” *Oxidative Medicine and Cellular Longevity*, vol. 2013, Article ID 957947, 11 pages, 2013.

## Research Article

# Gene Ontology and Expression Studies of Strigolactone Analogues on a Hepatocellular Carcinoma Cell Line

**Mohammed Nihal Hasan,<sup>1,2</sup> Syed Shoeb Razvi,<sup>1,3,4</sup> Hani Choudhry<sup>1,5,6</sup> Mohammed A. Hassan,<sup>1,7</sup> Said Salama Moselhy,<sup>1,8,9,10</sup> Taha Abdullallah Kumosani,<sup>1,9,11</sup> Mazin A. Zamzami<sup>1,5,6</sup> Khalid Omer Abualnaja,<sup>1,9,11</sup> Majed A. Halwani<sup>12</sup> Abdulrahman Labeed Al-Malki<sup>1,5</sup> Jiannis Ragoussis,<sup>13,14</sup> Wei Wu,<sup>15</sup> Christian Bronner,<sup>16</sup> Tadao Asami<sup>1,17</sup> and Mahmoud Alhosin<sup>1,5,6</sup>**

<sup>1</sup>Department of Biochemistry, Faculty of Science, King Abdulaziz University, Jeddah, Saudi Arabia

<sup>2</sup>Department of Biochemistry, All India Institutes of Medical Sciences, New Delhi, India

<sup>3</sup>MS Research Foundation, Hyderabad, India

<sup>4</sup>Department of Genetics, Vasavi Medical Research Center, Hyderabad, India

<sup>5</sup>Cancer Metabolism and Epigenetic Unit, Faculty of Science, King Abdulaziz University, Jeddah, Saudi Arabia

<sup>6</sup>Cancer and Mutagenesis Unit, King Fahd Medical Research Centre, King Abdulaziz University, Jeddah, Saudi Arabia

<sup>7</sup>Department of Basic Medical Sciences, College of Medicine and Health Sciences, Hadhramout University, Mukalla, Yemen

<sup>8</sup>Bioactive Natural Products Research Group, King Abdulaziz University, Jeddah, Saudi Arabia

<sup>9</sup>Experimental Biochemistry Unit, King Fahd Medical Research Center, King Abdulaziz University, Jeddah, Saudi Arabia

<sup>10</sup>Biochemistry Department, Faculty of Science, Ain Shams University, Cairo, Egypt

<sup>11</sup>Production of Bioproducts for Industrial Applications Research Group, King Abdulaziz University, Jeddah, Saudi Arabia

<sup>12</sup>Nanomedicine Department, King Abdullah International Medical Research Center (KAIMRC), King Saud bin Abdulaziz University for Health Sciences, Riyadh, Saudi Arabia

<sup>13</sup>Department of Human Genetics, McGill University, Montréal, QC, Canada H3A 0C7

<sup>14</sup>McGill University and Genome Québec Innovation Centre, Montréal, QC, Canada H3A 1A4

<sup>15</sup>Department of Medicine, University of California, San Francisco, CA 94143, USA

<sup>16</sup>Institut de Génétique et de Biologie Moléculaire et Cellulaire (IGBMC), INSERM U1258 CNRS UMR 7104, Université de Strasbourg, Illkirch, France

<sup>17</sup>Graduate School of Agricultural and Life Sciences, The University of Tokyo, Bunkyo, Tokyo 112-8657, Japan

Correspondence should be addressed to Majed A. Halwani; [halawanima@ngha.med.sa](mailto:halawanima@ngha.med.sa), Tadao Asami; [brassinazole@gmail.com](mailto:brassinazole@gmail.com), and Mahmoud Alhosin; [malhaseen@kau.edu.sa](mailto:malhaseen@kau.edu.sa)

Received 25 December 2018; Accepted 8 May 2019; Published 4 August 2019

Guest Editor: Xinhua Chen

Copyright © 2019 Mohammed Nihal Hasan et al. This is an open access article distributed under the Creative Commons Attribution License, which permits unrestricted use, distribution, and reproduction in any medium, provided the original work is properly cited.

Human hepatocellular carcinoma (HCC) is the most common and recurrent type of primary adult liver cancer without any effective therapy. Plant-derived compounds acting as anticancer agents can induce apoptosis by targeting several signaling pathways. Strigolactone (SL) is a novel class of phytohormone, whose analogues have been reported to possess anticancer properties on a panel of human cancer cell lines through inducing cell cycle arrest, destabilizing microtubular integrity, reducing damaged in the DNA repair machinery, and inducing apoptosis. In our previous study, we reported that a novel SL analogue, TIT3, reduces HepG2 cell proliferation, inhibits cell migration, and induces apoptosis. To decipher the mechanisms of TIT3-induced anticancer activity in HepG2, we performed RNA sequencing and the differential expression of genes was analyzed using different tools. RNA-Seq data showed that the genes responsible for microtubule organization such as TUBB, BUB1B, TUBG2,

TUBGCP6, TPX2, and MAP7 were significantly downregulated. Several epigenetic modulators such as UHRF1, HDAC7, and DNMT1 were also considerably downregulated, and this effect was associated with significant upregulation of various proapoptotic genes including CASP3, TNF- $\alpha$ , CASP7, and CDKN1A (p21). Likewise, damaged DNA repair genes such as RAD51, RAD52, and DDB2 were also significantly downregulated. This study indicates that TIT3-induced antiproliferative and proapoptotic activities on HCC cells could involve several signaling pathways. Our results suggest that TIT3 might be a promising drug to treat HCC.

## 1. Introduction

In 2012, 0.8 million patients were diagnosed with liver cancer, the seventh highest age-related incidence rate globally [1]. Human hepatocellular carcinoma (HCC) is the most common type of primary liver cancer in adults, as well as the most frequently recurrent malignancy without any effective therapy [2, 3]. HCC is the third most common cancer-related cause of mortality globally [1]. Several etiological factors could lead to the development of HCC including hepatitis B virus (HBV), hepatitis C virus (HCV), alcohol, cirrhosis, and nonalcoholic fatty liver disease (NAFLD) [1].

There exists an inveterate history of compounds, derived from plants, serving as anticancer agents [4]. These compounds can exert their inhibitory effects on cancer cells by targeting several pathways including cell cycle arrest, cell proliferation, and apoptosis. Strigolactones (SLs) are a novel class of phytohormones, which control the branching of shoot architecture by hindering growth and self-renewal of axillary meristem cells [5, 6]. It has previously been reported that synthetic SL analogues instigate G2/M cell cycle arrest and apoptosis by regulating the p38 and JNK1/2 MAPKs signaling pathways, causing the induction of stress in an array of solid and nonsolid human cancer cells, including prostate, colon, leukemia, osteosarcoma, and lung cancer cell lines.

It has only slight effects on the growth, survival, and viability of nontransformed human fibroblasts, healthy primary prostate cells, and mammary epithelial cells [7, 8]. SL analogues demonstrated their anticancer effects in a xenograft model of breast cancer [9] and have also been shown to affect the integrity of the microtubule network by impeding the migration of highly invasive breast cancer cell lines [9].

Recently, SL analogues have been found to destabilize the genomic DNA of cancer cells by inducing DNA double-strand breaks (DSBs) and activating the DNA damage and simultaneously hindering DNA repair, resulting in cell death. It is noteworthy that these activities of SL analogues have not been reported in nontransformed BJ fibroblast cells [10]. Furthermore, the efficiency of the delivery of SL analogues (hence their therapeutic efficacy) to prostate cancer cells may get enhanced by encapsulation of SL analogues in glutathione/pH-responsive nanosponges [11].

Synthetic SL analogues have been reported to downregulate RAD51 expression through ubiquitination in a proteasome-dependent way, hence, reducing the localization of RAD51 to DSB sites [10]. RAD51 is a crucial component of a prominent DNA repair pathway, the homology-directed repair (HDR) machinery. Overexpression of RAD51 causes an increase in DNA repair activity,

which could result in resistance to DNA damage that is usually imposed by radiotherapy or chemotherapy [12, 13].

In our previous study, we found that the newly synthesized SL analogue, TIT3, inhibits proliferation and induces apoptosis of HepG2 (hepatocellular carcinoma) cells with minimal effects on healthy cells [14]. The molecular structure of TIT3 is shown in Figure 1.

In the present study, we performed RNA sequencing and the differential expression of genes was analyzed using different tools to analyze and investigate the differential gene expression of HepG2 cells treated with TIT3 and to disclose the possible signaling pathways leading to the inhibition of cell proliferation and induction of apoptosis.

## 2. Materials and Methods

**2.1. Cell Culture and Treatment.** HepG2 cells were obtained from ATCC (Manassas, Virginia, USA). These cells were then sustained at 37°C, in a humidified incubator, at 5% CO<sub>2</sub>. DMEM (UFC Biotech, Riyadh, KSA) supplemented with 10% fetal bovine serum (FBS) (LifeTech, catalogue no: 16000-044) and 1% (100 U/ml) penicillin-streptomycin (LifeTech, catalogue no: 15140-122) was used to maintain cells.

**2.2. RNA-Seq, Differentially Expressed Genes, and Bioinformatics Analysis.** HepG2 cells were treated with 60  $\mu$ M of SL analogue TIT3 (IC<sub>50</sub> of 63.46  $\mu$ M) [14] for 24 hours, in triplicate. An RNeasy kit (QIAGEN) was used to extract the total RNA, and the concentration of RNA was quantified. A bioanalyzer was used to analyze the quality of the total RNA (RIN score > 7.0). Sequencing libraries were then generated using TruSeq Stranded mRNA Sample Preparation Kits (Illumina, CA) from 2500 ng of the total RNA from each of the three replicates. The Illumina HiSeq 2000 system was used to conduct 50 bp long single-end deep sequencing. The FASTX-Toolkit was used to remove the adaptor sequence and filtering of low-quality base call and low-quality reads. The short filtered sequencing reads that were acquired were mapped to the human genome by the TopHat2 and Subreads package; the featureCounts function was used to quantify the gene expression values. These gene expression values were then used to calculate the size of the library and dataset dispersion for the analysis of differentially expressed genes [15]. Differential gene expression was examined using the R/Bioconductor package edgeR and established by log fold change (LogFC) and false discovery rate (FDR) (LogFC  $\geq$  1 or  $\leq$  -1; FDR  $\leq$  0.05).

**2.3. Bioinformatics Analysis.** The gene set functional analysis and pathway analysis were analyzed using the gene ontology

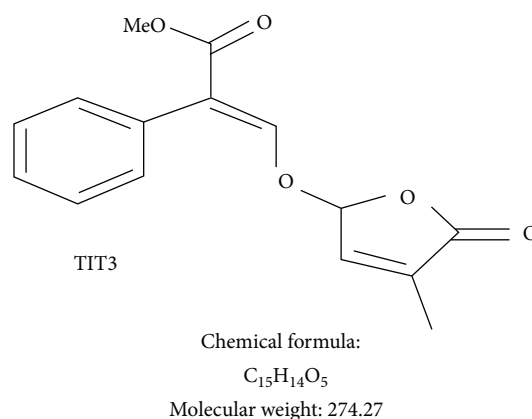


FIGURE 1: Molecular structure, chemical formula, and molecular weight of SL analogue TIT3.

TABLE 1: Classification based on  $p$  values; total number of transcripts altered in TIT3-treated HepG2 cells.

Range of $p$ value of genes in the transcriptome	Number of upregulated transcript genes	Range of upregulated LogFC	Number of downregulated transcript genes	Range of downregulated LogFC
$\leq 0.05$	1026	+1 to +7	968	-6.63 to -1.5
$\leq 0.01$	293	+1.5 to 7.3	511	-7.28 to -1.5
$\leq 0.001$	154	+1.55 to 12.47	288	-7.99 to -1.5

TABLE 2: Classification based on log fold change (LogFC) values; total number of transcripts altered in TIT3-treated HepG2 cells.

LogFC of the genes in transcriptome	Number of transcript-upregulated genes	LogFC	Number of transcript-downregulated genes	Range of $p$ values
+12.5 to +3	503	-8 to -3	290	$\leq 0.05$
+2.9 to +2	478	-2.9 to -2	693	$\leq 0.05$
+1.5 to +1.9	491	-1.5 to -1.99	810	$\leq 0.05$

(GO) and KEGG pathway. The gene IDs of interest were converted to EntrezID and uploaded to DAVID bioinformatics tools. GO and KEGG pathway analysis were performed by setting all the GO terms and KEGG pathway genes as background genes. Overrepresented GO terms or pathways are determined by the enrichment score (EASE  $\leq 0.1$ , gene count  $\geq 2$ ).

### 3. Results

**3.1. Gene Expression Is Regulated by TIT3.** Data obtained from HepG2 cells treated with 60  $\mu\text{M}$  of SL analogue of TIT3 revealed that the mRNA expression of 3240 genes was modulated, with 1473 genes being upregulated (log fold change  $< 1.5$ ;  $p < 0.05$ ) and 1767 genes being downregulated (log fold change  $> -1.5$ ;  $p < 0.05$ ). The number of altered transcripts has been organized based on the log fold change (LogFC) or the  $p$  value (Tables 1 and 2). Overall, the number of transcripts being upregulated was fewer than the number of transcripts being downregulated.

**3.2. Gene Enrichment Analysis of Altered Transcripts.** The gene enrichment analysis of gene ontology (GO) terms ( $p < 0.0001$ ) revealed that there was a significant increase in the negative regulation of transcription by the RNA polymerase II promoter and negative regulation of G1/S transition of mitosis and a substantial decrease in the damaged DNA repair genes. A summary of GO analysis with different biological processes, cell components, and molecular functions of upregulated and downregulated transcripts in HepG2 cells treated with TIT3 is shown in Figures 2 and 3, respectively.

**3.3. KEGG Pathway Analysis.** The KEGG pathway analysis revealed the probability of the involvement of apoptosis pathways involving TNF and PI3K-Akt (Figures 4–6). There was a significant decrease in the genes involved in the organization of microtubules such as BUB1B, TUBB, TUBG2, TUBGCP6, TPX2, and MAP7 (LogFC  $< -2.0$ ;  $p < 0.0001$ ). A significant decrease was also found in the expression levels of crucial epigenetic players UHRF1, DNMT1, and HDAC7, known to inhibit the expression of several tumor suppressor genes in cancer (LogFC  $< -1.7$ ;  $p < 0.001$ ).

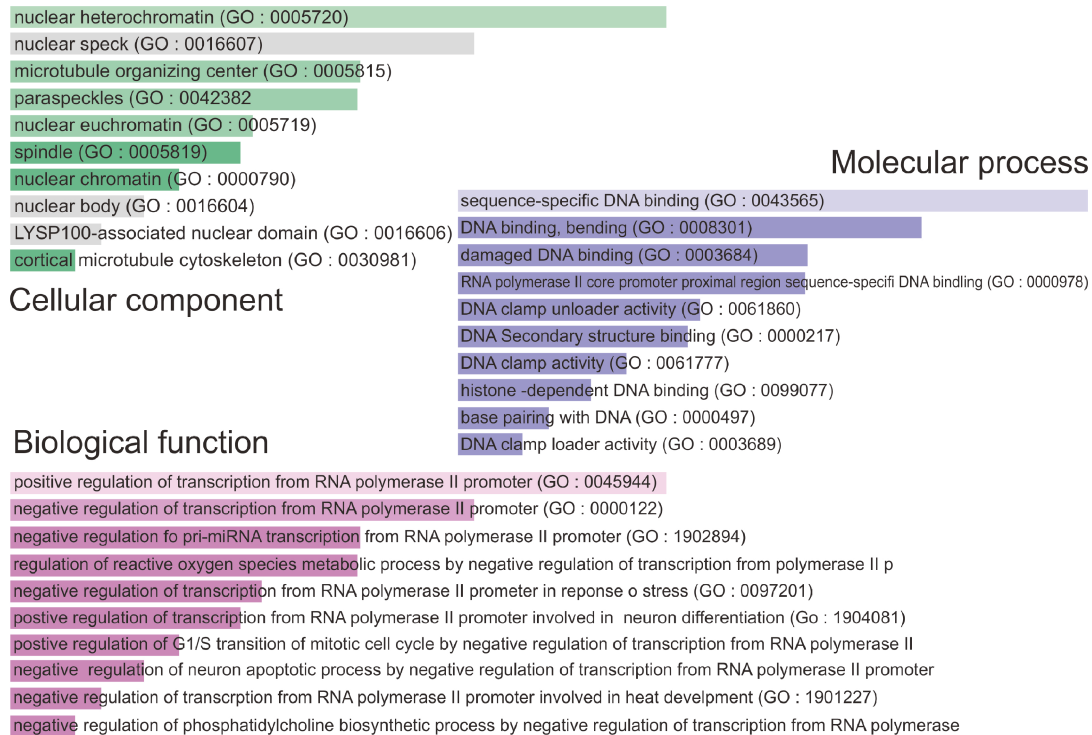


FIGURE 2: Gene ontology (GO) of upregulated genes in TIT3-treated HepG2 cells. The bar length represents the significance of that specific gene set or term, and the degree of the brightness of the color denotes the significance ( $p < 0.001$ ) of the differentially expressed genes.

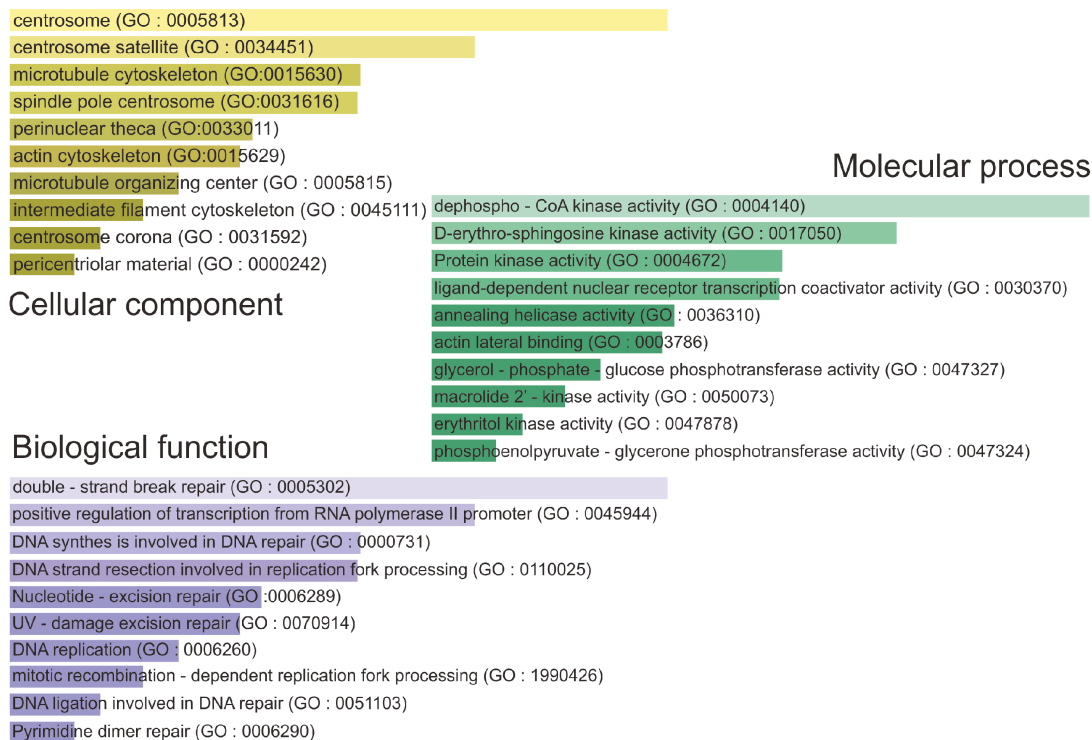


FIGURE 3: Gene ontology (GO) of downregulated genes in TIT3-treated HepG2 cells. The bar length represents the significance of that specific gene set or term, and the degree of the brightness of the color denotes the significance ( $p < 0.001$ ) of the differentially expressed genes.

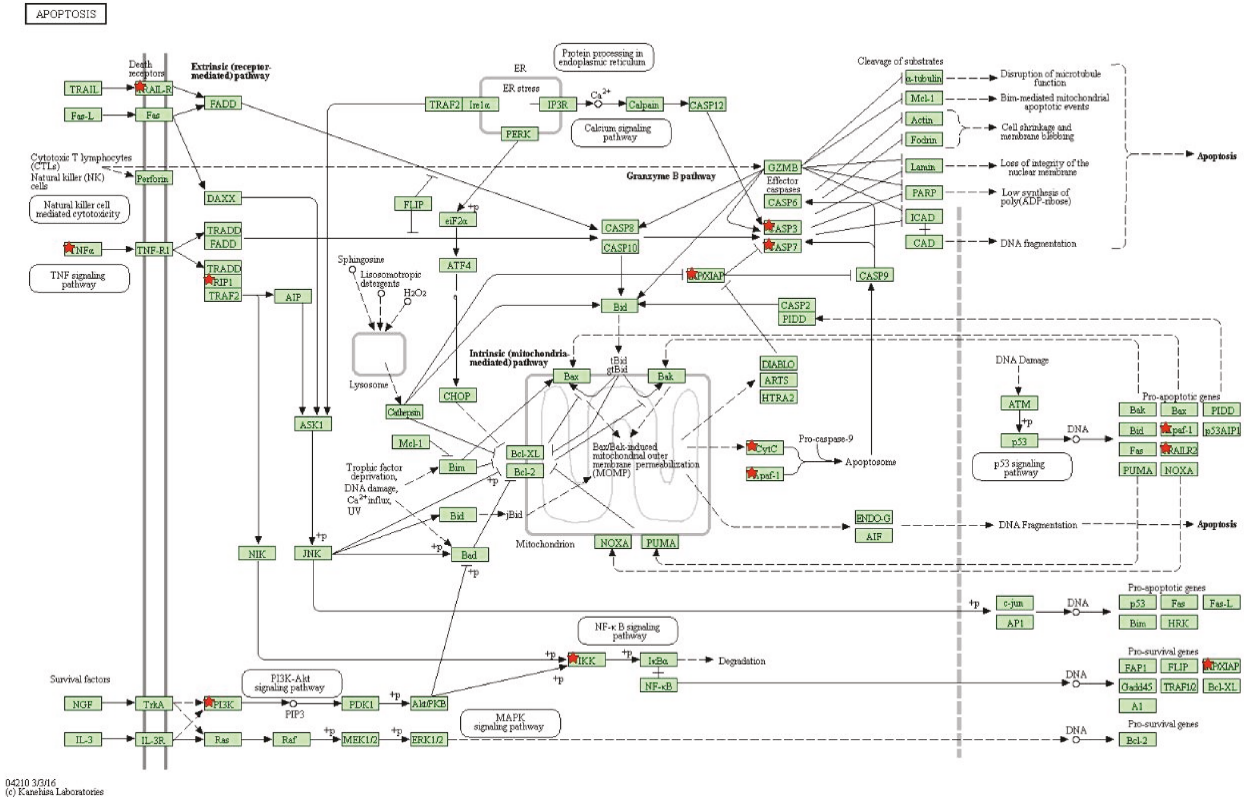


FIGURE 4: Analysis of the KEGG pathway in HepG2 cells after treatment with TIT3 illustrating the upregulated genes in apoptosis pathways; the genes regulated are marked.

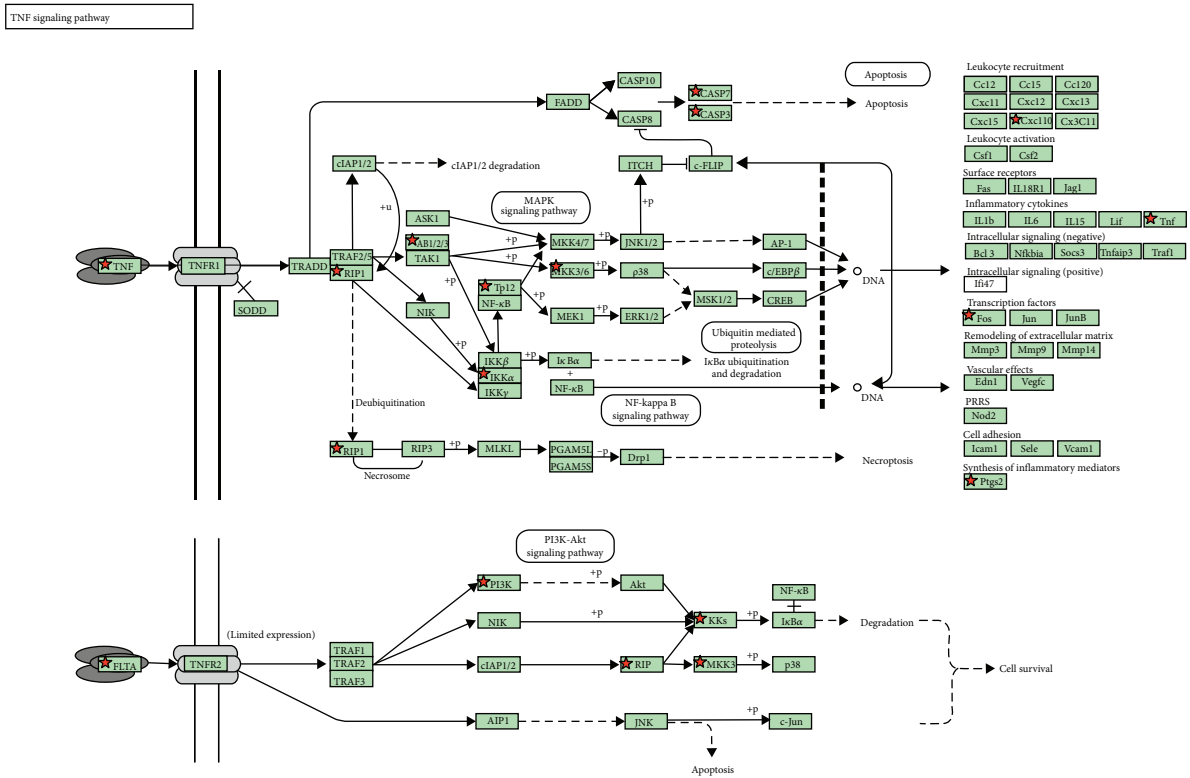


FIGURE 5: KEGG pathway analysis for HepG2 cells depicting the upregulated genes in the TNF signaling pathway after the treatment with TIT3; the altered genes are marked.

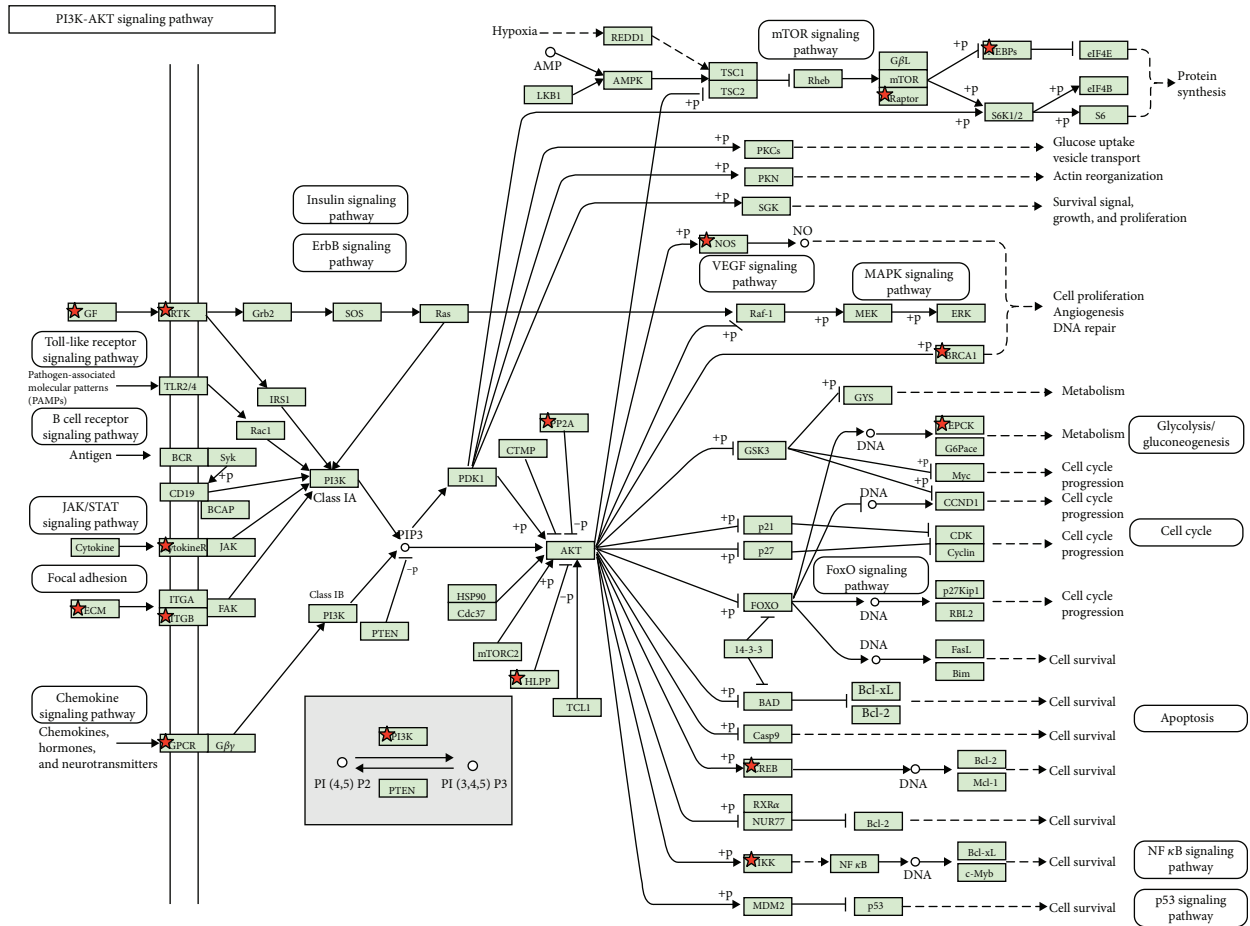


FIGURE 6: Significantly downregulated genes in the PI3K/Akt pathway after the treatment of HepG2 cells with TIT3 in this KEGG pathway analysis; the depicted downregulated genes are marked.

TABLE 3: Downregulated genes in TIT3-treated HepG2 cells as compared with untreated cells.

Genes	LogFC	p value
BUB1B	-2.018	3.71E-05
TUBB	-2.247	3.03E-06
TUBG2	-2.271	8.41E-06
TUBGCP6	-2.582	6.82E-06
TPX2	-2.054	2.44E-05
MAP7	-2.185	4.42E-05
UHRF1	-2.627	4.63E-06
DNMT1	-1.867	1.16E-04
HDAC7	-2.103	4.96E-05
KAT7	-2.026	4.65E-05
DDB2	-2.351	5.80E-06
RAD51	-2.463	1.29E-05
RAD52	-7.507	3.78E-04

\*Fold change treated vs control.

Additionally, genes responsible for DNA damage repair including DDB2, RAD51, and RAD52 were substantially downregulated (Table 3). The expression levels of several tumor suppressor genes such as NKX-3, FLCN, ING1,

TABLE 4: Upregulated genes in TIT3-treated HepG2 cells as compared with untreated cells.

Genes	LogFC	p value
CASP3	3.506	2.35E-11
CASP7	1.605	2.36E-03
TNF-α	4.686	6.96E-08
LTA (TNF-β)	8.148	1.02E-05
MOAP1	2.131	1.95E-04
CDKN1A (p21)	2.420	7.69E-07
NKX3-1	2.522	1.89E-06
FLCN	2.556	5.82E-07
ING1	2.094	3.43E-05
SIK1	3.947	1.70E-13
TP53INP1	3.046	3.08E-09

\*Fold change treated vs control.

SIK1, and TP53INP1 (LogFC > 2.0; p < 0.001), and genes exhibiting proapoptotic activities such as TNF-α, LTA (TNF-β), CASP3, MOAP1, and CASP7 (LogFC > 1.6; p < 0.01) as well as genes having antiproliferative effects such as CDKN1A (p21) (LogFC > 2.2; p < 0.001) were significantly increased in response to TIT3 treatment (Table 4).

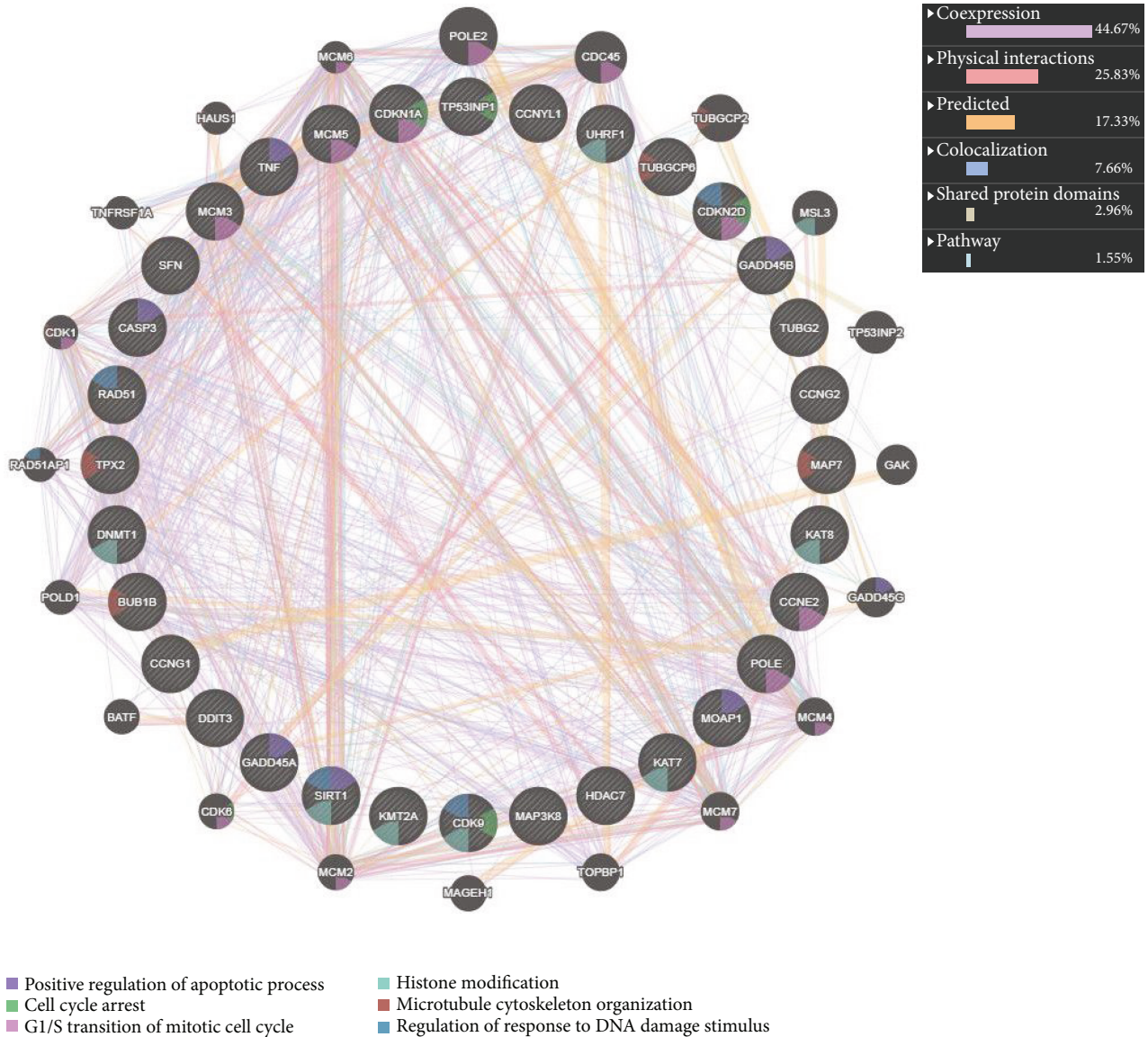


FIGURE 7: Outline of the interactions of different altered genes with their functions in HepG2 cells after treatment with TIT3.

Figure 7 shows the probable interactions of genes of the different transcriptional regulators, and Figure 8 depicts a heat map, representing the comprehensive regulation of gene expressions in terms of their  $p$  values and LogFC.

#### 4. Discussion

Synthetic SL analogues have been reported to induce cell cycle arrest and apoptosis in both solid and hematological tumors by targeting several signaling pathways [7, 8]. Our previous study showed that synthetic SL analogue TIT3 inhibited the proliferation and migration and induced apoptosis of HepG2 cells with minimal toxicity towards healthy noncancerous cells [14]. Since TIT3 impeded the migration of HepG2 cells, we suggested that such an effect is a result of the interference with the organization of the microtubular network. Data obtained from RNA-Seq showed significant downregulation of BUB1B, TUBB,

TUBG2, TUBGCP6, TPX2, and MAP7 genes, which are known to be involved in the microtubular organization, suggesting that the antimetastatic and proapoptotic effects of TIT3 could be challenged by mechanisms involved in the organization of microtubules. Our results are consistent with several studies showing that SL analogues can induce apoptosis in breast cancer cells [9]. Other cancer cell lines such as melanoma, colon, lung, prostate, and osteosarcoma were also reported to be affected by SL analogues through targeting of the microtubular network [8].

Furthermore, our results showed that the histone deacetylase 7 (HDAC7) was downregulated in response to TIT3 treatment. Interestingly, the unusual activity of the histone deacetylases including HDAC7 has been reported in many types of cancers [16]. HDAC inhibitors such as TSA, SAHA, and MS-275 are useful in the chemotherapeutic regimens of many cancers including HCC and significantly inhibit cell proliferation, and migration/invasion

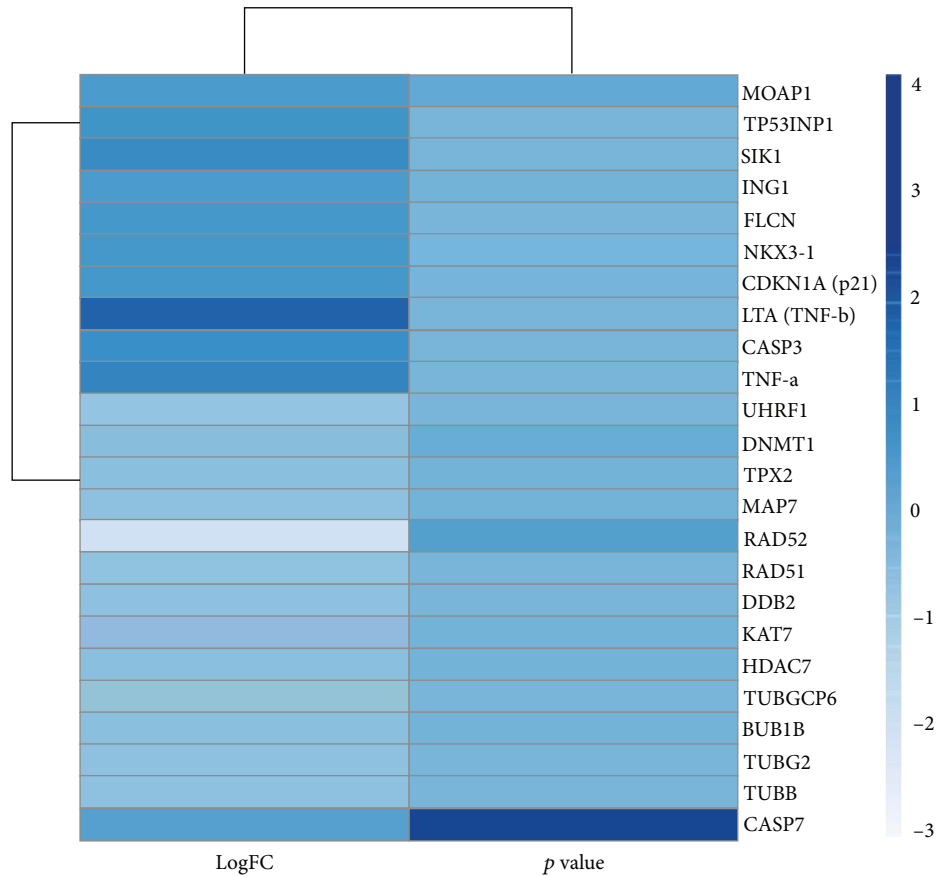


FIGURE 8: The heat map of the significantly deregulated genes represents the change with the intensity of the variation in color; with the alteration of LogFC (fold change) from -3 to +4 in TIT3-treated HepG2 cells as compared to untreated cells.

induces cell cycle arrest and apoptosis of HCC [17]. Knock-down of HDAC7 led to G1/S arrest in different cancer cells through the upregulation of the cell cycle inhibitor CDKN1A (p21). Interestingly, an increase in the expression levels of p21 mRNA has also been observed in TIT3-treated HepG2 cancer cell lines [18]. All the evidences above suggest that TIT3 could act as a HDAC inhibitor causing cell cycle arrest through a p21-dependent mechanism inducing inhibition of HepG2 cell proliferation.

Moreover, UHRF1, a well-documented regulator of gene expression in cancer [19, 20], was downregulated by TIT3 suggesting that UHRF1 could be a potent target for TIT3 in HCC. In alignment with our results, UHRF1 overexpression has been demonstrated to cause tumorigenesis in different cancer types including HCC [21]. UHRF1 inhibition by using pharmacological compounds is associated with the reactivation of various tumor suppressor genes, thus suppressing the proliferation of cancer cells by inducing apoptosis [22].

Double-strand breaks (DSBs) are the most notable form of DNA damage, and once the DSBs are formed, cells may undergo either of the two repair mechanisms: nonhomologous end joining (NHEJ) or homology-directed repair (HDR) [23, 24]. Previous studies have revealed that cancer cells which lack HDR are quite sensitive to DNA-damaging agents [25]. Our data obtained from RNA-Seq showed that TIT3 induced the downregulation of damaged DNA repair

genes including DDB2, RAD51, and RAD52. Therefore, TIT3 could be an inhibitor of DNA repair proteins. In support of our results, the evidence is available in the literature that SL analogues can hamper HDR and impair DSB repair [10].

Caspase 3 (CASP 3) is known as an executioner caspase in apoptosis resulting in the inhibition of proliferation of HepG2 cancer cells [26]. TNF- $\alpha$  is also known to modulate proliferation, differentiation, and apoptosis or necrotic cell death in several different cell types including HepG2 cancer cells [27, 28]. Our results illustrated that the primary genes responsible for apoptosis including CASP 3, CASP 7, TNF- $\alpha$ , TNF- $\beta$ , and MOAP1 were significantly upregulated by TIT3 treatment on HepG2 cancer cells.

Overall, we propose that the inhibition of HepG2 cancer cell growth was due to an interplay of genes wherein the treatment of TIT3 significantly altered their expression levels. Altered gene expressions affected cell proliferation, cell cycle, metastasis, and apoptosis. TIT3 could also be an inhibitor of HDAC and can target the organization of the microtubular network as well as affect the genes involved in DNA repair.

## 5. Conclusion

We provided evidence that TIT3 targets several critical pathways in HepG2 cells. Therefore, to obtain and establish

a deeper understanding of the molecular mechanisms exerted by TIT3, molecular biology techniques such as Western blotting, qPCR, microarray, and proteomics must be done to reveal the specific targets.

### Data Availability

The data used to support the findings of this study are available from the corresponding author upon request.

### Disclosure

The data and material presented in this manuscript neither have been published before nor have been submitted for publication to another scientific journal or are being considered for publication elsewhere.

### Conflicts of Interest

The authors have no relevant affiliations or financial involvement with any organization or entity with a financial interest in or financial conflict with the subject matter or materials discussed in the manuscript. This includes employment, consultancies, honoraria, stock ownership, grants, or patents received or pending and royalties.

### Authors' Contributions

MNH, SR, and MAH conducted experiments under the supervision of MA, TA, and HC. JR, WW, and SM analyzed the data. MA, MH, SR, CB, and MZ wrote most of the manuscript. SSM, AA, TK, and KA applied for funding and helped in the data analysis. All authors read and approved the final manuscript.

### Acknowledgments

The authors acknowledge the technical support from the Deanship of Scientific Research, King Abdulaziz University, Jeddah, and KFMRC for providing the RNA-Seq facility. This work was funded by the Deanship of Scientific Research (DSR), King Abdulaziz University, Jeddah, under grant no. RG-43-130-40. The authors, therefore, acknowledge with thanks DSR for the technical and financial support.

### References

- [1] Y. A. Ghouri, I. Mian, and J. H. Rowe, "Review of hepatocellular carcinoma: epidemiology, etiology, and carcinogenesis," *Journal of Carcinogenesis*, vol. 16, no. 1, p. 1, 2017.
- [2] C.-J. Liu, J.-H. Yang, F.-Z. Huang et al., "The role of MiR-99b in mediating hepatocellular carcinoma invasion and migration," *European Review for Medical and Pharmacological Sciences*, vol. 22, no. 8, pp. 2273–2281, 2018.
- [3] V. Zahir, M. N. Niki, P. Hajian, F. H. Shirazi, and H. Mirzaei, "Evaluation of silibinin effects on the viability of HepG2 (human hepatocellular liver carcinoma) and HUVEC (human umbilical vein endothelial) cell lines," *Iranian Journal of Pharmaceutical Research*, vol. 17, no. 1, pp. 261–267, 2018.
- [4] D. J. Newman and G. M. Cragg, "Advanced preclinical and clinical trials of natural products and related compounds from marine sources," *Current Medicinal Chemistry*, vol. 11, no. 13, pp. 1693–1713, 2004.
- [5] V. Gomez-Roldan, S. Fermas, P. B. Brewer et al., "Strigolactone inhibition of shoot branching," *Nature*, vol. 455, no. 7210, pp. 189–194, 2008.
- [6] M. Umehara, A. Hanada, S. Yoshida et al., "Inhibition of shoot branching by new terpenoid plant hormones," *Nature*, vol. 455, no. 7210, pp. 195–200, 2008.
- [7] C. B. Pollock, H. Koltai, Y. Kapulnik, C. Prandi, and R. I. Yarden, "Strigolactones: a novel class of phytohormones that inhibit the growth and survival of breast cancer cells and breast cancer stem-like enriched mammosphere cells," *Breast Cancer Research and Treatment*, vol. 134, no. 3, pp. 1041–1055, 2012.
- [8] C. B. Pollock, S. McDonough, V. S. Wang et al., "Strigolactone analogues induce apoptosis through activation of P38 and the stress response pathway in cancer cell lines and in conditionally reprogrammed primary prostate cancer cells," *Oncotarget*, vol. 5, no. 6, pp. 1683–1698, 2014.
- [9] E. Mayzlish-Gati, D. Laufer, C. F. Grivas et al., "Strigolactone analogs act as new anti-cancer agents in inhibition of breast cancer in xenograft model," *Cancer Biology and Therapy*, vol. 16, no. 11, pp. 1682–1688, 2015.
- [10] M. P. Croglio, J. M. Haake, C. P. Ryan et al., "Analogues of the novel phytohormone, strigolactone, trigger apoptosis and synergize with PARP inhibitors by inducing DNA damage and inhibiting DNA repair," *Oncotarget*, vol. 7, no. 12, pp. 13984–14001, 2016.
- [11] M. Argenziano, C. Lombardi, B. Ferrara et al., "Glutathione/PH-responsive nanosponges enhance strigolactone delivery to prostate cancer cells," *Oncotarget*, vol. 9, no. 88, pp. 35813–35829, 2018.
- [12] D. Schild and C. Wiese, "Overexpression of RAD51 suppresses recombination defects: a possible mechanism to reverse genomic instability," *Nucleic Acids Research*, vol. 38, no. 4, pp. 1061–1070, 2010.
- [13] A. Ward, K. K. Khanna, and A. P. Wiegman, "Targeting homologous recombination, new pre-clinical and clinical therapeutic combinations inhibiting RAD51," *Cancer Treatment Reviews*, vol. 41, no. 1, pp. 35–45, 2015.
- [14] M. N. Hasan, H. Choudhry, S. S. Razvi et al., "Synthetic strigolactone analogues reveal anti-cancer activities on hepatocellular carcinoma cells," *Bioorganic and Medicinal Chemistry Letters*, vol. 28, no. 6, pp. 1077–1083, 2018.
- [15] Y. Lu, N. Starkey, W. Lei et al., "Inhibition of hedgehog-signaling driven genes in prostate cancer cells by *Sutherlandia frutescens* extract," *PLoS One*, vol. 10, no. 12, article e0145507, 2015.
- [16] W. Weichert, "HDAC expression and clinical prognosis in human malignancies," *Cancer Letters*, vol. 280, no. 2, pp. 168–176, 2009.
- [17] S.-O. Kim, B.-T. Choi, I.-W. Choi et al., "Anti-invasive activity of histone deacetylase inhibitors via the induction of Egr-1 and the modulation of tight junction-related proteins in human hepatocarcinoma cells," *BMB Reports*, vol. 42, no. 10, pp. 655–660, 2009.
- [18] K. Qu, T. Lin, J. Wei et al., "Cisplatin induces cell cycle arrest and senescence via upregulating P53 and P21 expression in HepG2 cells," *Journal of Southern Medical University*, vol. 33, no. 9, pp. 1253–1259, 2013.
- [19] P. Bashtrykov, G. Jankevicius, R. Z. Jurkowska, S. Ragozin, and A. Jeltsch, "The UHRF1 protein stimulates the activity and

- specificity of the maintenance DNA methyltransferase DNMT1 by an allosteric mechanism," *The Journal of Biological Chemistry*, vol. 289, no. 7, pp. 4106–4115, 2014.
- [20] C. Bianchi and R. Zangi, "UHRF1 discriminates against binding to fully-methylated CpG-sites by steric repulsion," *Biophysical Chemistry*, vol. 171, pp. 38–45, 2013.
- [21] R. Mudbhary, Y. Hoshida, Y. Chernyavskaya et al., "UHRF1 overexpression drives DNA hypomethylation and hepatocellular carcinoma," *Cancer Cell*, vol. 25, no. 2, pp. 196–209, 2014.
- [22] M. Alhosin, T. Sharif, M. Mousli et al., "Down-regulation of UHRF1, associated with re-expression of tumor suppressor genes, is a common feature of natural compounds exhibiting anti-Cancer properties," *Journal of Experimental & Clinical Cancer Research*, vol. 30, no. 1, p. 41, 2011.
- [23] F. Liang, M. Han, P. J. Romanienko, and M. Jasin, "Homology-directed repair is a major double-strand break repair pathway in mammalian cells," *Proceedings of the National Academy of Sciences of the United States of America*, vol. 95, no. 9, pp. 5172–5177, 1998.
- [24] M. Zimmermann and T. de Lange, "53BP1: pro choice in DNA repair," *Trends in Cell Biology*, vol. 24, no. 2, pp. 108–117, 2014.
- [25] C. J. Lord and A. Ashworth, "The DNA damage response and cancer therapy," *Nature*, vol. 481, no. 7381, pp. 287–294, 2012.
- [26] Y. Kondoh, T. Kawada, and R. Urade, "Activation of caspase 3 in HepG2 cells by elaidic acid (T18:1)," *Biochimica et Biophysica Acta*, vol. 1771, no. 4, pp. 500–505, 2007.
- [27] J. Chen, X. Sun, T. Xia, Q. Mao, and L. Zhong, "Pretreatment with dihydroquercetin, a dietary flavonoid, protected against concanavalin A-induced immunological hepatic injury in mice and TNF- $\alpha$ /ActD-induced apoptosis in HepG2 cells," *Food & Function*, vol. 9, no. 4, pp. 2341–2352, 2018.
- [28] L. A. Tartaglia and D. V. Goeddel, "Two TNF receptors," *Immunology Today*, vol. 13, no. 5, pp. 151–153, 1992.

## Research Article

# Dynamics of the *O. felineus* Infestation Intensity and Egg Production in Carcinogenesis and Partial Hepatectomy in the Setting of Superinvasive Opisthorchiasis

Vitaly G. Bychkov,<sup>1</sup> Ludmila F. Kalyonova,<sup>2</sup> Elena D. Khadieva,<sup>3</sup> Semen D. Lazarev,<sup>1</sup> Ilgiz R. Lukmanov,<sup>3</sup> Vladimir A. Shidin,<sup>1</sup> and Evgeny N. Morozov <sup>4,5</sup>

<sup>1</sup>Tyumen State Medical University, Tyumen, Russia

<sup>2</sup>Tyumen Scientific Centre, Tyumen, Russia

<sup>3</sup>Khanty-Mansiysk State Medical Academy, Khanty-Mansiysk, Russia

<sup>4</sup>Sechenov University, Moscow, Russia

<sup>5</sup>Russian Medical Academy of Continuing Professional Education, Moscow, Russia

Correspondence should be addressed to Evgeny N. Morozov; emorozov@mail.ru

Received 31 December 2018; Revised 20 May 2019; Accepted 10 June 2019; Published 24 July 2019

Guest Editor: Zhigang Ren

Copyright © 2019 Vitaly G. Bychkov et al. This is an open access article distributed under the Creative Commons Attribution License, which permits unrestricted use, distribution, and reproduction in any medium, provided the original work is properly cited.

Clinical and experimental studies have shown that opisthorchii tend to evade tumour growth foci to colonize more distant areas of the liver. When modelling tumours with various carcinogens in the setting of superinvasive opisthorchiasis, the intensity of invasion is reduced both before the formation of neoplasms (>120 days) and after the development of tumours of various histogeneses (liver, pancreas, and stomach) (>240 days). Egg production was observed to increase with the decrease in the number of parasites in the liver. The smallest changes in the infestation intensity indicators and egg production were observed in the experimental stomach tumours ( $p > 0.05$ ). A partial hepatectomy in the setting of opisthorchiasis did not affect the number of parasites in the ecological niche (liver) or the production of eggs by the helminth. With the deterioration of the vegetation state, parasite clumps of opisthorchii increase egg production under the conditions of distress.

## 1. Introduction

Human opisthorchiasis is a parasitic disease discovered by Professor K.N. Vinogradov in 1891 in the city of Tomsk (Eastern Siberia), the causative agent of the disease—the trematode *Opisthorchis felineus*, Rivolta, 1884. The literature describes the changes in the internal organs with this helminthiasis [1]: features of tissue regeneration and development of atherosclerosis [2, 3]; pathologies of the liver and pancreas, where parasites vegetate [4, 5]; and morphological changes in the lungs with SO [6]. Of particular importance is the study of the cardiovascular system in opisthorchiasis invasion with repeated infections [7, 8]. Currently, the role of superinvasive opisthorchiasis in the development of liver malignant neoplasms, which in the hyperendemic foci of helminthiasis are significantly more frequent than in regions

without this invasion, has been identified: CO is a strong promoter in the carcinogenesis of not only the liver but also the pancreas, stomach, and other organs [9, 10]. The aim of the current study is to identify patterns of the intensity of the invasion and egg production of *Opisthorchis felineus* in the carcinogenesis of various organs and partial hepatectomy in the setting of superinvasive opisthorchiasis.

## 2. Materials and Methods

According to the data from postmortem examinations, loci of *O. felineus* vegetation were found in the liver in superinvasion ( $n = 88$ ), liver cancer ( $n = 42$ ), pancreas ( $n = 18$ ), and gastrointestinal stomach tumours (GIST) ( $n = 29$ ) in the setting of SO. In this study, tumours were simulated by chemical carcinogens: N-DMNA, N-DENA, N-MNNG, NDMM, NDOP,

and DMBA (N-dimethylnitrosamine, N-diethylnitrosamine, and N-diethyl-ironitroso-guanidine, 2,6-nitrosodimethylmorpholine, 2,2-nitrozodioxypropylalanine, etc.). Repeated infestations occurred on days 16, 32, 60, 120, and 240 after the primary infection. Methodological aspects of tumour modeling in the setting of SO were published previously [11].

Partial hepatectomy in Syrian hamsters ( $n = 48$ ) was performed by removing a liver lobe, which accounted for 17.3-17.7% of the organ weight. The opisthorchiasis and SO model was developed in mature Syrian hamsters ( $n = 280$ ) weighing 98.0-110.0 g. The larvae of opisthorchii were prepared by means of artificial gastric juice (pepsin+hydrochloric acid+water) according to the method of Glazkov [12]. The invasive material, *O. felineus* metacercariae, was introduced into the stomach; repeated infestations were performed 16 and 32 days after the primary infection. The animals were etherized (lethal overdose). The reproductive activity of opisthorchii was determined by the native smear, Fülleborn, and Thalemann methods. The infestation intensity was determined via incomplete helminthological dissection of animals according to K.I. Skryabin.

Liver and stomach preparations were stained with Mayer's haematoxylin and eosin according to Van Gieson and with alcian blue and Schiff's reagent according to McManus. The IHC test was performed with antibodies against the CD117, DOGI, and CD34 protein receptors and cytokeratins 7 and 19 according to the manufacturer's recommendations (Leica Biosystems and Spring Biosciences; the ultrastructural study was performed on a JEM-1011 microscope (Japan)).

Animal experiments were carried out in accordance with the principles set forth in the European Convention for the Protection of Vertebrate Animals used for Experimental and Other Scientific Purposes (Strasbourg, 1986), with the rules of laboratory practice of the Russian Federation, and with Order No. 724 of 1984 of the Ministry of Higher Education of the USSR, "Rules for carrying out work with experimental animals," after obtaining permission from the ethical committee of the FSBEIHE Tyumen State Medical University of the Russian Ministry of Health.

Statistical analyses of the actual data were carried out using the licensed software SPSS Statistics (USA) and Microsoft Excel by MS Office 2016 for Windows; single-factor ANOVA was used. The differences were statistically significant at  $p < 0.05$ .

### 3. Results and Discussion

A study of the dynamics of the infestation intensity and the reproduction of the population and individuals of *O. felineus* during a single infection showed that after 21 days, opisthorchii of different degrees of maturity were simultaneously detected in the liver and pancreas, and in faeces, helminth eggs with a low reproductive potential were detected ( $2.0 \pm 0.7$  eggs per parasite). The most pronounced rise of all of the indicators was observed on days 30-40 after infestation (infestation intensity—40.2, number of eggs per parasite— $57.3 \pm 12.3$ ). The highest indices were observed on days 48-56 after the start of the experiment (egg production by 1 parasite was  $76.0 \pm 11.4$ ).

TABLE 1: Dynamics of the infestation intensity and egg production of *O. felineus* in experimental opisthorchiasis (SO).

Time of infestation/superinvasion (days)	Number of opisthorchii in ecological niches	Number of eggs in 1 g of faeces	Number of eggs per parasite
21/6	$34.2 \pm 3.3$	$57 \pm 28$	$1.7 \pm 0.9$
28/13	$54.5 \pm 2.6$	$1277 \pm 162$	$23.4 \pm 7.9$
35/20	$62.2 \pm 2.5$	$3937 \pm 288$	$54.5 \pm 13$
48/33	$86.8 \pm 2.7$	$4714 \pm 375$	$54.3 \pm 10$
60/45	$87.9 \pm 3.1$	$4731 \pm 291$	$53.8 \pm 9.6$
85/65	$88.2 \pm 4.0$	$4683 \pm 214$	$53.1 \pm 8.3$
120/100	$86.6 \pm 3.9$	$4614 \pm 183$	$53.3 \pm 7.8$
240/120	$86.8 \pm 2.6$	$4583 \pm 101$	$52.8 \pm 8.1$
320/200	$85.6 \pm 3.1$	$4566 \pm 116$	$53.3 \pm 9.4$

Note: ecological niches—liver, pancreas, and gall bladder.

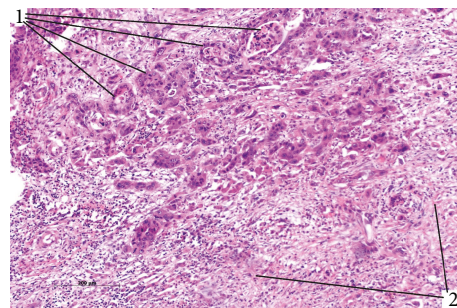


FIGURE 1: Cholangiocellular tumour with a forming coarse stroma in the setting of superinvasive opisthorchiasis (SO) was visualized with haematoxylin and eosin (HE) staining, magnification 200x (1: tumour glandular complexes; 2: forming coarse stroma).

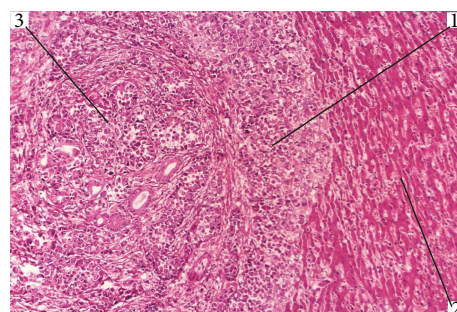


FIGURE 2: Undifferentiated cancer in the setting of SO. Opposition growth. HE staining, magnification 200x (1: undifferentiated tumour cells; 2: normal liver cells; 3: cholangiocyte adenomatous proliferates).

Statistical analysis of the results in the setting of SO showed a significant increase in mature opisthorchii after 48 days, with a maximum reproductive potential (54.5 eggs); as the duration of superinfestation increased, the intensity of the mature opisthorchii increased as well (88.2) but did not double (infection—50 metacercariae, repeated inflows—50

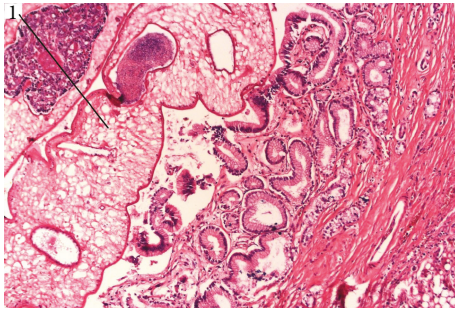


FIGURE 3: Opisthorchii in a duct located remotely from the tumour (showed by arrow). HE staining, magnification 200x.

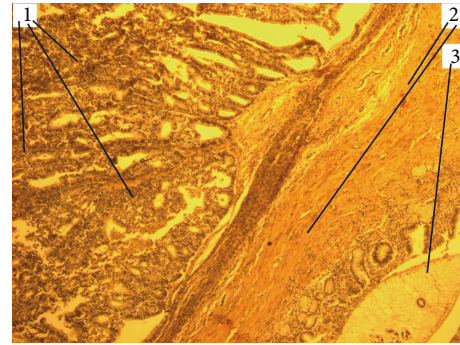


FIGURE 7: Experimental cholangiocarcinoma with a tender stroma in the setting of SO. HE staining, magnification 200x (1: adenocarcinoma; 2: coarse cholangiectasis wall; 3: opisthorchii in cholangiectasis).

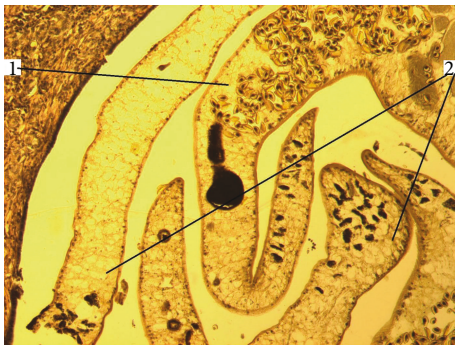


FIGURE 4: Clumps of opisthorchii in cholangiectasis in liver cancer in the setting of SO. HE staining, magnification 100x (1: mature parasites; 2: immature parasites).

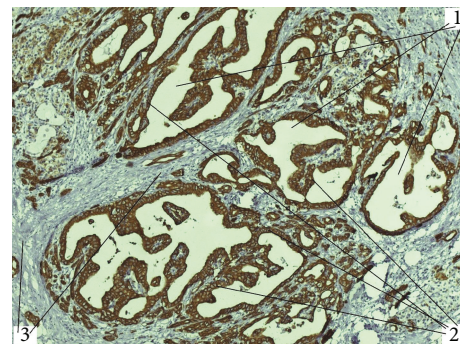


FIGURE 8: Experimental pancreatic cancer in the setting of SO, IHC reaction with antibodies against cytokeratin-19 receptors, magnification 100x (1: cyst component; 2: papillary component; 3: tumour stroma).

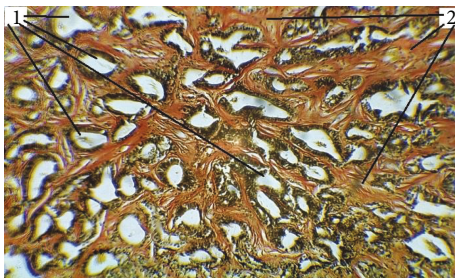


FIGURE 5: Experimental cholangiocarcinoma with a coarse stroma in the setting of SO. Van Gieson's staining, light microscopy magnification 20x (1: tumour glandular complexes; 2: coarse stroma).

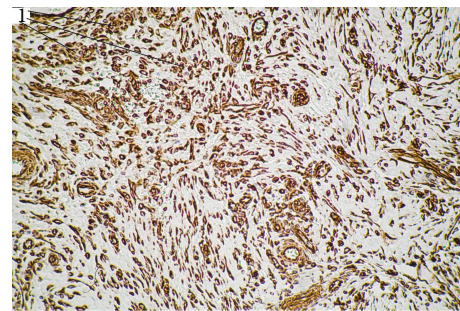


FIGURE 9: Experimental gastrointestinal stromal tumour (GIST), IHC reaction with antibodies against CD117 receptors, magnification 200x (1: tumour elements from cells of Cajal).

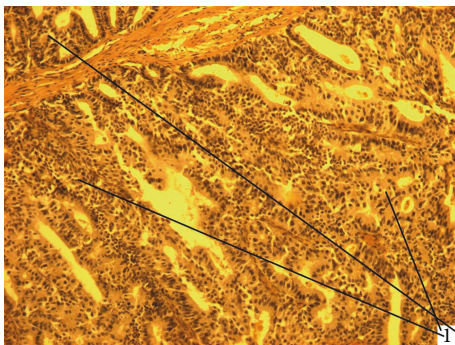


FIGURE 6: Experimental cholangiocarcinoma with a tender stroma in the setting of SO. HE staining, magnification 200x (1: adenocarcinoma).

larvae) until the end of the experiment (320 days). The parasite quantities in hamsters with SO are shown in Table 1.

A pathoanatomical examination of the liver of animals that died from cholangiocarcinoma (CCR) and other histological forms of tumours (Figures 1 and 2) showed the presence of 1 or more nodes; the largest number of tumours was observed in the left lobe of the organ, and intraorgan metastases were noted as foci with a rounded shape and clear edges.

Parasites were not found in the ductal system adjacent to the tumour. Clumps of opisthorchii were found in areas

TABLE 2: Dynamics of the infestation intensity and egg production of *O. felineus* in carcinogenesis (experiment).

Experiment period	SO		SO+liver cancer		SO+pancreas cancer		SO+GIST	
	No. of opisthorchii in ecological niches ( $M \pm m$ )	Number of eggs per parasite ( $M \pm m$ )	No. of opisthorchii in ecological niches ( $M \pm m$ )	Number of eggs per parasite ( $M \pm m$ )	No. of opisthorchii in ecological niches ( $M \pm m$ )	Number of eggs per parasite ( $M \pm m$ )	No. of opisthorchii in ecological niches ( $M \pm m$ )	Number of eggs per parasite ( $M \pm m$ )
85/65	88.2 $\pm$ 4.0	53.1 $\pm$ 8.3	62.2 $\pm$ 2.8*	62.5 $\pm$ 3.1	76.4 $\pm$ 4.3*	55.3 $\pm$ 6.2	79.1 $\pm$ 8.1*	57.2 $\pm$ 7.8
120/100	86.6 $\pm$ 3.9	53.3 $\pm$ 7.8	56.3 $\pm$ 3.2*	65.4 $\pm$ 4.8	72.8 $\pm$ 4.0*	61.0 $\pm$ 4.2	78.3 $\pm$ 4.8*	56.2 $\pm$ 2.7
240/120	86.8 $\pm$ 2.6	52.8 $\pm$ 8.1	48.4 $\pm$ 4.1	73.7 $\pm$ 4.9*	68.7 $\pm$ 4.6	59.3 $\pm$ 3.9*	77.8 $\pm$ 3.17	56.1 $\pm$ 1.9*
320/200	85.6 $\pm$ 3.1	53.3 $\pm$ 9.4	46.7 $\pm$ 3.7	60.32 $\pm$ 3.7*	62.4 $\pm$ 4.1	68.6 $\pm$ 2.4*	75.2 $\pm$ 2.9	56.7 $\pm$ 1.8*

Note: \*Statistically significant differences in comparison with the SO group ( $p < 0.05$ ).

remote from tumour nodes (Figure 3). Observations of CCR with metastases into portal lymph nodes showed bile hypertension syndrome and formed cholangiectasis, where a large number of helminths predominantly grew in the form of small “lumps” consisting of 12-16 individuals. In a larger ectasias, such cooperation consisted of 22 or more parasites (Figure 4). Single, smaller knots of opisthorchii were detected in enlarged bile ducts, mainly in other parts of the liver that were free of tumour growth.

Parasites in tumour-free segments were closely attached to the lining of the duct, occupying the surface along the entire length of the helminth, i.e., they occupied a position that facilitated contact with the largest area of the mucous membrane of the ducts.

Simulation of tumours in the setting of SO revealed the development of neoplasms in 38.4-76.9% of all cases, and the multiplicity factor varied: 1.46 in the liver (Figures 5–7), 1.32 in the pancreas (Figure 8), 1.27 in the stomach (Figure 9), 1.11 in the mammary gland, and 1.32 in the skin, without tumours; all of the tumours were nonlethal. Tumours with metastases to the lymph nodes were identified in CCR and adenocarcinoma of the pancreas. GISTs and metastases to the liver were also observed. In groups with numerous superinvasions, the numbers of tumour formations in the liver, pancreas, and stomach increased by 16.7-22.3%, and metastases of tumours into lymph nodes and other organs were more often noted. A sharp decrease in the intensity of infestation and an increase in egg production were observed on day 85 of invasion and day 65 of superinvasion (Table 2).

In the experiments for partial hepatectomy in the setting of SO, by day 48, the number of parasites in the liver was  $46.3 \pm 3.17$ , the number of eggs in 1 g of faeces was  $2673 \pm 94$ , and the egg production index of 1 opisthorchis was  $55.7 \pm 8.2$ . The morphological examination showed a uniform distribution of helminths throughout the organ, but the most populated ducts were noted in areas adjacent to the liver stump, where multiple newly formed ducts and vessels were formed.

#### 4. Conclusion

The development of tumour processes in the human liver makes opisthorchii move away from the sites of neoplasm localization. The main areas where opisthorchii are found

are large ducts and cholangiectases, where helminths create more compact populations, which indicates an insufficient nutraceutical supply.

Model tumours with SO induce a similar effect: initiators (carcinogens) provide a partial anthelmintic effect—a decrease in the intensity of infestation preceding the formation of neoplasms; the further population-level depression might be due to a lack of nutrition for parasites and the disruption of homeostasis.

A decrease in the infestation intensity regardless of the cause (carcinogens, reduction of the nutraceutical substrate) stimulates egg production of the remaining helminths, which is a trend of species preservation. Negative effects on helminths or their death results in an increase in egg production by surviving individuals, which indicates the intraspecies social relations of opisthorchii.

#### Data Availability

All data underlying the findings described in the manuscript are fully available without restriction. All relevant data are within the manuscript.

#### Conflicts of Interest

The authors declare that they have no competing interests.

#### Acknowledgments

The research was partially supported by the Russian Foundation for Basic Research (Grant No. 01-04-49239).

#### References

- [1] D. F. Avgustinovich, I. A. Orlovskaya, L. B. Toporkova et al., “Experimental opisthorchiasis: study of blood cell composition, hematopoiesis, and startle reflex in laboratory animals,” *Russian Journal of Genetics: Applied Research*, vol. 7, no. 1, pp. 82–92, 2017.
- [2] V. G. Bychkov, *Dynamics of Serum Cholesterol and Aortic Atherosclerosis in Chronic Opisthorchiasis Invasion*, Martsinovskiy Institute of Medical Parasitology and Tropical Medicine, Moscow, 1975.
- [3] E. Magen, V. Bychkov, A. Ginovker, and E. Kashuba, “Chronic *Opisthorchis felineus* infection attenuates atherosclerosis—

- an autopsy study,” *International Journal for Parasitology*, vol. 43, no. 10, pp. 819–824, 2013.
- [4] O. É. Vakulina, E. D. Khadieva, I. V. Garchuk et al., “The specific features of regenerative processes of hip and shin fractures in patients with superinvasion opisthorchiasis,” *Meditssinskaia Parazitologiia i Parazitarnye Bolezni*, vol. 1, pp. 20–22, 2011.
- [5] S. Lazarev, E. Oparina, and V. Bychkov, “Cytogenesis of Liver Recovery after Partial Hepatectomy in the Settings of Superinvasive Opisthorchiasis,” in *9th Therapeutic Forum*, Tyumen, Russia, 2017.
- [6] E. Khadieva, R. Uruzbaev, S. Lazarev, N. Pakhtyshev, and V. Bychkov, “Proliferative Reactions in the Liver and Pancreas in Chronic Superinvasive Opisthorchiasis,” in *2nd All-Russia Scientific-Practical Conference with International Participation*, Chelyabinsk, Russia, 2016.
- [7] S. Kulikova, E. Khadieva, S. Orlov, O. Solovyova, V. Zolotukhin, and V. Bychkov, “Heart involvement in superinvasive opisthorchiasis,” *Medical Science and Education of the Urals*, vol. 1, pp. 66–68, 2011.
- [8] V. G. Bychkov, V. M. Zolotukhin, E. D. Khadieva et al., “Hypereosinophilic syndrome, cardiomyopathies, and sudden cardiac death in superinvasive opisthorchiasis,” *Cardiology Research and Practice*, vol. 2019, Article ID 4836948, 5 pages, 2019.
- [9] V. P. Zuevsky, V. G. Bychkov, P. V. Tselishcheva, and E. D. Khadieva, “Opisthorchiasis as a promoter of gastric carcinogenesis,” *Meditssinskaia Parazitologiia i Parazitarnye Bolezni*, vol. 4, pp. 7–10, 2015.
- [10] S. Boonjaraspinyo, T. Boonmars, C. Aromdee et al., “Turmeric reduces inflammatory cells in hamster opisthorchiasis,” *Parasitology Research*, vol. 105, no. 5, pp. 1459–1463, 2009.
- [11] V. G. Bychkov, S. D. Lazarev, V. P. Zuevsky, V. L. Yanin, E. D. Khadieva, and I. R. Lukmanov, “Methodological aspects of modeling tumours in the setting of superinvasive opisthorchiasis,” *Morfologiia*, vol. 149, no. 3, pp. 44–48, 2016.
- [12] G. A. Glazkov, *To the Method of Isolation of Metacercariae of the Siberian Fluke from the Muscle Tissue of the Affected Fish*, Pasteur Institute of Epidemiology and Microbiology, Leningrad, USSR, 1977.

## Review Article

# Current Research Progress on Long Noncoding RNAs Associated with Hepatocellular Carcinoma

Haihong Shi <sup>1</sup>, Yuxin Xu,<sup>2</sup> Xin Yi,<sup>1</sup> Dandan Fang,<sup>3</sup> and Xia Hou <sup>1,4</sup>

<sup>1</sup>Department of Biochemistry and Molecular Biology, Jiamusi University School of Basic Medicine, Jiamusi, Heilongjiang 154007, China

<sup>2</sup>Jiamusi Maternal and Child Health Hospital, Jiamusi, Heilongjiang 154001, China

<sup>3</sup>Hospital of Traditional Chinese Medicine of Qiqihar, Qiqihar, Heilongjiang 161000, China

<sup>4</sup>Department of Physiology, Wayne State University School of Medicine, Detroit, MI 48201, USA

Correspondence should be addressed to Xia Hou; [hou\\_xia@hotmail.com](mailto:hou_xia@hotmail.com)

Received 6 December 2018; Revised 20 February 2019; Accepted 10 March 2019; Published 24 June 2019

Guest Editor: Zhigang Ren

Copyright © 2019 Haihong Shi et al. This is an open access article distributed under the Creative Commons Attribution License, which permits unrestricted use, distribution, and reproduction in any medium, provided the original work is properly cited.

Hepatocellular carcinoma (HCC) is the second leading cause of mortality among cancers. It has been found that long noncoding RNAs (lncRNAs) are involved in many human cancers, including liver cancer. It has been identified that carcinogenic and tumor-suppressing lncRNAs are associated with complex processes in liver cancer. These lncRNAs may participate in a variety of pathological and biological activities, such as cell proliferation, apoptosis, invasion, and metastasis. Here, we review the regulation and function of lncRNA in liver cancer and evaluate the potential of lncRNA as a new goal for liver cancer.

## 1. Introduction

Hepatocellular carcinoma (HCC), the most common form of liver cancer, is involved in 90% of primary liver cancers. In the last few decades, liver cancer has become the most important commonly diagnosed tumor type worldwide. It is also considered to be the most lethal cancer, related to approximately 34% of all malignancies [1, 2]. HCC is a highly invasive and fatal type of tumor that is often involved in relapse and metastasis, and the prognosis is poor. The incidence of liver cancer is related to a variety of risk factors, such as hepatitis B virus (HBV) and hepatitis C virus (HCV) infections, alcoholic cirrhosis, smoking, and aflatoxin B1 intake [3]. However, the molecular mechanism of the occurrence and development of liver cancer is complicated, which is related to different processes, e.g., cell cycle dysregulation, apoptosis, tumor cell invasion, and metastasis [4]. Accumulating proofs show that long noncoding RNA (lncRNA) expression is altered in liver cancer and involved in tumorigenesis [5].

In recent decades, most researches concerning the relationship between tumorigenesis and human genes have

focused on structural genes and their related regulatory sequences. However, some studies show that noncoding sequences of human genes play crucial roles in tumorigenesis. The human genome contains approximately 3 billion base pairs, of which less than 2% encode proteins, whereas the remaining ~98% of the genome consists of non-protein-coding sequences. RNAs that cannot be translated into proteins are called noncoding RNAs (ncRNAs), which include lncRNA, siRNA, miRNA, and other types [6]. lncRNA consists of more than 200 nucleotides without protein-coding potential but with gene regulatory functions. lncRNAs are classified based on the related locations of their protein-encoding genes in the genome, including (1) sense, (2) antisense, (3) bidirectional, (4) intronic, and (5) intergenic (Figure 1). This positional relationship is helpful in predicting the lncRNA function. lncRNA is involved in the proliferation, migration, invasion, apoptosis, angiogenesis, and drug resistance of tumor cells, although it was previously considered as “transcriptional noise” [7–9]. lncRNA is also related to the regulation of biological functions and gene expression under physiological and pathological conditions [10]. However, only a few functional

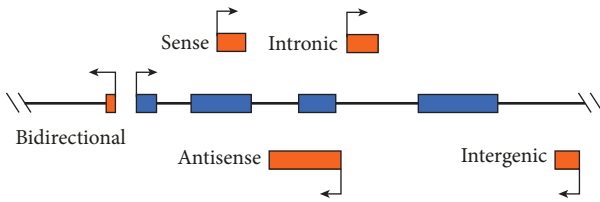


FIGURE 1: Based on the location of the lncRNA on the genome, it can be divided into five types: (1) sense, (2) antisense, (3) bidirectional, (4) intronic, and (5) intergenic. The coding RNA and noncoding RNA exons are shown in blue and red, respectively.

lncRNAs have been well characterized to date; several mechanistic topics of lncRNA function have been reviewed elsewhere [11, 12]. In this review, a summary of the four well-known molecular functions of lncRNAs is shown (Figure 2): (1) signal function—lncRNA has the function of stimulating the combination of transcription factors, suggesting that it may act as a signal molecule regulating the expression of genes; (2) decoy function—transcription of a class of lncRNAs can then bind to and titrate protein or RNA targets without performing any other functions. (these lncRNAs may negatively regulate the expression of their targets by acting as molecular bait); (3) manipulation function—lncRNAs can recruit the chromatin-modifying enzyme to regulate or control the positioning of these enzymes close to or away from the target gene; and (4) scaffolding function—lncRNAs can aggregate with many proteins to form a nuclear protein complex, which is involved in the modification of histones. lncRNAs have been proven to play an essential biological role in carcinogenesis by regulating gene expression, such as carcinogenic and antitumor functions. lncRNAs can be used as a criterion for the diagnosis and prognosis of hepatocellular carcinoma [13–16].

In this review, we mainly discuss HCC-associated lncRNAs. Here, we summarized the differences in the expression of lncRNAs in HCC; then, we reviewed the participation of lncRNAs in HCC cell proliferation, apoptosis, and migration. Finally, we discussed the prospect of lncRNAs as potential biomarkers and therapeutic targets for HCC.

## 2. Molecular Mechanisms of lncRNAs in HCC

lncRNA is involved in the development of various molecular mechanisms of hepatocellular carcinoma: epigenetic regulation, the regulation of DNA damage and cell cycle progression, microRNA regulation, signal transduction pathways, and hormone-induced cancer [17]. In liver cancer, lncRNAs are used as transcriptional regulatory molecules for oncogenes and tumor suppressor genes [17]. For instance, lncRNA HOTAIR overexpression is associated with the development of liver cancer. In contrast, the lncRNA TARID can prevent cancer formation by causing the demethylation of tumor suppressor gene promoters [18]. Epigenetic regulation refers to genetic phenotypes and genetic changes in gene expression, including DNA methylation, histone modification, and chromatin remodelling, and does not result in any changes in DNA sequencing. Studies show that a crucial role

in liver cancer development is that lncRNAs are accomplished by epigenetic regulation. lncRNAs can regulate gene expression through epigenetic regulation, transcriptional and posttranscriptional regulation, etc. lncRNAs participate in various biological processes in liver cancer cells, such as proliferation, differentiation, and apoptosis [19]. Besides, lncRNAs are involved in the regulation of a variety of epigenetic complexes, thus resulting in the activation and inactivation of genes. For example, lncRNA TCF7 is highly expressed in HCC cells and plays an important role in the maintenance of the self-renewal ability of the liver cancer stem cell [20]. The TCF7 gene is activated by recruiting SWI/SNF complexes to the gene and produces lncRNA TCF7, which can activate the Wnt signalling pathway and lead to the occurrence of hepatocarcinoma. The repair of DNA damage and the regulation of cell cycle checkpoints are important to maintain cell integrity. lncRNAs are also involved in DNA damage repair and in the regulation of physiological or pathological processes such as cell cycle, through which lncRNAs can regulate the occurrence and development of tumors [20]. The p53 gene, a tumor suppressor gene, also owns a robust ability to encode transcription factors in cells, which is at a low expression level under normal conditions. p53 can be activated by different signalling pathways under cellular stresses such as DNA damage, which results in cell cycle arrest, apoptosis or fading by enhancing the transcription of multiple downstream genes, maintaining cell genome integrity, and clearing damaged cells [21, 22]. As an example, lncRNA-p21 recruits ribonucleoprotein hnRNP-k to promote P21 transcription, a key molecule regulating the p53 signalling pathway. Downregulation of lincRNA-p21 causes losing control of G1/S checkpoints and leads to enhanced cell proliferation [23]. Furthermore, the mechanism of lncRNAs regulating microRNAs is that microRNAs (miRNAs) are related to the development of many diseases, including liver cancer [24]. miRNAs can bind to lncRNA sponges to inhibit gene expression and protein synthesis [25]; therefore, they affect the function of the cell, e.g., lncRNA XIST promotes HCC proliferation and inhibits apoptosis by regulating miR-139-5p/PDK1/AKT axis [26]. Finally, lncRNAs take part in signalling pathways and hormonal regulation. Evidence shows that liver cancer development is associated with the abnormal activation of signalling pathways. The role of lncRNAs in these signalling pathways is an essential part of the mechanism of liver cancer. Therefore, future studies on lncRNAs are also expected to find candidate drugs for the treatment of liver cancer. Studies have confirmed the roles of transforming growth factor beta (TGF- $\beta$ ), the AKT signalling pathway, and the Wnt signalling pathway in tumor development [27–29]. For example, TGF- $\beta$  promotes liver cancer cell metastasis via lncRNA-ATB. Abnormal AKT signalling leads to increased expression of lncRNA PTTG3P and promotes proliferation and migration of hepatoma cells.

## 3. lncRNAs in HCC

**3.1. Dysregulation of lncRNAs in HCC.** lncRNAs play irreplaceable roles in the progression of HCC because lncRNAs are known to be involved in the regulation of tumor

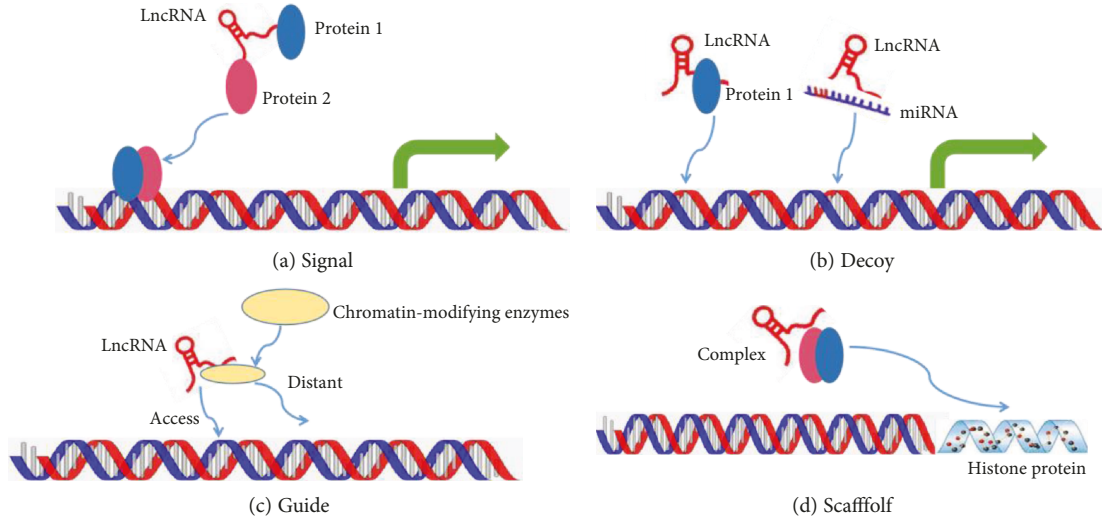


FIGURE 2: Four typical molecular functions of lncRNA: (a) LncRNAs can be used as molecular signalling mediators to regulate the expression of certain genes together with specific transcription factors or chromatin modifiers. (b) LncRNAs can bind to and titrate the expression of proteins or RNA, which indirectly play a variety of biological functions. (c) LncRNAs recruit chromatin-modifying enzymes that can enter or leave the target gene. (d) LncRNAs can pool multiple proteins to form ribonucleoprotein complexes and affect histone modifications.

TABLE 1: Dysregulated long noncoding RNAs (lncRNAs) associated with HCC.

LncRNAs	Expression	Affected target genes and pathways	Affected clinicopathological characteristics of HCC	References
HOTAIR	Upregulated	HOXD/VEGF/MMP-9/PRC2/H3K27/rbm38/Bmi-1/P14/P16	TNM stage, distant metastasis	[31–34]
HULC	Upregulated	P18/PRKACB/CREB	TNM stage, intrahepatic metastases	[38, 39, 54]
H19	Upregulated	Cdc25A/E2F1/hnRNP U/PCAF/DMC/ZEB1/2		[51, 55]
URHC	Upregulated	ZAK	Tumor size, tumor number	[9]
ROR	Upregulated	TGF- $\beta$ /PDK1/P53		[56]
PVT1	Upregulated	TGF- $\beta$ /NOP2	AFP level, tumor size, tumor number, tumor stage	[14, 57]
PTTG3P	Upregulated	PPTG1/AKT signalling	Tumor size, TNM stage	[43]
XIST	Upregulated	miR-139-5p/PDK1/AKT signalling	Tumor size	[26]
DBH-AS1	Upregulated	P53/ERK/MAPK signalling	HBsAg, tumor size	[58]
MEG3	Downregulated	UHRF1/P53	Tumor size, Edmondson grade	[47, 59]
DREH	Downregulated	HBx/vimentin	Tumor size, HBsAg	[48, 49]
PTENP1	Downregulated	miR-17/miR-19b/miR-20a/AKT/PI3K signalling	Tumor size, TNM stage	[60]
LET	Downregulated	P53/NF90/HIF-1 $\alpha$		[50]
uc002mbe.2	Downregulated	TAS	Tumor size	[52]

differentiation at the tumor node metastasis stage (TNM) and cell growth processes, including cell proliferation and apoptosis, invasion, and metastasis. LncRNAs play an irreplaceable role in the progression of HCC. The key biological functions of lncRNA are related to certain signalling pathways. LncRNA expression in liver cancer tissues is associated with clinicopathological features. Deregulated lncRNAs can be a novel biomarker for diagnosing or assessing treatment efficiencies. The dysregulation of lncRNA in HCC marks a disease spectrum and is proposed to be associated with liver cancer. Many oncogenes are known as targets for liver cancer-associated lncRNAs (Table 1). LncRNA participates in HCC processes by binding to oncogenes. In addition,

lncRNA can also participate in HCC through regulatory signalling pathways, even though the underlying mechanisms are still unknown. Differential expression and potential functional roles of lncRNAs in HCC are essential.

### 3.2. Upregulation of lncRNAs in HCC

3.2.1. *HOTAIR*. HOTAIR, a 2158 bp lncRNA, is encoded in the HOXC locus on chromosome 12q13.1 [30]. It has been found that HOTAIR is more highly expressed in HCC tissues than in paracancerous nontumor tissues. The increased expression of HOTAIR is associated with lymph node metastasis; therefore, the HOTAIR expression level is associated

with lymph node metastasis. Thus, the high HOTAIR levels in LT patients indicate a significantly shorter recurrence-free survival. Patients with tumors and high HOTAIR gene expression levels have a higher risk of recurrence after hepatectomy [31]. It is reported that HOTAIR promotes cell proliferation, autophagy, and invasion and reduces the response of hepatoma cells to the apoptosis stimulator  $\text{TNF-}\alpha$  and the chemotherapeutic drugs cisplatin and doxorubicin [31–33]. Further studies revealed that tumorigenesis is suppressed in HCC after silencing HOTAIR, which resulted in the activation of P16 and P14 signalling via increased miR-218 expression and decreasing Bmi-1 expression, respectively. It is suggested that HOTAIR expression is associated with liver tumor differentiation, metastasis, and early recurrence [34]. These findings suggest that HOTAIR plays an important role in the development of hepatocarcinoma, so HOTAIR is the possible target for the diagnosis and treatment of liver cancer.

**3.2.2. MALAT1.** MALAT1 (metastasis-associated lung adenocarcinoma transcript 1) was initially discovered in human non-small-cell lung cancer (NSCLC). MALAT1 is the first identified metastasis-associated lncRNA, which is found upregulated in HCC cell lines and patients [35, 36]. Functionally, MALAT1 promotes proliferation, invasion, metastasis, chemosensitivity, and autophagy in HCC cells. MALAT1 is upregulated in HCC and associated with cell proliferation and migration by regulating Bax, bcl-2, bcl-xl, caspase-3, and caspase-8 [36]. Moreover, MALAT1 is thought to promote proliferation during liver regeneration through the stimulation of the Wnt/catenin pathway, which is negatively regulated by p53. Silencing MALAT1 reduces cell viability, migration, and invasion and increases the sensitivity of cells to apoptotic stimuli such as cisplatin and doxorubicin, TNF-alpha, and glucose-brain toxins [37]. Thus, MALAT1 is probably involved in tumor development and could be a new biomarker for predicting tumor recurrence after LT.

**3.2.3. HULC.** HULC is the first identified lncRNA specifically upregulated in HCC [38]. Its coding sequence is located on chromosome 6p24.3 and is highly conserved among primates. In clinical tissues, HULC expression in HCC and hepatic colorectal metastasis samples is highly upregulated compared with that in the normal control. HULC expression is positively correlated with the Edmondson histological classification and the HBV/HBV X protein- (HBx-) positive state [39–41]. Similar results were detected in plasma samples from hepatocellular carcinoma [41]. HULC promotes lipogenesis and cell proliferation, induces apoptosis and enhanced epithelial-mesenchymal transformation (EMT), and also increases the risk of liver cancer development and metastasis [40]. Previous studies illustrated that HBx-mediated HULC upregulation promotes the increase of mRNA and protein levels in liver cancer by downregulating the tumor suppressor gene CDKN2C (p18). CDKN2C is thought to be a tumor suppressor gene that regulates cell cycle and plays a role in signal transduction pathways, including ATM/ATR and p53 pathways. These results

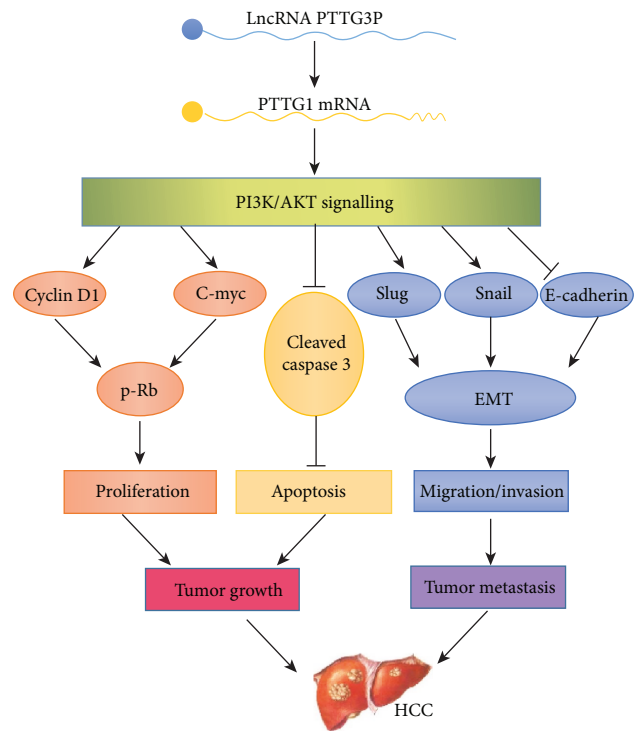


FIGURE 3: Functional diagram of lncRNA PTTG3P in HCC tumor growth and metastasis.

indicated that HULC could be used as a potential biomarker for HCC diagnosis.

**3.2.4. PTTG3P.** PTTG3P (pituitary tumor-transforming 3 pseudogene) is a novel lncRNA. Expression and localization of PTTG3P were analyzed using quantitative real-time polymerase chain reaction (qRT-PCR) and in situ hybridization (ISH) in two patients with liver cancer [42]. It has been shown that the expression of PTTG3P in liver cancer is significantly increased. The upregulation of PTTG3P is positively correlated with a poor prognosis of liver cancer patients. PTTG3P promotes cell proliferation, inhibits apoptosis, and accelerates migration and invasion of HCC cells. Mechanically, PTTG3P is involved in tumor growth, while PTTG3P metastatic cascade promotes cells by the upregulation of PTTG1 and activation of the PI3K/AKT signalling pathway. Growth and metastasis follows, which in turn affect downstream signal transduction, through the regulation of cell cycle regulators and EMT-related factors as shown in Figure 3. Therefore, PTTG3P may be a potential target for the prevention and treatment of liver cancer [43].

**3.2.5. PVT1.** lncRNA PVT1 is located at 8q24.21 [44]. Studies showed that PVT1 is highly expressed in HCC tissues and associated with the number and grade of tumors. PVT1 promotes tumor growth by accelerating cell proliferation and cell cycle progression and enhancing stem cell-related properties [45]. Functionally, PVT1 can increase NOP2 levels by enhancing the stability of the NOP2 protein, and the function of PVT1 is dependent on the presence of the NOP2 protein. The hPVT1/NOP2/cell cycle gene pathway

is involved in promoting carcinogenesis, cell proliferation, and stem cell-like properties in HCC cells [14]. Furthermore, it has been reported that PVT1 promotes proliferation, invasion, and migration of liver cancer cells by modulating the mir-150/HIG2 axis [44]. Therefore, PVT1 can be used as a diagnosis marker for HCC.

### 3.3. Downregulation of LncRNAs in HCC

**3.3.1. MEG3.** MEG3 is highly expressed in the human pituitary gland and is a maternal imprinting gene. The MEG3 gene is located at the imprinted DLK1-MEG3 locus on chromosome 14q32.3 in humans. MEG3 expression is observed in several types of cancer [46]. MEG3 was confirmed downregulated in HCC. MEG3 regulates proliferation and apoptosis in HCC cells [47]. Mechanistically, MEG3 improves the protein stability, increases the transcriptional activity of p53 in hepatocellular carcinoma cells, and influences the expression of p53 target genes. In liver cancer tissues, MEG3 is negatively correlated with UHRF1 that plays an important role in DNA methylation by recruiting DNA methyltransferase DNMT1 during DNA replication. In the same study, UHRF1 is identified as involved in the upstream regulation of MEG3 in liver cancer by regulating DNMT1 [47]. These results indicate that MEG3 is a tumor suppressor gene and can be considered as a biomarker for liver cancer.

**3.3.2. DREH.** DREH is involved in HBx-mediated hepatocellular carcinoma. DREH and mouse homologous DREH were significantly downregulated in human HBV-related HCC tissues and HBx transgenic mice, respectively. DREH is a highly conserved lncRNA. The DREH reduction is significantly associated with poor survival in patients with liver cancer [48]. DREH is linked to the proliferation and metastasis of HBV-related HCC. A previous study revealed the negative correlation between DREH expression and HBx and HBs [49]. DREH is downregulated by HBx via the downregulation of vimentin, which results in the suppression of HCC growth and migration [48, 49]. These results indicate that DREH is a tumor suppressor in the development of HBx-related hepatocellular carcinoma and may be a new target for the treatment of HBV-related hepatocellular carcinoma.

**3.3.3. LET.** “Low expression in the tumor,” or LET, is present at significantly reduced levels in HCC tumor tissues and is linked to metastasis [50]. LET influences the invasiveness and metastasis of HCC cells. LET is inhibited by histone deacetylase 3 (HDAC3). LET inhibition increases the stability of nuclear factor 90 (NF90), thus promoting hypoxia-induced invasion [50]. HDAC3 induced by hypoxia inhibits lncRNA-let by reducing the lncRNA-let promoter region regulation mediated by histone acetylation. Interestingly, downregulation of lncRNA-let is a key step in stabilizing the NF90 protein, leading to hypoxic-induced infiltration of cancer cells. In addition, the relationship between hypoxia, histone acetylation disorders, low lncRNA-let expression, and metastasis has been demonstrated in clinical HCC samples. These findings demonstrated the role of lncRNA-let as a regulator of hypoxia signal transduction and provide new methods for therapeutic intervention in cancer progression.

Moreover, these findings also indicate that hypoxia can inhibit lncRNA-let expression by reducing the level of acetylation of histones H3 and H4 in its promoter region [50]. In addition, downregulation of lncRNA-let may affect the accumulation and stability of hif-1 $\alpha$  mRNA under hypoxia.

## 4. Biological Roles of LncRNAs in HCC

**4.1. Proliferation.** To date, it has been proven that many lncRNAs maladjusted in hepatocellular carcinoma play a vital role in the growth of hepatocellular carcinoma in vitro or in vivo. It has been found that upregulated URHC promotes tumor and cell proliferation, which is directly related to poor prognosis in liver cancer tissues and cell lines. Further studies showed that URHC promotes cell proliferation by regulating ZAK protein during the activation of the ERK/MAPK signalling pathway [9]. Researchers found that H19 knockdown abolishes the tumorigenicity of HCC in vivo, and significantly, hypoxic recovery reduces growth independent of the adherent wall [51]. Moreover, the detection of the hepatoma cell line Bel7402 in vitro showed that silencing lncRNA HOTAIR could inhibit cell proliferation [31].

**4.2. Apoptosis.** Apoptosis is the gene-controlled autonomous and orderly death of cells. The decrease of apoptosis can promote the survival and accumulation of abnormal cells and lead to cancer development. It has been reported that lncRNA affects liver cancer by acting on apoptosis. The expression of uc002mbe.2 is lower in liver cancer cell tissues than in normal ones. The histone deacetylase inhibitor Trichostatin A (TSA) exerts an antitumor effect by promoting the apoptosis of liver cancer cells. Apoptosis induced by TSA is significantly inhibited by uc002mbe.2 knockdown [52]. Thus, uc002mbe.2 is very important in TSA-mediated hepatocyte apoptosis.

**4.3. Invasion and Metastasis.** The most crucial reasons for mortality and poor prognosis in patients with liver cancer are tumor metastasis and invasion, which are related to HCC both in vitro and in vivo. More and more evidences showed that lncRNA plays an important role in the invasion and metastasis of liver cancer. For example, lncRNA-related microvascular invasion in HCC (MVIH) are a class of lncRNA molecules that are highly expressed in liver cancer and are involved in angiogenesis. When the expression of these lncRNAs is high, the survival rate and prognosis are the opposite. Overexpression of MVIH in animal models promotes angiogenesis and facilitates tumor growth and metastasis. Furthermore, the expression of MVIH in liver cancer patients is significantly negatively correlated with the angiogenesis inhibitor PGK1, suggesting that MVIH promotes liver cancer metastasis by inhibiting the secretion of PGK1 [16]. In addition, recent studies indicated that lncRNA-ATB activated by TGF- $\beta$  induces EMT and cell invasion in vitro, promoting the invasion of hepatocellular carcinoma cells [53].

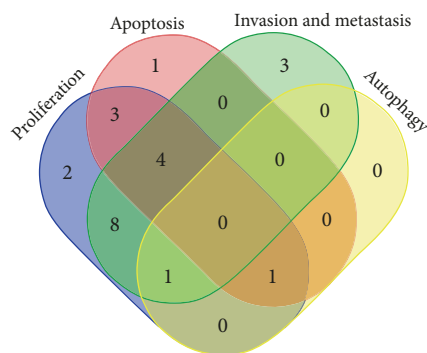


FIGURE 4: Informatics analysis of the biological functions of lncRNAs in HCC.

TABLE 2: Statistical analysis of lncRNAs and tumor biological functions.

Biological functions	Number	lncRNAs	References
Apoptosis, invasion, metastasis, and proliferation	4	PTTG3P	[43]
		DREH	[49]
		ANRIL	[61]
		HULC	[53]
Apoptosis, autophagy, and proliferation	1	PTENP1	[60]
Autophagy, invasion, metastasis, and proliferation	1	HOTAIR	[33]
Apoptosis and proliferation	3	uc002mbe.2	[52]
		DBH-AS1	[58]
		MEG3	[59]
Invasion, metastasis, and proliferation	8	CCAT1	[62]
		HOTTIP	[63]
		AFAP1-AS1	[64]
		UCA1	[65]
		H19	[55]
		XIST	[26]
		ZEB1-AS1	[66]
HEIH	[67]		
Proliferation	2	PVT1	[57]
		ROR	[56]
Apoptosis	1	URHC	[9]
Invasion and metastasis	3	HBx-LINE1	[68]
		LET	[50]
		ATB'	[69]

## 5. Conclusions and Future Perspectives

In conclusion, lncRNAs play important roles in the biological processes of the occurrence, development, metastasis, and recurrence of liver cancer, which impact on the treatment and prognosis of liver cancer. Furthermore, the dysregulation of liver cancer-associated lncRNA in tumor tissues is often associated with these biological processes. lncRNA dysregulation is associated with the progression and prognosis of

liver cancer. Therefore, lncRNA should be a candidate biomarker for the diagnosis, prognosis, recurrence prediction, and treatment of liver cancer. The characteristics of the biological functions related to HCC lncRNA enable researchers to have a more comprehensive understanding of the occurrence of liver cancer (Figure 4, Table 2). Further research on the mechanism of lncRNA involvement in the development and progression of liver cancer is conducive to clinical diagnosis and treatment. Although a small number of lncRNAs have been studied in liver cancer, a large part of them needs to be further discovered. Therefore, further research is needed on the role and mechanism of liver-specific lncRNA in the progression of liver cancer. The knowledge of the function of lncRNA in liver cancer development is increasing, which is laying the foundation for the design of new treatment methods for liver cancer.

## Conflicts of Interest

The authors declare that there is no conflict of interest regarding the publication of this paper.

## References

- [1] L. A. Torre, F. Bray, R. L. Siegel, J. Ferlay, J. Lortet-Tieulent, and A. Jemal, "Global cancer statistics, 2012," *CA: a Cancer Journal for Clinicians*, vol. 65, no. 2, pp. 87–108, 2015.
- [2] H. B. El-Serag and K. L. Rudolph, "Hepatocellular carcinoma: epidemiology and molecular carcinogenesis," *Gastroenterology*, vol. 132, no. 7, pp. 2557–2576, 2007.
- [3] R. N. Aravalli, C. J. Steer, and E. N. Cressman, "Molecular mechanisms of hepatocellular carcinoma," *Hepatology*, vol. 48, no. 6, pp. 2047–2063, 2008.
- [4] P. Merle and C. Trepo, "Molecular mechanisms underlying hepatocellular carcinoma," *Viruses*, vol. 1, no. 3, pp. 852–872, 2009.
- [5] F. J. Yu, J. J. Zheng, P. H. Dong, and X. M. Fan, "Long non-coding RNAs and hepatocellular carcinoma (Review)," *Molecular and Clinical Oncology*, vol. 3, no. 1, pp. 13–17, 2015.
- [6] C. P. Ponting, P. L. Oliver, and W. Reik, "Evolution and functions of long noncoding RNAs," *Cell*, vol. 136, no. 4, pp. 629–641, 2009.
- [7] P. G. Mansourian, M. Yoneda, M. Krishna Rao, F. J. Martinez, E. Thomas, and E. R. Schiff, "Effects of statins on the risk of hepatocellular carcinoma," *Gastroenterology & Hepatology*, vol. 10, no. 7, pp. 417–426, 2014.
- [8] M. D. Huang, W. M. Chen, F. Z. Qi et al., "Long non-coding RNA ANRIL is upregulated in hepatocellular carcinoma and regulates cell proliferation by epigenetic silencing of KLF2," *Journal of Hematology & Oncology*, vol. 8, no. 1, p. 57, 2015.
- [9] W. H. Xu, J. B. Zhang, Z. Dang et al., "Long non-coding RNA URHC regulates cell proliferation and apoptosis via ZAK through the ERK/MAPK signaling pathway in hepatocellular carcinoma," *International Journal of Biological Sciences*, vol. 10, no. 7, pp. 664–676, 2014.
- [10] M. C. Tsai, O. Manor, Y. Wan et al., "Long noncoding RNA as modular scaffold of histone modification complexes," *Science*, vol. 329, no. 5992, pp. 689–693, 2010.

- [11] J. L. Rinn and H. Y. Chang, "Genome regulation by long noncoding RNAs," *Annual Review of Biochemistry*, vol. 81, no. 1, pp. 145–166, 2012.
- [12] K. C. Wang and H. Y. Chang, "Molecular mechanisms of long noncoding RNAs," *Molecular Cell*, vol. 43, no. 6, pp. 904–914, 2011.
- [13] Y. Li, S. D. Egranov, L. Yang, and C. Lin, "Molecular mechanisms of long noncoding RNAs-mediated cancer metastasis," *Genes, Chromosomes & Cancer*, vol. 58, no. 4, pp. 200–207, 2018.
- [14] F. Wang, J. H. Yuan, S. B. Wang et al., "Oncofetal long non-coding RNA PVT1 promotes proliferation and stem cell-like property of hepatocellular carcinoma cells by stabilizing NOP2," *Hepatology*, vol. 60, no. 4, pp. 1278–1290, 2014.
- [15] F. Yang, L. Zhang, X. S. Huo et al., "Long noncoding RNA high expression in hepatocellular carcinoma facilitates tumor growth through enhancer of zeste homolog 2 in humans," *Hepatology*, vol. 54, no. 5, pp. 1679–1689, 2011.
- [16] S. X. Yuan, F. Yang, Y. Yang et al., "Long noncoding RNA associated with microvascular invasion in hepatocellular carcinoma promotes angiogenesis and serves as a predictor for hepatocellular carcinoma patients' poor recurrence-free survival after hepatectomy," *Hepatology*, vol. 56, no. 6, pp. 2231–2241, 2012.
- [17] A. Sahu, U. Singhal, and A. M. Chinnaiyan, "Long noncoding RNAs in cancer: from function to translation," *Trends in Cancer*, vol. 1, no. 2, pp. 93–109, 2015.
- [18] K. Arab, Y. J. Park, A. M. Lindroth et al., "Long noncoding RNA *TARID* directs demethylation and activation of the tumor suppressor *TCF21* via *GADD45A*," *Molecular Cell*, vol. 55, no. 4, pp. 604–614, 2014.
- [19] R. Taby and J. P. Issa, "Cancer epigenetics," *CA: a Cancer Journal for Clinicians*, vol. 60, no. 6, pp. 376–392, 2010.
- [20] Y. Wang, L. He, Y. Du et al., "The long noncoding RNA *lncTCF7* promotes self-renewal of human liver cancer stem cells through activation of Wnt signaling," *Cell Stem Cell*, vol. 16, no. 4, pp. 413–425, 2015.
- [21] M. Nakayama and M. Oshima, "Mutant p53 in colon cancer," *Journal of Molecular Cell Biology*, vol. 11, no. 4, pp. 267–276, 2018.
- [22] A. Vazquez, E. E. Bond, A. J. Levine, and G. L. Bond, "The genetics of the p53 pathway, apoptosis and cancer therapy," *Nature Reviews Drug Discovery*, vol. 7, no. 12, pp. 979–987, 2008.
- [23] N. Dimitrova, J. R. Zamudio, R. M. Jong et al., "LincRNA-p21 activates p21 in cis to promote polycomb target gene expression and to enforce the G1/S checkpoint," *Molecular Cell*, vol. 54, no. 5, pp. 777–790, 2014.
- [24] M. V. Iorio and C. M. Croce, "MicroRNA dysregulation in cancer: diagnostics, monitoring and therapeutics. A comprehensive review," *EMBO Molecular Medicine*, vol. 9, no. 6, p. 852, 2017.
- [25] L. Salmena, L. Poliseno, Y. Tay, L. Kats, and P. P. Pandolfi, "A ceRNA hypothesis: the Rosetta Stone of a hidden RNA language?," *Cell*, vol. 146, no. 3, pp. 353–358, 2011.
- [26] Y. Mo, Y. Lu, P. Wang et al., "Long non-coding RNA *XIST* promotes cell growth by regulating miR-139-5p/PDK1/AKT axis in hepatocellular carcinoma," *Tumour biology: the journal of the International Society for Oncodevelopmental Biology and Medicine*, vol. 39, no. 2, article 1010428317690999, 2017.
- [27] S. Colak and P. Ten Dijke, "Targeting TGF- $\beta$  signaling in cancer," *Trends in Cancer*, vol. 3, no. 1, pp. 56–71, 2017.
- [28] J. Taipale and P. A. Beachy, "The Hedgehog and Wnt signalling pathways in cancer," *Nature*, vol. 411, no. 6835, pp. 349–354, 2001.
- [29] F. Liu and S. E. Millar, "Wnt/beta-catenin signaling in oral tissue development and disease," *Journal of Dental Research*, vol. 89, no. 4, pp. 318–330, 2010.
- [30] J. Zhang, P. Zhang, L. Wang, H. L. Piao, and L. Ma, "Long non-coding RNA *HOTAIR* in carcinogenesis and metastasis," *Acta Biochimica et Biophysica Sinica*, vol. 46, no. 1, pp. 1–5, 2014.
- [31] Y. J. Geng, S. L. Xie, Q. Li, J. Ma, and G. Y. Wang, "Large intervening non-coding RNA *HOTAIR* is associated with hepatocellular carcinoma progression," *The Journal of International Medical Research*, vol. 39, no. 6, pp. 2119–2128, 2011.
- [32] W. M. Fu, X. Zhu, W. M. Wang et al., "Hotair mediates hepatocarcinogenesis through suppressing miRNA-218 expression and activating P14 and P16 signaling," *Journal of Hepatology*, vol. 63, no. 4, pp. 886–895, 2015.
- [33] E. Li, Z. Zhao, B. Ma, and J. Zhang, "Long noncoding RNA *HOTAIR* promotes the proliferation and metastasis of osteosarcoma cells through the AKT/mTOR signaling pathway," *Experimental and Therapeutic Medicine*, vol. 14, no. 6, pp. 5321–5328, 2017.
- [34] Z. Yang, L. Zhou, L. M. Wu et al., "Overexpression of long non-coding RNA *HOTAIR* predicts tumor recurrence in hepatocellular carcinoma patients following liver transplantation," *Annals of Surgical Oncology*, vol. 18, no. 5, pp. 1243–1250, 2011.
- [35] R. Lin, S. Maeda, C. Liu, M. Karin, and T. S. Edgington, "A large noncoding RNA is a marker for murine hepatocellular carcinomas and a spectrum of human carcinomas," *Oncogene*, vol. 26, no. 6, pp. 851–858, 2007.
- [36] M. C. Lai, Z. Yang, L. Zhou et al., "Long non-coding RNA *MALAT-1* overexpression predicts tumor recurrence of hepatocellular carcinoma after liver transplantation," *Medical Oncology*, vol. 29, no. 3, pp. 1810–1816, 2012.
- [37] C. Li, L. Chang, Z. Chen, Z. Liu, Y. Wang, and Q. Ye, "The role of lncRNA *MALAT1* in the regulation of hepatocyte proliferation during liver regeneration," *International Journal of Molecular Medicine*, vol. 39, no. 2, pp. 347–356, 2017.
- [38] K. Panzitt, M. M. Tschernatsch, C. Guelly et al., "Characterization of *HULC*, a novel gene with striking up-regulation in hepatocellular carcinoma, as noncoding RNA," *Gastroenterology*, vol. 132, no. 1, pp. 330–342, 2007.
- [39] H. Xie, H. Ma, and D. Zhou, "Plasma *HULC* as a promising novel biomarker for the detection of hepatocellular carcinoma," *BioMed Research International*, vol. 2013, Article ID 136106, 5 pages, 2013.
- [40] Y. Du, G. Kong, X. You et al., "Elevation of highly up-regulated in liver cancer (*HULC*) by hepatitis B virus X protein promotes hepatoma cell proliferation via down-regulating p18," *The Journal of Biological Chemistry*, vol. 287, no. 31, pp. 26302–26311, 2012.
- [41] I. J. Matouk, I. Abbasi, A. Hochberg, E. Galun, H. Dweik, and M. Akkawi, "Highly upregulated in liver cancer noncoding RNA is overexpressed in hepatic colorectal metastasis," *European Journal of Gastroenterology & Hepatology*, vol. 21, no. 6, pp. 688–692, 2009.
- [42] W. Weng, S. Ni, Y. Wang et al., "PTTG3P promotes gastric tumour cell proliferation and invasion and is an indicator of

- poor prognosis," *Journal of Cellular and Molecular Medicine*, vol. 21, no. 12, pp. 3360–3371, 2017.
- [43] J. L. Huang, S. W. Cao, Q. S. Ou et al., "The long non-coding RNA PTTG3P promotes cell growth and metastasis via up-regulating PTTG1 and activating PI3K/AKT signaling in hepatocellular carcinoma," *Molecular Cancer*, vol. 17, no. 1, p. 93, 2018.
- [44] Y. Xu, X. Luo, W. He et al., "Long non-coding RNA PVT1/miR-150/HIG2 axis regulates the proliferation, invasion and the balance of iron metabolism of hepatocellular carcinoma," *Cellular Physiology and Biochemistry : International Journal of Experimental Cellular Physiology, Biochemistry, and Pharmacology*, vol. 49, no. 4, pp. 1403–1419, 2018.
- [45] Y. Zhang, W. J. Mo, X. Wang et al., "Microarray-based bioinformatics analysis of the prospective target gene network of key miRNAs influenced by long non-coding RNA PVT1 in HCC," *Oncology Reports*, vol. 40, no. 1, pp. 226–240, 2018.
- [46] L. Benetatos, G. Vartholomatos, and E. Hatzimichael, "MEG3 imprinted gene contribution in tumorigenesis," *International Journal of Cancer*, vol. 129, no. 4, pp. 773–779, 2011.
- [47] J. Zhu, S. Liu, F. Ye et al., "Long noncoding RNA MEG3 interacts with p53 protein and regulates partial p53 target genes in hepatoma cells," *PLoS One*, vol. 10, no. 10, article e0139790, 2015.
- [48] J. F. Huang, Y. J. Guo, C. X. Zhao et al., "Hepatitis B virus X protein (HBx)-related long noncoding RNA (lncRNA) down-regulated expression by HBx (Dreh) inhibits hepatocellular carcinoma metastasis by targeting the intermediate filament protein vimentin," *Hepatology*, vol. 57, no. 5, pp. 1882–1892, 2013.
- [49] D. Lv, Y. Wang, Y. Zhang, P. Cui, and Y. Xu, "Downregulated long non-coding RNA DREH promotes cell proliferation in hepatitis B virus-associated hepatocellular carcinoma," *Oncology Letters*, vol. 14, no. 2, pp. 2025–2032, 2017.
- [50] F. Yang, X. S. Huo, S. X. Yuan et al., "Repression of the long noncoding RNA-LET by histone deacetylase 3 contributes to hypoxia-mediated metastasis," *Molecular Cell*, vol. 49, no. 6, pp. 1083–1096, 2013.
- [51] I. J. Matouk, N. DeGroot, S. Mezan et al., "The H19 non-coding RNA is essential for human tumor growth," *PLoS One*, vol. 2, no. 9, article e845, 2007.
- [52] H. Yang, Y. Zhong, H. Xie et al., "Induction of the liver cancer-down-regulated long noncoding RNA uc002mbe.2 mediates trichostatin-induced apoptosis of liver cancer cells," *Biochemical Pharmacology*, vol. 85, no. 12, pp. 1761–1769, 2013.
- [53] H. Xiong, B. Li, J. He, Y. Zeng, Y. Zhang, and F. He, "lncRNA HULC promotes the growth of hepatocellular carcinoma cells via stabilizing COX-2 protein," *Biochemical and Biophysical Research Communications*, vol. 490, no. 3, pp. 693–699, 2017.
- [54] X. Xin, M. Wu, Q. Meng et al., "Long noncoding RNA HULC accelerates liver cancer by inhibiting PTEN via autophagy cooperation to miR15a," *Molecular Cancer*, vol. 17, no. 1, p. 94, 2018.
- [55] M. L. Yang, Z. Huang, Q. Wang et al., "The association of polymorphisms in lncRNA-H19 with hepatocellular cancer risk and prognosis," *Bioscience Reports*, vol. 38, no. 5, article BSR20171652, 2018.
- [56] A. Zhang, N. Zhou, J. Huang et al., "The human long non-coding RNA-RoR is a p53 repressor in response to DNA damage," *Cell Research*, vol. 23, no. 3, pp. 340–350, 2013.
- [57] J. Guo, C. Hao, C. Wang, and L. Li, "Long noncoding RNA PVT1 modulates hepatocellular carcinoma cell proliferation and apoptosis by recruiting EZH2," *Cancer Cell International*, vol. 18, no. 1, p. 98, 2018.
- [58] J. Bao, X. Chen, Y. Hou, G. Kang, Q. Li, and Y. Xu, "LncRNA DBH-AS1 facilitates the tumorigenesis of hepatocellular carcinoma by targeting miR-138 via FAK/Src/ERK pathway," *Biomedicine & Pharmacotherapy*, vol. 107, pp. 824–833, 2018.
- [59] H. Zhuo, J. Tang, Z. Lin et al., "The aberrant expression of MEG3 regulated by UHRF1 predicts the prognosis of hepatocellular carcinoma," *Molecular Carcinogenesis*, vol. 55, no. 2, pp. 209–219, 2016.
- [60] C. L. Chen, Y. W. Tseng, J. C. Wu et al., "Suppression of hepatocellular carcinoma by baculovirus-mediated expression of long non-coding RNA PTENP1 and microRNA regulation," *Biomaterials*, vol. 44, pp. 71–81, 2015.
- [61] J. Ma, T. Li, X. Han, and H. Yuan, "Knockdown of lncRNA ANRIL suppresses cell proliferation, metastasis, and invasion via regulating miR-122-5p expression in hepatocellular carcinoma," *Journal of Cancer Research and Clinical Oncology*, vol. 144, no. 2, pp. 205–214, 2018.
- [62] H. Zhu, X. Zhou, H. Chang et al., "CCAT1 promotes hepatocellular carcinoma cell proliferation and invasion," *International Journal of Clinical & Experimental Pathology*, vol. 8, no. 5, pp. 5427–5434, 2015.
- [63] F. H. Tsang, S. L. Au, L. Wei et al., "Long non-coding RNA HOTTIP is frequently up-regulated in hepatocellular carcinoma and is targeted by tumour suppressive miR-125b," *Liver International*, vol. 35, no. 5, pp. 1597–1606, 2015.
- [64] J. Y. Zhang, M. Z. Weng, F. B. Song et al., "Long noncoding RNA AFAP1-AS1 indicates a poor prognosis of hepatocellular carcinoma and promotes cell proliferation and invasion via upregulation of the RhoA/Rac2 signaling," *International Journal of Oncology*, vol. 48, no. 4, pp. 1590–1598, 2016.
- [65] J. J. Hu, W. Song, S. D. Zhang et al., "HBx-upregulated lncRNA UCA1 promotes cell growth and tumorigenesis by recruiting EZH2 and repressing p27Kip1/CDK2 signaling," *Scientific Reports*, vol. 6, no. 1, article 23521, 2016.
- [66] T. Li, J. Xie, C. Shen et al., "Upregulation of long noncoding RNA ZEB1-AS1 promotes tumor metastasis and predicts poor prognosis in hepatocellular carcinoma," *Oncogene*, vol. 35, no. 12, pp. 1575–1584, 2016.
- [67] Y. Zhang, Z. Li, Y. Zhang, Q. Zhong, Q. Chen, and L. Zhang, "Molecular mechanism of HEIH and HULC in the proliferation and invasion of hepatoma cells," *International Journal of Clinical and Experimental Medicine*, vol. 8, no. 8, pp. 12956–12962, 2015.
- [68] H. W. Liang, N. Wang, Y. Wang et al., "Hepatitis B virus-human chimeric transcript HBx-LINE1 promotes hepatic injury via sequestering cellular microRNA-122," *Journal of Hepatology*, vol. 64, no. 2, pp. 278–291, 2016.
- [69] Y. Li, Y. Ye, and H. Chen, "Astragaloside IV inhibits cell migration and viability of hepatocellular carcinoma cells via suppressing long noncoding RNA ATB," *Biomedicine & Pharmacotherapy*, vol. 99, pp. 134–141, 2018.

## Review Article

# The Security Rating on Local Ablation and Interventional Therapy for Hepatocellular Carcinoma (HCC) and the Comparison among Multiple Anesthesia Methods

Qianhui Jin <sup>1,2,3</sup> Xinhua Chen <sup>1,2,3</sup> and Shusen Zheng <sup>1,2,3</sup>

<sup>1</sup>Division of Hepatobiliary Pancreatic Surgery, Department of Surgery, The First Affiliated Hospital, College of Medicine, Zhejiang University, Zhejiang Province, Hangzhou, China

<sup>2</sup>Key Laboratory of Combined Multi-Organ Transplantation, Ministry of Public Health, Key Laboratory of the Diagnosis and Treatment of Organ Transplantation, CAMS Key Laboratory of Organ Transplantation, Zhejiang Province, Hangzhou, China

<sup>3</sup>Collaborative Innovation Center for Diagnosis Treatment of Infectious Diseases, Zhejiang Province, Hangzhou, China

Correspondence should be addressed to Shusen Zheng; [shusenzheng@zju.edu.cn](mailto:shusenzheng@zju.edu.cn)

Received 21 November 2018; Revised 6 January 2019; Accepted 3 February 2019; Published 19 February 2019

Academic Editor: Alain Chapel

Copyright © 2019 Qianhui Jin et al. This is an open access article distributed under the Creative Commons Attribution License, which permits unrestricted use, distribution, and reproduction in any medium, provided the original work is properly cited.

Recently, the interventional therapies are used more often in clinical practice for hepatocellular carcinoma. The most commonly used methodologies include radiofrequency ablation, microwave ablation, laser ablation, and cryotherapy. Most of the interventional operations need local anesthesia combined with intravenous sedation. Also, some interventional therapy centers apply general anesthesia. However, different anesthesia methods can cause diverse effects on patients' pain management, recovery time, and hospitalization time. For the better understanding of the current anesthesia application status, we summarize and analyze multiple anesthesia methods while being applied in interventional therapy for hepatocellular carcinoma; in addition, their characters are also compared in this paper.

## 1. Introduction

As a curative therapy, the interventional ablations are used more often in clinical practice for hepatocellular carcinoma, e.g., radiofrequency ablation, microwave ablation, laser ablation, and cryotherapy. Most of the interventional operations need local anesthesia combined with intravenous sedation or general anesthesia. For better understanding of the current anesthesia application status and diverse effect, the multiple anesthesia methods applied in interventional therapy for hepatocellular carcinoma are reviewed.

## 2. The Development of Interventional Therapy for Hepatic Carcinoma

Hepatocellular carcinoma (HCC) is a malignant tumor with high global incidence which is ranked as the 7th highest incidence among malignant tumors in male and 5th in female [1]. In China, primary hepatocellular carcinoma has the

2nd highest incidence in malignant tumors and the mortality is in the third position among global malignant tumors [2]. At present, the main radical therapies for hepatocellular carcinoma include surgical resection and liver transplantation; however, most of the hepatocellular carcinoma patients have had cirrhosis, lymphatic metastasis, or distant metastasis when they were diagnosed; therefore, 70% of those patients have already lost the opportunity of getting radical surgery. With regard to those hepatocellular carcinomas which are impossible to be radically resected, such as advanced hepatocellular carcinoma and small hepatocellular carcinoma, interventional therapy has been noticed as an increasingly significant adjuvant method of treating advanced HCC and a radical therapy for small HCC. It is featured by the small trauma and obvious curative effect, providing patients who are intolerant to surgical resection a chance to be radically cured. If 2-3 neoplastic foci spread deep in the liver or are central type (less or equal to 5 centimeters), the effect of local ablation is similar to surgical resection which can achieve

radical ablation after mini-invasive treatment. The local ablation therapy for hepatocellular carcinoma is applicable for treating patients whose tumor is smaller than 5 cm; whose tumor nodes are less than 3 and the diameter of the largest tumor is smaller than 3 cm; and whose tumors have no vessels, bile ducts, and adjacent organ invasion and metastasis and liver function is Child-Pugh A or B. As for those patients having single or multiple tumors with a diameter of 3 cm to 7 cm, further TACE should be considered.

**2.1. Radiofrequency Ablation (RFA).** Radiofrequency ablation can ablate tumor by heating local liver tissues causing tumors' necrosis. For small hepatocellular carcinoma, especially with a diameter smaller than 5 centimeters, RFA has an equal effect to surgical resection, which is recognized as one of the efficient approaches to radically cure hepatocellular carcinoma [3]. Hocquet et al. [4] compared the efficacy of monopole radiofrequency ablation and nontouch bipolar radiofrequency ablations, finding that bipolar radiofrequency ablation can destruct local tumor. Kawamura et al. [5] studied the nontouch bipolar radiofrequency ablative effect on the relapse of single tumor and small hepatocellular carcinoma and found that it reduces the tumor recurrence compared with touch radiofrequency ablations. The curative effect and complication of radiofrequency ablations depend on tumors' anatomy positions. When hepatocellular carcinoma is close to vessels, bile ducts, liver capsule, and other adjacent organs, the ablation-caused complications, such as great vascular injury [6], rise.

**2.2. Microwave Ablation (MWA).** Microwave ablation transfers high-frequency electromagnetic energy to microwave radiation energy, and then, the heat causes coagulative necrosis and eliminates tumors. Xiang et al. [7] and Hui-xiong and Ming-yan [8] compared the effects of RFA and MWA on treating hepatocellular carcinoma. They concluded that there is no obvious difference between MWA and RFA in terms of curative effect and complications. Livraghi [9] found there is no difference between MWA's complications and RFA's; they both have a low rate of serious complications [10] and no death cases; thus, they are safe therapies to treat hepatocellular carcinoma.

**2.3. Cryotherapy.** Cryotherapy is a therapy to kill tumor with low temperature. After technical upgrade, its curative effect has been significantly improved, and its complications have been substantially decreased. In addition, percutaneous minimally invasive approach has had replaced the quondam open surgery. Orlacchio et al. [11] retrospectively studied the feasibility and safety of percutaneous cryoablation guided by B-mode ultrasound and CT, and they found 4 patients' tumors were eliminated efficiently without complications which meant cryotherapy is potent, safe, and feasible. Dunne et al. [12] found there is no statistical difference between cryotherapy and RFA by comparing complications. Both of them are safe.

**2.4. Transcatheter Arterial Chemoembolization (TACE).** The major chemical ablation method to interventional therapy for hepatocellular carcinoma is TACE. It infuses

chemotherapeutic drugs and embolic agents through the hepatic artery to deprive the blood supply of the tumor. This therapy is the first fine choice of chemical ablation [13]. TACE is suitable for high vascular hepatocellular carcinoma. It is able to reduce tumors' size to meet the surgical indication so that radical surgical therapy can be operated. It can also be used in patients with multiple or locally unresectable hepatocellular carcinoma, or postoperative recurrence and postoperative recurrence prevention. Xue et al. [14] found that TACE causes less-severe complications after being applied to massive hepatocellular carcinoma, which proved that it is a safe and efficient therapy. Besides, patients with better preoperative hepatic function and lower alpha fetoprotein level can achieve better curative results and prolonged survival.

### 3. Curative Evaluation and Follow-Up

The local therapy is evaluated by CT, MRI, and B-mode ultrasound. The effect can be classified as complete ablation and incomplete ablation. If patients have incomplete ablation, they can be operated again. If after twice ablation, still, patients have tumors, the ablation therapy should be considered failed; it should be abandoned and replaced by other therapies.

When the tumors are completely ablated, patients should get a periodic follow-up. Usually, every 2-3 months, the tumor marker test, color Doppler ultrasound, MRI, or CT should be done so as to discover potential recrudescence local tumor focuses and new focuses within the life in time.

### 4. Comparison among Multiple Anesthesia Methods in Interventional Therapy for Hepatocellular Carcinoma

**4.1. Local Anesthesia.** Local anesthesia has a certain antiproliferative effect on the tumor. Because simple local anesthesia cannot satisfy the analgesic requirement, more interventional therapies for hepatocellular carcinoma are performed under local anesthesia combined with intravenous analgesia. However, pain controls is often difficult to manage, especially in some cases where the tumor is large or in a special position, for example, under the diaphragm or near the liver capsule [15, 16]. If intraoperative pain is not well controlled, interventional operation will be affected. On the other hand, local anesthesia is simple and convenient, with fewer postoperative complications, and there is no need for resuscitation.

**4.2. General Anesthesia.** Although interventional therapy for hepatocellular carcinoma is local treatment, the requirement for anesthesia is slightly higher. Several situations, for example, the pain control during the intervention, the ache by tumor necrosis after operation, and the respiratory activity's impact on the diaphragm activity, would also affect the accuracy of operators, which could influence the effect of treatment and the time of operation. General anesthesia has a good analgesic effect. It can reduce the intraoperative pain caused by body movement which may influence the treatment effect. Besides, during the general anesthesia, using appropriate anesthetics can reduce the dosage of

intraoperative drugs, shorten the time to resuscitation, and improve patient recovery.

Currently, local anesthesia is still widely used in interventional therapy; sometimes intravenous analgesics are used to relieve intraoperative pain. While using lidocaine local anesthesia, the intraoperative blood pressure and heart rate are increased, affecting patients' hemodynamic stability. And intraoperative pain is often difficult to control. The position of the tumor also influences pain scoring [16]. For example, the tumor located at the septum or under the capsule is an important factor; the tumor diameter [17] is also an important factor affecting blood pressure and heart rate of patients with large tumors changing more than those with small tumors during the treatment. Moreover, local anesthesia may affect respiratory activity and cause anesthesia-related complications, such as respiratory depression or respiratory arrest. Applying intravenous general anesthesia can ensure more stable hemodynamics, blood pressure, and heart rate compared with using local anesthesia. General anesthesia's incidence of postoperative complications such as pleural effusion and gas accumulation is lower than that of the local anesthesia group as well. Compared with local anesthesia, intravenous general anesthesia has a longer postoperative recovery time, but intraoperative hemodynamics is more stable. And local anesthesia [18] has less postoperative complications and shorter hospitalization time. The comparison between local anesthesia and general anesthesia is shown in Table 1. And the comparison of complications is shown in Table 2.

## 5. The Effect of Different Anesthetics on Interventional Therapy for Hepatocellular Carcinoma

With the application of abundant new anesthetics, more literature has compared the effects of different anesthetics in interventional therapy.

*5.1. The Effect of Sevoflurane on Interventional Therapy for Hepatocellular Carcinoma.* Sevoflurane is a type of inhalation anesthetic which has the advantages of fast induction, muscle relaxation, and rapid postoperative recovery. In the past researches, for hepatocellular carcinoma surgery or interventional therapy, sevoflurane has little influence on hepatic function and is relatively safe. Nishiyama et al. [19] found that sevoflurane and isoflurane have a certain effect on hepatic function after hepatectomy, but sevoflurane's is less. Yi et al. [20] studied the anesthetic safety of sevoflurane inhalation anesthesia and intravenous anesthesia with propofol in microwave ablation. Propofol is a routine surgical anesthetic. The adverse drug effects of that are mainly on the inhibition of the respiratory system and the cardiovascular system; therefore, increasing the dose of propofol will reduce the security of anesthesia. Compared with propofol and sevoflurane inhalation anesthesia, cardiovascular and respiratory depression is not obvious; hemodynamics and respiration are more stable, and induction of anesthesia is more smooth. However, the incidence of nausea and vomiting after sevoflurane is higher than that of propofol which could affect

the electrolyte balance of the body and cause food to be inhaled into the trachea. Ling-xi et al. [21] did research on the postoperative effect of different densities of sevoflurane on hepatectomy. It turned out that the usage of sevoflurane in surgical anesthesia could reduce the dosage of propofol, accelerate the recovery and extubation after the operation, and reduce the postoperative complications. Song et al. [22] compared sevoflurane and propofol's effects on hepatic function finding that both of them have no obvious difference on the peak value of hepatic function items such as aminotransferase, bilirubin, and alkaline phosphatase, which indicates that, in clinical application, they have similar effects on hepatic function.

*5.2. The Effect of Dexmedetomidine on Interventional Therapy for Hepatocellular Carcinoma.* Dexmedetomidine is a kind of alpha-2 receptor agonist and highly selective agonist which has analgesic, sedative, and antianxiety functionality, and it can maintain hemodynamic stability, widely used in general anesthesia. A large amount of research indicated that dexmedetomidine, to some degree, can protect organs, such as myocardial cell. Sulaiman et al.'s research [23] showed that dexmedetomidine can reduce intraoperative blood pressure and heart rate. It can prevent cardiac ischemia by regulating the blood flow of the heart, which has a certain protective effect on the heart. Wang et al.'s [24] study found that dexmedetomidine did not affect immune function, stabilize hemodynamics, and reduce inflammatory response. Feld et al.'s study [25] has shown that dexmedetomidine can replace fentanyl's analgesic effect and reduce blood pressure and heart rate. Some studies [26–28] show the effect of dexmedetomidine combined with that of sufentanil during perioperation and found that the use of dexmedetomidine can reduce the dosage of anesthetics and the sedation level is higher. During the operation, the group in which patients use dexmedetomidine has lower blood pressure and heart rate. It may be related to the increment of vagus tension after using dexmedetomidine. Nonetheless, the incidence of postoperative complications like respiratory depression, nausea, and vomiting is lower than that of those without using medetomidine. Meanwhile, it does not increase adverse reactions such as hypertension and tachycardia. It effectively reduces the proportion of postoperative complications. And it can increase the security of anesthesia. Joung et al. [29] found that compared with propofol, medetomidine can maintain respiratory stability and reduce the dosage of anesthetics in radiofrequency ablation.

*5.3. The Effect of Opioids on Interventional Therapy.* Opioids are good analgesic drugs, widely used in clinical anesthesia. They can inhibit cellular immunity and humoral immunity, affecting the recurrence rate of tumors after the surgery [30]. Studies [31, 32] show that using fentanyl and sufentanil during perioperation will not affect postoperative recurrence. Studies [33] show that compared with general anesthesia combined with epidural anesthesia, there is no significant difference in the survival rate and recurrence rate of general anesthesia combined with morphine intravenous analgesia. Yi et al. [34] studied the application of remifentanyl

TABLE 1: Comparison between local anesthesia and general anesthesia.

	Advantage	Disadvantage
Local anesthesia	No need for recovery [44]	No satisfy the analgesic requirement [15, 16]
	Simple, convenient [44]	More postoperative complications [45]
	Shorter hospitalization time [18]	
General anesthesia	Satisfy the analgesic requirement [45]	Longer postoperative recovery time [18, 45]
	Stable heart rate and blood pressure	

TABLE 2: Comparison of local anesthesia and general anesthesia complications in interventional therapy.

	Local anesthesia	General anesthesia
Complications	Unstable blood pressure [45]	Hypotension [46, 47]
	Unstable heart rate [45]	Slow heart rate [47]
	Pleural effusion [15, 45]	Respiratory depression
	Poor pain control [17]	Postoperative nausea and vomiting [47, 48]

combined with propofol intravenous anesthesia in radiofrequency ablation for hepatocellular carcinoma, and they found that remifentanyl could reduce the recovery time, decrease the dosage of propofol in anesthesia, and lower the fluctuation of mean arterial pressure. But it will increase the risk of apnea and add respiratory management during the surgery. Guohua and Li [35] found that patients maintained their awareness during the treatment, which made them possible to follow doctors' instructions and the operation would not be disturbed by the patient's unconscious movements. Besides, it not easy to get synergies with other drugs, and thus, the effects of sedation and analgesia not meeting the requirements of surgery will not happen. Li-hong et al. [36] studied the application of propofol combined with remifentanyl in radiofrequency ablation for hepatocellular carcinoma. It is found that the combination of them is helpful to maintain the stability of blood pressure and heart rate during the treatment, and the degree of sedation in the operation makes the patient slightly uncomfortable. The patient can follow the doctor's instructions in the treatment which helps the treatment to proceed smoothly. Lingyan et al. [37] compared the effects of tramadol and fentanyl in the treatment of hepatocellular carcinoma by microwave ablation. They found that if patients use fentanyl combined with propofol during the operation, the proportion of hypotension, bradycardia, and hypoxemia was higher. Tramadol affects blood circulation less than fentanyl does, which means it is relatively secure.

## 6. The Effect of Anesthesia on Therapy Result

**6.1. The Effect of Anesthesia on Immune Function.** Various methods of anesthesia and anesthetic drugs have effects on immune function after operation. Using anesthetic methods and drugs with less influence on postoperative immune function has certain advantages for patients' curative effect and tumor's metastasis and recurrence after the surgery. In surgery for hepatocellular carcinoma, Sun et al. [38] found that compared with intravenous inhalation-combined anesthesia,

after the surgery for hepatocellular carcinoma, there is a significant increase in the amount of CD4+/CD8+ T cells when patients use general anesthesia combined with epidural anesthesia. The two different anesthesia ways have obvious difference effects. The study found that general anesthesia combined with epidural anesthesia can reduce immunosuppression and speed up the recovery of immune function after the surgery. Fu et al.'s [39] study found that patients with combined general anesthesia and epidural anesthesia have more stable immune function than those with intravenous anesthesia. Wada [40] found that sevoflurane could reduce the metastasis of cancer cells and reduce postoperative immunosuppression. Moreover, compared with general anesthesia with sevoflurane, sevoflurane general anesthesia combined with spinal block anesthesia can reduce immunosuppression and the metastasis of cancer cells. Huimin et al. [41] found that propofol anesthesia can influence the level of serum interleukins and HSP70 when patients were treated with radiofrequency ablation for hepatocellular carcinoma. And they found that the increased level of IL-6, IL-8, and HSP70 in patients who had got propofol anesthesia was lower than that in the local anesthetic group, which could reduce the nociceptive inflammation of patients. However, in Cho et al.'s study [42], propofol-remifentanyl anesthesia can preserve NKCC to achieve good immunity compared with sevoflurane-remifentanyl anesthesia. Levins et al. [43] compared immune cell markers for general anesthesia opioid analgesia with propofol-epidural anesthesia and found no significant difference between the two.

**6.2. The Effect of Anesthesia on Coagulation Function.** We can judge hepatic blood coagulation function by comparing general anesthesia's and epidural anesthesia's effect on blood coagulation function; through comparing coagulation indexes (prothrombin time, partial thromboplastin time, platelet count, and more), 3 days before and after the operation, we can compare the variation of the coagulation function. Using the hemostasis test and fibrinolysis test (vWF, tPA, sP-selectin, PAI-1, D-dimer, and PF1z2), we compare

the effects of those two methods of anesthesia before and after the operation. Compared with general anesthesia, after 3 days of the operation, those indexes mentioned above restored and got close to the normal range when patients use epidural anesthesia. It was also found that epidural anesthesia can make coagulation indexes of patients with hepatocellular carcinoma restore quicker and can maintain hemostatic stability better.

**6.3. Pain Management.** Local ablation and interventional procedures for hepatocellular carcinoma should follow the WHO three-step analgesic therapy principle and NCCN adult cancer pain guideline. 80% to 90% cancer patients' pain symptoms can be alleviated by standard and effective therapies.

## 7. The Key Points for Safe Operations of the Ablation for Hepatocellular Carcinoma

Local ablation and interventional operations for hepatocellular carcinoma should follow the guidelines for the therapy of hepatocellular carcinoma, and operators should get strict training and sufficient accumulation of practice. Before the treatment, the patient's overall condition and liver function should be assessed comprehensively and adequately. Besides, we should assess tumor size, location, and number location of tumors and their adjacent organs, formulating reasonable puncture path and ablation scope, and achieve enough safety edge. Based on the size and position of tumors, choosing appropriate imaging-guided techniques (ultrasound or CT) and ablation methods (RFA, MWA, or PEI) is emphasized. In addition, the distance from tumors to the common bile duct and the left and right hepatic ducts should be at least 5 mm. It is not recommended to treat tumor foci that are larger than 5 cm only by ablation. For multiple tumor foci or larger tumors, according to the patient's hepatic function, we can apply TACE combined with ablation treatment before the therapy and it is superior to simple ablation therapy. In order to get the "safe edge" and kill the tumors thoroughly, the ablation range should include 5 mm paracarcinoma tissues. And for invasive carcinoma or metastatic neoplastic foci whose boundary is clear and the shape is irregular, if the condition of adjacent liver tissues and structure is suitable, it is suggested that the ablation range should be expended properly.

## Conflicts of Interest

All authors have no conflicts of interest to declare.

## Acknowledgments

This work was supported by the National S&T Major Project (no. 2018ZX10301201). The authors thank Danjing Guo and Liangje Hong from the Key Laboratory of Combined Multi-Organ Transplantation, Ministry of Public Health, for their comments.

## References

- [1] C. Bosetti, F. Turati, and C. La Vecchia, "Hepatocellular carcinoma epidemiology," *Best Practice & Research Clinical Gastroenterology*, vol. 28, no. 5, pp. 753–770, 2014.
- [2] J. G. Chen and S. W. Zhang, "Liver cancer epidemic in China: past, present and future," *Seminars in Cancer Biology*, vol. 21, no. 1, pp. 59–69, 2011.
- [3] C. Yin, Z. Jian, F. Jia et al., "Clinical effect and prognostic factors analysis of intraoperative radiofrequency ablation in treatment of hepatocellular carcinoma with severe cirrhosis," *Chinese Journal of Digestive Surgery*, vol. 16, no. 2, pp. 159–163, 2017.
- [4] A. Hocquelet, C. Aubé, A. Rode et al., "Comparison of no-touch multi-bipolar vs. monopolar radiofrequency ablation for small HCC," *Journal of Hepatology*, vol. 66, no. 1, pp. 67–74, 2017.
- [5] Y. Kawamura, K. Ikeda, S. Fujiyama et al., "Potential of a no-touch pincer ablation procedure that uses a multipolar radiofrequency ablation system to prevent intrasubsegmental recurrence of small and single hepatocellular carcinomas," *Hepatology Research*, vol. 47, no. 10, pp. 1008–1020, 2017.
- [6] T. de Baère, O. Risse, V. Kuoch et al., "Adverse events during radiofrequency treatment of 582 hepatic tumors," *American Journal of Roentgenology*, vol. 181, no. 3, pp. 695–700, 2003.
- [7] J. Xiang, D. Jian-min, W. Yan-dong, W. Feng-mei, W. Yi-jun, and D. Zhi, "Ultrasound-guided percutaneous radiofrequency ablation and microwave ablation for the treatment of hepatocellular carcinoma: a comparison study," *Journal of Interventional Radiology*, vol. 23, no. 4, pp. 306–310, 2014.
- [8] X. Hui-xiong and L. Ming-yan, "A clinical comparison of ultrasound-guided percutaneous microwave and radiofrequency ablation for treatment of hepatocellular carcinoma," *Chinese Journal of Hepatobiliary Surgery*, vol. 13, no. 8, pp. 528–530, 2007.
- [9] T. Livraghi, For the Collaborative Italian Group using AMICA system, F. Meloni, L. Solbiati, and G. Zanusi, "Complications of microwave ablation for liver tumors: results of a multicenter study," *CardioVascular and Interventional Radiology*, vol. 35, no. 4, pp. 868–874, 2012.
- [10] P. Liang, Y. Wang, X. Yu, and B. Dong, "Malignant liver tumors: treatment with percutaneous microwave ablation—complications among cohort of 1136 patients," *Radiology*, vol. 251, no. 3, pp. 933–940, 2009.
- [11] A. Orlicchio, G. Bazzocchi, D. Pastorelli et al., "Percutaneous cryoablation of small hepatocellular carcinoma with US guidance and CT monitoring: initial experience," *CardioVascular and Interventional Radiology*, vol. 31, no. 3, pp. 587–594, 2008.
- [12] R. M. Dunne, P. B. Shyn, J. C. Sung et al., "Percutaneous treatment of hepatocellular carcinoma in patients with cirrhosis: a comparison of the safety of cryoablation and radiofrequency ablation," *European Journal of Radiology*, vol. 83, no. 4, pp. 632–638, 2014.
- [13] M. Tsurusaki and T. Murakami, "Surgical and locoregional therapy of HCC: TACE," *Liver Cancer*, vol. 4, no. 3, pp. 165–175, 2015.
- [14] T. Xue, F. Le, R. Chen et al., "Transarterial chemoembolization for huge hepatocellular carcinoma with diameter over ten centimeters: a large cohort study," *Medical Oncology*, vol. 32, no. 3, p. 64, 2015.
- [15] Z. Junchao, L. Su, and Z. Yueyong, "Complications of radiofrequency ablation for liver cancer in high-risk locations and

- their prevention," *Linchuang Gandanbing Zazhi*, vol. 33, no. 5, pp. 969–973, 2017.
- [16] L. Jinghua, C. Shichang, and S. Jian, "Relationship between tumor location and pain level in CT-guided percutaneous microwave ablation of hepatocellular carcinoma," *Journal of Clinical Hepatology*, vol. 31, no. 6, pp. 903–906, 2015.
- [17] X. Mian, W. Zhao, H. Yin, and L. Ke, "Relationship between tumor location and intraoperative pain during CT-guided microwave ablation under local anesthesia," *Chinese Journal of General Surgery*, vol. 25, no. 7, pp. 979–984, 2016.
- [18] G. F. Attizzani, S. M. Patel, G. D. Dangas et al., "Comparison of local versus general anesthesia following transfemoral transcatheter self-expanding aortic valve implantation (from the Transcatheter Valve Therapeutics Registry)," *The American Journal of Cardiology*, vol. 123, no. 3, pp. 419–425, 2019.
- [19] T. Nishiyama, T. Fujimoto, and K. Hanaoka, "A comparison of liver function after hepatectomy in cirrhotic patients between sevoflurane and isoflurane in anesthesia with nitrous oxide and epidural block," *Anesthesia & Analgesia*, vol. 98, no. 4, pp. 990–993, 2004.
- [20] Z. Yi, Z. Hong, and L. Ping, "Application of general anesthesia with sevoflurane or intravenous propofol in percutaneous sonographically guided microwave coagulation therapy for hepatocellular carcinoma," *Journal of Clinical Anesthesiology*, vol. 23, no. 4, pp. 291–293, 2007.
- [21] Z. Ling-xi, L. Qing, P. Juan-bao, and N. Yu-xia, "The effects of different concentrations of sevoflurane combined with propofol on recovery quality in patients undergoing partial hepatic resection," *Journal of Clinical Anesthesiology*, vol. 30, no. 6, pp. 550–553, 2014.
- [22] J. C. Song, Y. M. Sun, L. Q. Yang, M. Z. Zhang, Z. J. Lu, and W. F. Yu, "A comparison of liver function after hepatectomy with inflow occlusion between sevoflurane and propofol anesthesia," *Anesthesia & Analgesia*, vol. 111, no. 4, pp. 1036–1041, 2010.
- [23] S. Sulaiman, R. B. Karthekeyan, M. Vakamudi, A. S. Sundar, H. Ravullapalli, and R. Gandham, "The effects of dexmedetomidine on attenuation of stress response to endotracheal intubation in patients undergoing elective off-pump coronary artery bypass grafting," *Annals of Cardiac Anaesthesia*, vol. 15, no. 1, pp. 39–43, 2012.
- [24] L. Wang, A. Zhang, W. Liu, H. Liu, F. Su, and L. Qi, "Effects of dexmedetomidine on perioperative stress response, inflammation and immune function in patients with different degrees of liver cirrhosis," *Experimental and Therapeutic Medicine*, vol. 16, no. 5, pp. 3869–3874, 2018.
- [25] J. M. Feld, W. E. Hoffman, M. M. Stechert, I. W. Hoffman, and R. C. Ananda, "Fentanyl or dexmedetomidine combined with desflurane for bariatric surgery," *Journal of Clinical Anesthesia*, vol. 18, no. 1, pp. 24–28, 2006.
- [26] C.-S. Dong, J. Zhang, Q. Lu et al., "Effect of Dexmedetomidine combined with sufentanil for post-thoracotomy intravenous analgesia: a randomized, controlled clinical study," *BMC Anesthesiology*, vol. 17, no. 1, p. 33, 2017.
- [27] X.-K. Zhang, Q.-H. Chen, W.-X. Wang, and Q. Hu, "Evaluation of dexmedetomidine in combination with sufentanil or butorphanol for postoperative analgesia in patients undergoing laparoscopic resection of gastrointestinal tumors: a quasi-experimental trial," *Medicine*, vol. 95, no. 50, article e5604, 2016.
- [28] Y. Nie, Y. Liu, Q. Luo, and S. Huang, "Effect of dexmedetomidine combined with sufentanil for post-caesarean section intravenous analgesia: a randomised, placebo-controlled study," *European Journal of Anaesthesiology*, vol. 31, no. 4, pp. 197–203, 2014.
- [29] K. W. Joung, S. S. Choi, D. M. Jang et al., "Comparative effects of dexmedetomidine and propofol on US-guided radiofrequency ablation of hepatic neoplasm under monitored anesthesia care: a randomized controlled study," *Medicine*, vol. 94, no. 32, article e1349, 2015.
- [30] G. L. Snyder and S. Greenberg, "Effect of anaesthetic technique and other perioperative factors on cancer recurrence," *British Journal of Anaesthesia*, vol. 105, no. 2, pp. 106–115, 2010.
- [31] P. Forget, J. Vandenhende, M. Berliere et al., "Do intraoperative analgesics influence breast cancer recurrence after mastectomy? A retrospective analysis," *Anesthesia & Analgesia*, vol. 110, no. 6, pp. 1630–1635, 2010.
- [32] K. Jaeger, D. Scheinichen, J. Heine et al., "Remifentanyl, fentanyl, and alfentanil have no influence on the respiratory burst of human neutrophils in vitro," *Acta Anaesthesiologica Scandinavica*, vol. 42, no. 9, pp. 1110–1113, 1998.
- [33] P. Y. Wuethrich, G. N. Thalmann, U. E. Studer, and F. C. Burkhard, "Epidural analgesia during open radical prostatectomy does not improve long-term cancer-related outcome: a retrospective study in patients with advanced prostate cancer," *PloS One*, vol. 8, no. 8, article e72873, 2013.
- [34] L. I. Yi, H. U. Wan, L. O. Yu-Hui et al., "Application of total intravenous anesthesia with remifentanyl and propofol to radiofrequency ablation," *Chinese Journal of Cancer*, vol. 26, no. 3, pp. 322–324, 2007.
- [35] Z. Guohua and S. Li, "Remifentanyl as a single agent to provide analgesia for percutaneous radiofrequency ablation of hepatic cancer," *Journal of Medical Research*, vol. 42, no. 9, pp. 100–102, 2013.
- [36] H. Li-hong, N. Yang-hong, and L. Xiao-qin, "Target-controlled infusion of propofol and remifentanyl in geriatric patients with hepatocellular carcinoma undergoing percutaneous radiofrequency ablation," *Chinese Journal of Geriatrics*, vol. 29, no. 7, pp. 579–581, 2010.
- [37] J. Lingyan, P. Lichao, and Z. N. S. Yanging, "Anesthetic effect of propofol combined with tramadol or fentanyl in ultrasonically guided percutaneous microwave coagulation therapy for hepatocellular carcinoma," *Chinese Journal of Clinical Medicine*, vol. 20, no. 1, pp. 72–74, 2013.
- [38] H. Z. Sun, Y. L. Song, and X. Y. Wang, "Effects of different anesthetic methods on cellular immune and neuroendocrine functions in patients with hepatocellular carcinoma before and after surgery," *Journal of Clinical Laboratory Analysis*, vol. 30, no. 6, pp. 1175–1182, 2016.
- [39] S. Fu, P.-S. Qu, and S.-N. Cai, "Effect of anesthetic methods on postoperative CD3+, CD4+ and CD4+CD25+ in patients with lung cancer undergoing radical operation," *Oncology Letters*, vol. 16, no. 5, pp. 6547–6551, 2018.
- [40] H. Wada, S. Seki, T. Takahashi et al., "Combined spinal and general anesthesia attenuates liver metastasis by preserving TH1/TH2 cytokine balance," *Anesthesiology*, vol. 106, no. 3, pp. 499–506, 2007.
- [41] F. Huimin, L. Tingkun, L. Shuaiguo, F. Yanping, and L. Changsheng, "Effects of propofol anesthesia on serum interleukins and HSP70 levels in patients with liver cancer after radiofrequency ablation," *Journal of Zhengzhou University*, vol. 50, no. 10, pp. 761–767, 2012.

- [42] J. S. Cho, M.-H. Lee, S. I. Kim et al., "The effects of perioperative anesthesia and analgesia on immune function in patients undergoing breast cancer resection: a prospective randomized study," *International Journal of Medical Sciences*, vol. 14, no. 10, pp. 970–976, 2017.
- [43] K. J. Levins, S. Prendeville, S. Conlon, and D. J. Buggy, "The effect of anesthetic technique on  $\mu$ -opioid receptor expression and immune cell infiltration in breast cancer," *Journal of Anesthesia*, vol. 32, no. 6, pp. 792–796, 2018.
- [44] S. Al Youha and D. H. Lalonde, "Update/Review: changing of use of local anesthesia in the hand," *Plastic and Reconstructive Surgery Global Open*, vol. 2, no. 5, p. e150, 2014.
- [45] W. Li-zhou, L. Xin, S. Jie, J. Tian-peng, W. Xiao-ping, and Z. Shi, "Discussion on the application of different anesthesia methods in performing radiofrequency ablation for hepatocellular carcinoma," *Journal of Interventional Radiology*, vol. 24, no. 9, pp. 781–784, 2015.
- [46] M. E. McCann, D. E. Withington, S. J. Arnup et al., "Differences in blood pressure in infants after general anesthesia compared to awake regional anesthesia (GAS study-a prospective randomized trial)," *Anesthesia & Analgesia*, vol. 125, no. 3, pp. 837–845, 2017.
- [47] M. A. Longo, B. T. Cavalheiro, and G. R. de Oliveira Filho, "Laparoscopic cholecystectomy under neuraxial anesthesia compared with general anesthesia: systematic review and meta-analyses," *Journal of Clinical Anesthesia*, vol. 41, pp. 48–54, 2017.
- [48] for the ADS study group, J. Sansonnens, P. Taffé, and B. Burnand, "Higher occurrence of nausea and vomiting after total hip arthroplasty using general versus spinal anesthesia: an observational study," *BMC anesthesiology*, vol. 16, no. 1, p. 44, 2016.